Characterization and modification of zeolites and related materials

Document status and date:
Published: 01/01/1989

Document Version:
Publisher's PDF, also known as Version of Record (includes final page, issue and volume numbers)

Please check the document version of this publication:

CHARACTERIZATION
AND
MODIFICATION
OF
ZEOLITES
AND
RELATED MATERIALS

BETTINA KRAUSHAAR-CZARNETZKI

CHARACTERIZATION AND MODIFICATION OF ZEOLITES AND RELATED MATERIALS

CHARACTERIZATION AND MODIFICATION OF ZEOLITES AND RELATED MATERIALS

PROEFSCHRIFT

TER VERKRIJGING VAN DE GRAAD VAN DOCTOR AAN
DE TECHNISCHE UNIVERSITEIT EINDHOVEN, OP GEZAG
VAN DE RECTOR MAGNIFICUS PROF. IR. M. TELS, VOOR
EEN COMMISSIE AANGEWEZEN DOOR HET COLLEGE
VAN DEKANEN, IN HET OPENBAAR TE VERDEDIGEN OP
VRIJDAG 7 APRIL 1989 TE 16.00 UUR

DOOR

BETTINA KRAUSHAAR-CZARNETZKI

GEBOREN TE ZWESTEN,
BONDSREPUBLIEK DUITSLAND

Dit proefschrift is goedgekeurd door de promotoren:
Prof.dr.ir. J.H.C. van Hooff
Prof.dr. R.A. van Santen.

Copromotor:
Dr.ir. J.W. de Haan.

Für meine Eltern.

CONTENTS

Zeolites and related crystalline, microporous materials become currently more important and popular because of the great variety of possible applications. Their unique molecular sieve properties, for instance, make them useful as sorbents in the separation of gaseous or liquid compounds. Their ion exchange properties enable applications in the purification of waste water or as detergent builders. In the field of industrial heterogeneous catalysis, zeolites are meanwhile indispensible for the cracking and upgrading of refinery streams. The invention and synthesis of new materials as well as the development of new applications play therefore a dominant role in the chemistry of zeolites and related molecular sieves. At the same time, the characterization by means of modern and currently refined spectroscopic techniques promotes a deeper understanding of the physico–chemical and catalytic properties.

The investigations described in this thesis are concerned with modification, a further important subject in zeolite chemistry. Modification means that a given material is manipulated by appropriate treatments in order to change its properties. Three examples for modifications will be described in this thesis, starting from quite different molecular sieves.

The first example concerns the manipulation of structural defects in zeolite ZSM–5. In acid catalyzed cracking, these structural defects will be shown to have a negative effect on the intrinsic activity and the deactivation characteristics. On the other hand, they can be used for the incorporation of titanium atoms into the framework yielding a new material useful as a catalyst in oxidation reactions.

As a second example for modification, the dealumination of zeolite Y by means of different methods will be investigated. Zeolite Y is the most important industrial

cracking catalyst, and its selectivity towards high–octane products can be improved by increasing the framework Si/Al ratio. However, the various dealumination reactions do not only alter the framework composition, but also result in the formation of structural defects. As in the case of zeolite ZSM–5, these defect sites may be used for the incorporation of titanium or other elements into the framework.

The third example does not concern the modification of the framework composition of a molecular sieve, but rather the deposition of catalytically active metal inside the channels. Metal loading in zeolites can be achieved by means of ion exchange and subsequent reduction of the metal ions, resulting in a material with acidic and metallic properties. However, there is also need of non–acidic molecular sieves that can act as shape selective high–surface supports for catalytically active metals or metal compounds in, i.e., (de–) hydrogenation, HDS and HDN catalysts. The aluminophosphate molecular sieves are promising candidates for this purpose since these materials exhibit no ion exchange capacity and hence no potential for Brønsted acidity. The the loading of $AlPO_4$–5 with nickel particles will be evaluated here as an example for this kind of modification.

This thesis will only document a small part of the numerous possibilities of modification. However, the examples presented may show that modification is a fascinating subject: even well investigated, "old fashioned" materials can suddenly reveal surprisingly new properties suitable for new applications.

I.   SOME UNIFYING CONCEPTS IN THE CHEMISTRY OF ZEOLITES AND RELATED MATERIALS

I.1.   ZEOLITES AND RELATED MATERIALS: DEFINITION

Zeolites are crystalline aluminosilicates with a threedimensional, open anion framework consisting of four–connected $TO_{4/2}$ tetrahedra (T = Si, Al) in which the charge–compensating cations and the water molecules have considerable freedom of movement, permitting ion exchange and reversible dehydration. The $TO_{4/2}$ tetrahedra are linked to each other by sharing all four oxygen atoms. The negative charge of the framework is generated by the presence of $AlO_{4/2}$ tetrahedra with formally charged Al^{3+} and O^{2-} ions.

Currently, zeolite chemistry is concerned with a wide range of novel materials that have some properties in common with zeolites, but do not exactly obey their definition. Isostructural analogues containing trivalent elements such as gallium or iron instead of aluminum, for instance, exhibit all features characteristic of zeolites except for the chemical composition. On the other hand, formal substitution of tetravalent elements such as silicon, germanium or titanium for aluminum results in materials without ion exchange properties and considerably changed sorption characteristics. It will be shown in part III and part IV of this thesis that the chemically substituted derivatives sometimes can or even must be prepared from a given zeolite by means of appropriate modification reactions. Therefore, it is justified to integrate these materials into zeolite chemistry.

This is also true for the novel microporous aluminophosphates and their substitutional analogues. Some of them have the same framework topology as found in

zeolites. Depending on their chemical composition they can, moreover, exhibit similar ion exchange and sorption properties.

From the practical and possibly also from the theoretical point of view it is useful to consider all crystalline molecular sieves with a three–dimensional framework structure as "zeolites and related materials". This term includes zeolites, microporous aluminophosphates and any possible derivative or modification.

The great variety of zeolites and related materials calls for unifying concepts which enable systematic classification as well as description and prediction of properties. Various promising attempts have been made in order to rationalize structures, sorption characteristics, acidities, activities and stabilities of zeolites, and some approaches are or may also be applicable to related materials. In the following sections, a short introduction to some recent concepts will be given.

I.2.   TOPOLOGICAL CONCEPTS

From the strictly topological point of view, zeolites and related materials can be described by considering only the four–connected tetrahedral T–atoms because each oxygen atom lies between two T–atoms. A TO_2 framework consisting of four connected T–atoms and two–coordinated oxygen atoms is called a (4;2)–3D net. This designation provides a clear distinction from other types of three–dimensional networks with different coordination numbers of the metal or oxygen atoms.

There is an infinite number of ways to construct (4;2)–3D nets from the $TO_{4/2}$ tetrahedra which can be considered as primary building units, and no systematic procedure exists for deriving all of them. The most convenient way to classify frameworks is to look for common subunits.

The concept of "secondary building units" (SBU)[1,2] was introduced on the assumption that each zeolite framework could be built with only one particular kind of

simple component consisting of a few TO_4 tetrahedra. Such a SBU might also be a precursor in the crystallization mixture from which the corresponding framework grows. Actually, the construction of many (4;2)–3D nets was found to require more than one type of SBU. Moreover, the original eight types of SBU[1,2] (4–ring, 6–ring, 8–ring, cube, hexagonal prism, 4^3 cluster, 5–ring plus one edge and $4^2 5^2 6$ cluster; $4^2 5^2 6$, for instance, is the face symbol for a polyhedron with two square faces, two pentagonal faces and one hexagonal face) must currently be completed with further complex clusters in order to enable the description of novel structures. The use of the SBU concept for the complete and systematic classification of (4;2)–3D nets is therefore limited.

A more rigorous topological approach to the systematic enumeration of possible (4;2)–3D nets was proposed by Smith on regarding polyhedra[3], coplanar and non–coplanar chains[4] and 2D nets (sheets) as subunits[5,6].

Most but not all polyhedra with three edges meeting at each vertex can be joined to each other by sharing faces in order to generate (4;2)–3D networks. An exception are, for instance, polyhedra with pentagonal faces. One of the simplest examples for the construction of a 3D net from polyhedra is the sodalite framework. This net can be described as a space–filling array of translated truncated octahedra. The faujasite net requires two types of polyhedra: the truncated octahedron and the hexagonal prism (see also Fig. IV.1). Two truncated octahedra are joined together with a hexagonal prism in trans configuration, resulting in a diamond–type array of the truncated octahedra.

Any sequence of edge–vertex–edge etc. is a chain and therefore, any (4;2)–3D net contains chains. Smith demonstrated that some of them are useful for classification. The simplest chains are coplanar arrays of two–connected vertices which can be linked into sheets. More complex chains consist of edge–sharing clusters. The pentasil chain, for instance, is obtained from a zigzag arrangement of edge–sharing 5^8 clusters (polyhedra with eight pentagonal faces)[4]. Pentasils such as zeolite ZSM–5 can be constructed by using these complex zigzag chains as a subunit (see Fig. II.1)[7].

Three–connected 2D nets are also convenient subunits for the classification and

description of four connected 3D nets, and there is an infinity of 2D nets that can be considered to start with. The net of $AlPO_4$–5, for instance, can be formed from parallel (4.6.12) 2D nets which are connected by alternating upward and downward bondings (4.6.12 is the Schläfli symbol for a net in which each node is part of one 4–ring, one 6–ring and one 12–ring). A framework model of $AlPO_4$–5 is shown in Fig. V.3. Actually, the $AlPO_4$–5 net (labeled Smith #81) was invented by Smith[6] four years before $AlPO_4$–5 was synthesized[8]. Starting from the $AlPO_4$–5 net and expanding the (4.6.12) sheets by insertion of 4–rings, Smith and Dytrych moreover predicted a new network (Smith #81(1)) containing 18–rings[9], which was recently found to be the topology of the novel aluminophosphate VPI–5[10].

These examples show that a systematic enumeration and classification of (4;2)–3D nets can be a powerful help in the elucidation of crystal structures and in the prediction of new framework types.

I.3   CONCEPTS OF FRAMEWORK ELECTRONEGATIVITY

Electronegativity is defined as the power of an atom to attract electrons. In a molecule consisting of atoms of different electronegativity the electrons will be redistributed until they are equally attracted to the corresponding nuclei. This principle of electronegativity equalization was first expressed by Sanderson[11]. For a compound $A_a B_b C_c$, the intermediate electronegativity (S_{int}) is postulated to be the geometric mean of the atomic electronegativities:

$$S_{int} = \left[S_A^a \, S_B^b \, S_C^c \right]^{1/(a + b + c)}$$

This intermediate electronegativity can be correlated with the partial atomic charges, and both magnitudes provide significant information about the properties of a

6

compound. Application of Sanderson's electronegativity equalization concept to zeolites was, for instance, successful in rationalizing Bronsted acidity and the corresponding physico–chemical properties[12-15]. However, structure related parameters are not taken into consideration, and therefore, Sanderson's formalism is only valid within a single structurally homogeneous series.

Mortier et al. recently developed a refined definition of the formalism for the calculation of charges and average electronegativities in solids[16,17]. The Sanderson electronegativity was replaced by an "effective" electronegativity which includes correction terms for the charge and the connectivity of atoms in a crystal. The equalization of these effective electronegativities leads to structure–dependent atomic charges. Atoms in different crystal structures, at different crystallographic positions or with different types of neighbours must therefore exhibit different charges, while the conventional Sanderson formalism gives only composition–dependent atomic charges. A correlation between the average electronegativity according to Mortier et al. and the framework density (refractive index) of different silica polymorphs has already been established[16]. Correlations with ESCA–shifts, NMR chemical shifts, hydroxyl stretching frequencies, catalytic activities etc. can be considered. The concept of framework electronegativity can become a useful approach for the understanding and prediction of physico–chemical properties of zeolites and related materials.

I.4.   THE CONCEPT OF CONFINEMENT EFFECTS

The so–called confinement effect has recently been proposed by Derouane[18-20] in order to describe the interactions of sorbed atoms or molecules with the curved surface of channels and cages in molecular sieves. It is, of course, convenient to assume that the whole framework can contribute to activation by close contact and strong interaction with reactant molecules. From the chemical point of view, the terms "solvatation" or

"supersolvatation" for sorbate–framework interactions in molecular sieves may therefore be more appropriate than the designation "confinement effects".

Derouane et al. derived a simple van der Waals model for the interaction energy, containing terms accounting for the polarizabilities of adsorbent and sorbate and a parameter accounting for the effects of the surface curvature. Strikingly, the model presented does not take the polarities of adsorbents and sorbates into consideration. This means, for instance, that factors such as electric field gradients, the influence of charge compensating cations or lattice defects are neglected. Nevertheless, measurements of the chemical shift characteristics of the apolar and spherical ^{129}Xe atoms entrapped in various molecular sieves could be used to estimate the contribution of surface curvature effects and framework polarizabilities[19]. Until now, however, only little data are available. Heats of sorption and ^{13}C NMR characteristics of non–spherical hydrocarbons, for instance, can provide direct information about the sorbate–framework interaction energy and the diffusivities, mobilities and conformational changes of the sorbate molecules.

The novel concept of confinement effects obviously needs some more experimental background and precision, but it is a promising attempt to rationalize the sorption characteristics and reactivities of molecular sieves.

I.5. REFERENCES

1   W.M. Meier, "Molecular Sieves", Society of the Chemical Industry, London 1968, p. 10.

2   W.M. Meier and D.H. Olson, Atlas of Zeolite Structure Types, Juris Druck & Verlag, Zürich 1978.

3   J.V. Smith and J.M. Bennet, Amer. Mineral. 66, 777 (1981).

4   J.V. Smith, Amer. Mineral. 64, 551 (1979).

5   J.V. Smith, Amer. Mineral. 62, 703 (1977).

6   J.V. Smith, Amer. Mineral. 63, 960 (1978).

7   D.H. Olson, G.T. Kokotailo, S.L. Lawton and W.M. Meier, J. Phys. Chem. 85, 2238 (1981).

8   S.T. Wilson, B.M. Lok and E.M. Flanigen, U.S. Patent 4.310.440 (1982).

9   J.V. Smith and W.J. Dytrych, Nature 309, 607 (1984).

10   M.E. Davis, C. Saldarriaga, C. Montes, J. Garces and C. Crowder, Zeolites 8, 362 (1988).

11   R.T. Sanderson, "Chemical Bonds and Bond Energy", Academic Press, New York 1976.

12   P.A. Jacobs and W.J. Mortier, Zeolites 2, 226 (1982).

13   P.A. Jacobs, Catal Rev. — Sci. Eng. 24, 415 (1982).

14   S. Hocevar and B. Drzaj, J. Catal. 73, 205 (1982).

15   A.K. Ghosh and G. Curthoys, J. Catal. 86, 454 (1984).

16   W.J. Mortier, K. van Genechten and J. Gasteiger, J. Am. Chem. Soc. 107, 829 (1985).

17   K. van Genechten, W.J. Mortier and P. Geerlings, J. Chem. Soc., Chem. Commun. 1278 (1986).

18   E.G. Derouane, A.A. Lucas and J.M. André, Chem. Phys. Letters 137, 336 (1987).

19   E.G. Derouane and J.B. Nagy, Chem. Phys. Letters 137, 341 (1987).

20   E.G. Derouane, Chem. Phys. Letters 142, 200 (1987).

CONTENTS

zeolite. The manufacturing costs of ZSM–5 could drastically be decreased if both, expensive use of templates during synthesis and subsequent exchange of alkaline ions against H^+ or NH_4^+, could be avoided. But the preparation of ZSM–5 from alkaline– and template–free reaction mixtures has not been reported.

The crystal structure of ZSM–5 was described in 1978 by Kokotailo et al.[14] and is depicted in Fig. II.1. According to Smith's topological concept (see part I), the ZSM–5 framework can be constructed from the so–called pentasil chains, which are, in their turn, obtained from a zig–zag arrangement of edge–sharing 5^8 clusters. The channels visible in Fig. II.1 are straight and point along the [010] direction. They are formed by elliptical 10–membered rings of 0.51 x 0.55 nm diameter. Another kind of channels,

Fig. II.1: Framework Model of Zeolite ZSM–5.
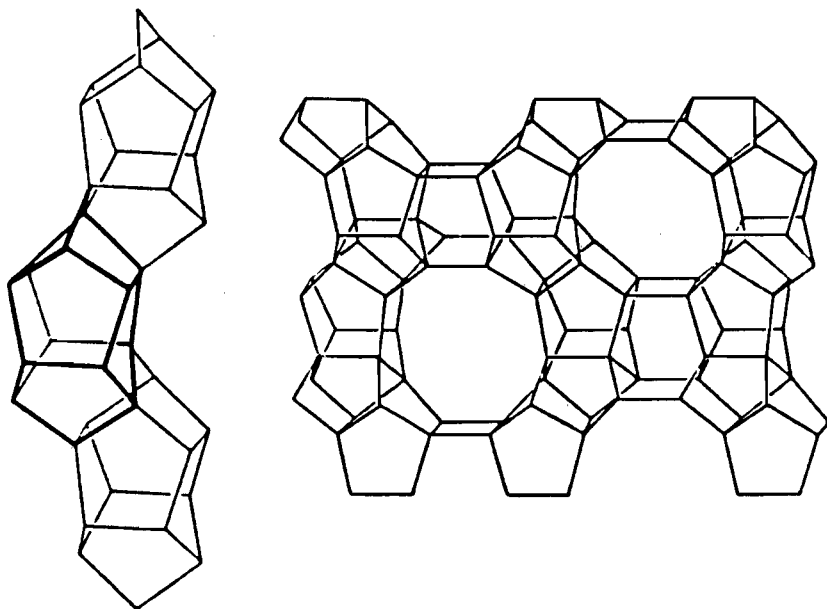
circumscribed by nearly circular 10—membered rings of 0.54 x 0.56 nm diameter, are not visible in Fig. II.1 because they run sinusoidally along the [100] direction. The two channel types are interconnected and form a three dimensional pore system. The distance between two channel intersections is very small. In fact, any framework atom can be considered as a part of an intersection. The unit cell exhibits orthorhombic symmetry and consists of 96 T—atoms (Si and Al) which are occupying 12 crystallographically non—equivalent lattice positions.

On the Difference between ZSM—5 and Silicalite—1

In 1978, Flanigen et al. reported a silica molecular sieve with similar structural features as ZSM—5 which was denoted as silicalite—1. This new material exhibited unusually high selectivity for the adsorption of apolar molecules, and application in the separation of hydrocarbons from polar compounds was suggested[15]. Earlier investigations had already shown that zeolites and particularly ZSM—5 become increasingly hydrophobic as the Si/Al ratio increases[16,17]. Therefore, Olson et al. assumed that silicalite—1 is no new molecular sieve but rather the high silica endmember of the ZSM—5 substitutional series[18]. However, this assumption was in conflict with results obtained from structure determinations: the framework of ZSM—5 must be described in the orthorhombic space group $Pnma$[14] while calcined silicalite was found to exhibit monoclinic framework symmetry (space group $P2_1/n$)[15]. On the other hand, Wu et al. demonstrated that both materials are orthorhombic before removal of the template[19].

Solid—state ^{29}Si and ^{27}Al NMR spectroscopy became a powerful tool in the eludication of this discussion. Fyfe et al. showed that the so—called silicalite—1 also contains traces of tetrahedrally coordinated framework aluminum[20]. Moreover it was demonstrated that the typical fine structure in the ^{29}Si MAS NMR spectra of calcined silicalite—1, which is ascribed to the presence of crystallographically non—equivalent sites for silicon atoms in the lattice, can also be observed after dealumination of zeolite ZSM—5[20,21]. Fyfe et al. concluded that the line broadening in the ^{29}Si NMR spectra of

12

ZSM–5 as compared with silicalite–1 is caused by the large number of silicon environments created by the random distribution of aluminum atoms in the lattice and predicted narrow ^{29}Si resonances for any perfectly ordered system[22].

However, the structural differences between ZSM–5 with orthorhombic and silicalite–1 with monoclinic framework symmetry were still a point of discussion until Hay et al. presented XRD evidence of reversible temperature induced phase changes monoclinic–orthorhombic in ZSM–5 and silicalite–1. The critical temperature, at which the phase change occurs was found to decrease with increasing concentration of framework aluminum[23]. Subsequent ^{29}Si MAS NMR investigations confirmed these results[24-26]. Moreover, some recent studies revealed that structural changes accompanied by a monoclinic–orthorhombic phase transition in silicalite–1 can also be induced by uptake of sorbates[27,28].

Obviously, silicalite–1 and high silica ZSM–5 are identical materials. The partly conflicting results concerning the structural properties can be ascribed to changes in the framework symmetry which can be influenced by the concentration of framework aluminum, the temperature and by the presence of template or sorbate molecules in the channels. As a consequence, the old and misleading denotation "silicalite–1" became less popular and is currently replaced by the more convenient denotation "ZSM–5" or "high silica ZSM–5".

Shape Selective Properties of ZSM–5

It has already been mentioned that ZSM–5 possesses unusual sorption properties that render potential use in the separation of hydrocarbons from polar compounds. The major applications of ZSM–5, however, are found in the field of chemical and fuel processing and are based on the unique shape selective properties of the ZSM–5 structure. The channels in ZSM–5 exhibit intermediate sizes between those of classical shape selective zeolites such as erionite, ferrierite, gmelinite, chabazite or zeolite A[29] and those of large–pore zeolites such as faujasite, mordenite and zeolite L. The classical shape

selective catalysts accept only straight chain paraffins whereas the channels of ZSM—5 are also accessible for isoparaffins and simple aromatics. On the other hand, the absence of large internal cages prevents formation of bulky and plugging products such as polyaromatic coke.

Commercial processes involving zeolite ZSM—5 are based on the shape selective properties of this catalyst. In the M—forming process, for instance, ZSM—5 cracks selectively the normal and slightly branched reactant paraffins from reformate streams. The cracked fragments can alkylate aromatics in the reformate stream, and an increase in liquid yield can be observed[30]. Dewaxing is a similar process and comprises selective conversion of long chain paraffins in heavy fractions of petroleum streams. The waxy crude oils are therefore upgraded into fluids with improved flow properties[31]. In the toluene disproportionation and xylene isomerization processes, high yields of p—xylene are realized. Although all three xylene isomers are formed within the ZSM—5 channel system, p—xylene has a diffusivity several orders of magnitude greater than for the meta and ortho isomers. The para isomer therefore easily leaves the pore system while the other isomers undergo further equilibration to p—xylene. Moreover, the formation of a bimolecular transition complex is restricted inside the channels of ZSM—5, resulting in very low rates of transalkylations[32-35]. The methanol—to—gasoline process (MTG) concerns complete dehydration of methanol and formation of hydrocarbons in the gasoline range[36]. The mechanism of this reaction has been the subject of numerous investigations and discussions. An up—to—date review has been presented by Engelen[37].

However, future technologies will most probably involve modifications of ZSM—5. Entrapment of catalytically active metals or metal compounds in the channels can yield bifunctional catalysts, and isomorphous substitution of Al atoms can modify the acidic properties. Diffusional and acidic characteristics can be altered by interaction or reaction with chemical reagents. A better understanding of the ZSM—5 system enables purposeful modifications which can be applied profitably to activity and selectivity enhancement in known processes or to development of novel catalytic reactions. In this

14

part, the characterization of ZSM–5 with respect to structural defects will be described, and it will be shown that manipulation of these defects alters the activity and deactivation characteristics of the catalyst.

II.2.   CHARACTERIZATION OF SILANOL GROUPS IN ZSM–5

Introduction

Modern spectroscopic techniques in combination with sorption and ion exchange experiments permit a clear distinction between acidic and non–acidic hydroxyl groups in zeolites. The acidic hydroxyl groups are forming a bridge between adjacent Al and Si atoms in the lattice and are also described as Brønsted hydroxyls (Fig. II.2, type I). In contrast, silanol groups are terminal hydroxyl groups attached to silicon atoms, and they exhibit only very weak acidic character (Fig. II.2, type II).

Silanol groups are required in order to terminate the external surface of the zeolite crystals. The amount of these external silanol groups (type II.1) can approximately be calculated from the zeolite particle size. In highly siliceous ZSM–5 the total amount of silanol groups was found to be much higher than the required amount of external silanol groups[38-41]. Therefore, the presence of internal silanol groups in structural defects was proposed.

Of course, the most convenient explanation for the occurence of internal silanol groups is the cleavage and hydration of strained Si–O–Si linkages e.g. in the small 4–rings[38,42]. Upon heating these paired silanol groups (type II.2.2) can condense and the zeolite framework is healed. Recently, Dessau et al. proposed the presence of isolated internal silanol groups which can condense after structural rearrangements[43]. Furthermore, a clustering of internal silanol groups may be considered, e.g. at missing T–atoms in the lattice (type II.2.3)[44].

Until now, the direct discrimination of external and different possible types of

15

internal silanol groups is not possible. Infrared spectroscopy (IR), magic angle spinning nuclear magnetic resonance of ^{1}H or of ^{29}Si in combination with cross–polarization (^{1}H MAS NMR or ^{29}Si CP MAS NMR), ion exchange experiments and temperature programmed desorption of bases can be applied, but these techniques give only little more than indication of silanol groups. However, a more detailed characterization is possible in an indirect way. If silanol groups are first silylated by reaction with e.g. trimethylchlorosilane, subsequent ^{29}Si CP MAS NMR analysis of the products will reveal information about their spatial arrangement and the location in the zeolite. This method will be introduced in the following section.

Fig. II.2: Possible Types of Hydroxyl Groups in Zeolites.

I:

H
|
O
≡Si⁄ ⎯ \Al≡   *Brønsted hydroxyl, bridging*

II: ≡Si–OH   *silanol group, terminal*
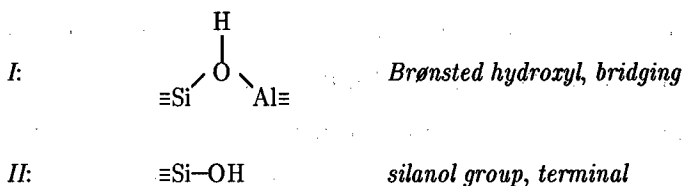
II.1: external silanol groups terminating the external surface of the zeolite crystals
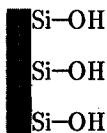
II.2: internal silanol groups at structural defects in the lattice

II.2.1: isolated

Si–OH

Si–OH

Si–OH

Si–OH

II.2.2: paires in broken Si–O–Si linkages

Si–OH   HO–Si

II.2.3: clusters surrounding T–atom vacancies

S i
|
OH
Si–OH   HO–Si
OH
|
S i
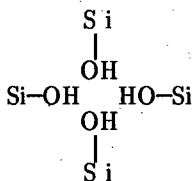
Experimental

The samples of ZSM–5 were synthesized according to a modified patent procedure described by Derouane et al.[45] but without addition of aluminum. Aerosil 200 (Degussa) or Davison Grade 360 (Grace) were used as silica sources. The crystallization products were washed and dried before and after removal of the template (3 h at 823 K). Chemical analyses revealed Si/Al ratios above 4000 and Si/Na ratios of about 80.

The silylations were performed in quartz ampoules with 26 μl trimethylchlorosilane (TCS) per 450 mg of carefully dried zeolite. After injection of the TCS in an atmosphere of dried nitrogen, the ampoules were cooled with solid carbon dioxide, evacuated and rapidly sealed. The ampoules were then heated with a rate of 4 K/min and kept for 16 h at the reaction temperature of 573 or 673 K. After cooling down, the ampoules were opened and the products were washed thoroughly with dried toluene and hexane. Finally, the products were dried in vacuo at 393 K overnight. The reaction of silylated materials with t.–butoxide ions was performed according to a procedure described by Price and Sowa[46], using potassium t.–butoxide dissolved in dimethylsulfoxide (DMSO). The products obtained were subsequently washed with DMSO and water and were dried at 393 K overnight.

The ^{29}Si CP MAS NMR spectra were obtained on a Bruker CXP 300 spectrometer at 59.63 MHz using a double bearing probe for spinning the samples (about 250 mg) at ca. 3.5 kHz. Single contacts with contact times of 8 ms and pulse interval times of 1 s were used. About 55000 free induction decays were accumulated in 1 k data points, zero–filled to 8 k prior to Fourier transformation. The δ values were determined relative to TMS.

XRD patterns of all samples revealed high crystallinities, indicating that the applied modification reactions did not affect the framework of the zeolites. Repeated NMR measurements affirmed that the silylation products were stable in air for at least several months. The pore volumes were determined on a Cahn RG electrobalance by sorption of n–butane. The procedure has been described elsewhere[47].

Results and Discussion

The silylation of silica gel or silica surfaces is a widely applied method for the preparation of stationary phases in chromatography. It is well–known that even monofunctional silanes such as trimethylchlorosilane (TCS) can react with more than one silanol group if sufficiently high reaction temperatures are provided[48]. The reaction scheme in Fig. II.3 illustrates the possible steps of the reaction of TCS with terminal groups. The primary silylation product (trimethylsiloxysilane) can be formed at a silanol group or $\equiv$SiO$^-$Na$^+$ group under elimination of HCl or NaCl and can be identified by a ^{29}Si NMR resonance at +12 ppm. Secondary and tertiary products can be formed with concomitant evolution of methane if further silanol groups are available at suitable distances. By means of ^{29}Si MAS NMR the silylation products carrying different numbers of methyl groups can easily be distinguished from each other and from silanol groups and Q^4 silicon atoms stemming from silica or the zeolite. Moreover, ^{1}H–^{29}Si cross polarization enables the application of shorter pulse interval times and provides

Fig. II.3: The Reaction of Trimethylchlorosilane with Silanol Groups.

Si–OH   CH$_3$
           /
Si–O–Si–CH$_3$ *trimethylsiloxysilane, primary product, δ = +12 ppm*
           \
Si–OH   CH$_3$

↓ – CH$_4$

Si–O
        \
Si–O–Si–CH$_3$ *dimethyldisiloxysilane, secondary product, δ = –18 ppm*
        \
Si–OH   CH$_3$

↓ – CH$_4$

Si–O
        \
Si–O–Si–CH$_3$ *methyltrisiloxysilane, tertiary product, δ = –66 ppm*
        /
Si–O
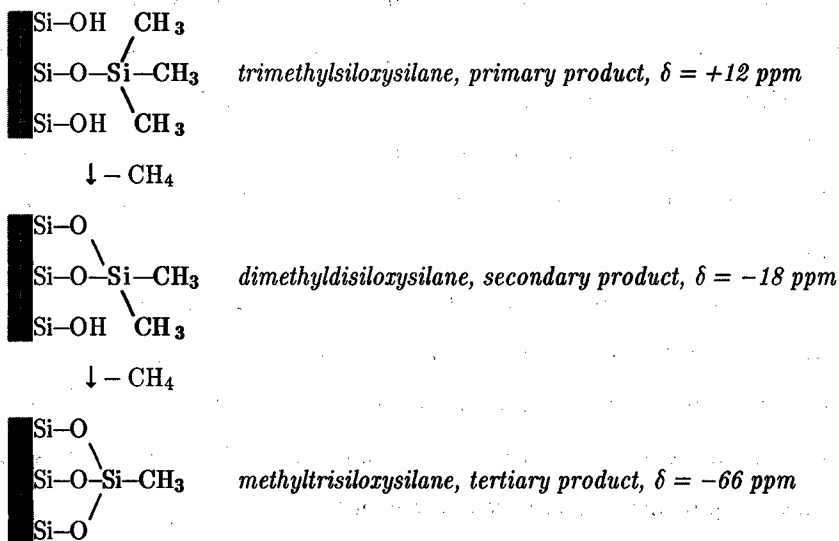
enhancement of signals stemming from silicon atoms in the neighbourhood of hydrogen atoms.

The course of the silylation reaction depends on the reaction temperature and on the spatial arrangement of the silanol groups. On silica gels, for instance, the formation of tertiary silylation products requires reaction temperatures of at least 773 K because of the unfavourable planar arrangement of the silanol groups at the surface.

Fig. II.4: ^{29}*Si CP MAS NMR Spectra of ZSM–5.*

(A) before reaction with TCS; (B) after reaction with TCS at 573 K; (C) after reaction with TCS at 673 K.
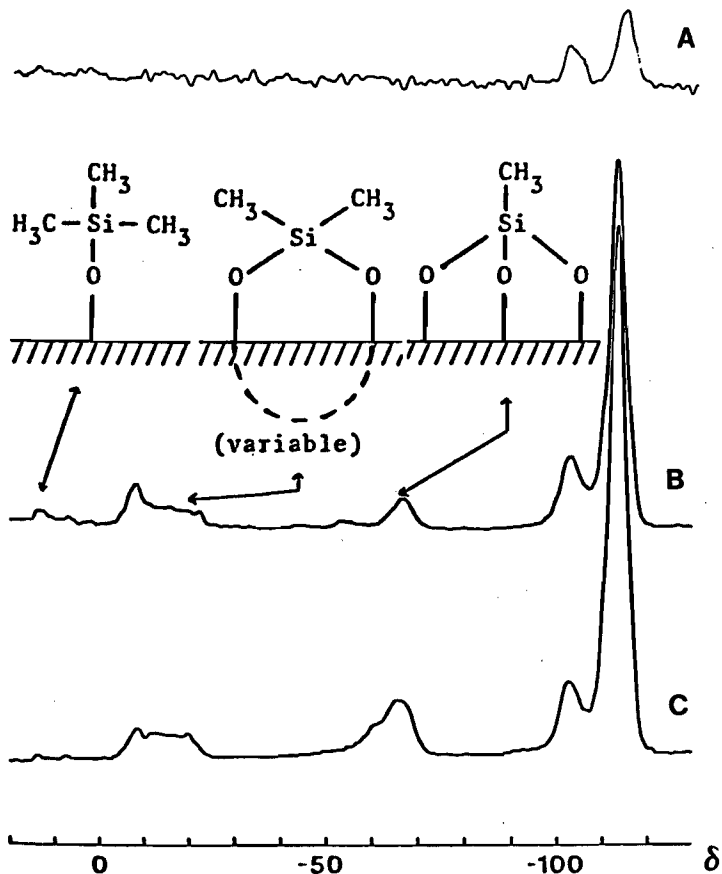
The ^{29}Si CP MAS NMR spectra of ZSM-5 before and after reaction with TCS are depicted in Fig. II.4. The starting material (spectrum A) gives only two resonances due to silanol groups connected to three siloxy groups (Q^3 sites) and silicon atoms connected to four siloxy groups (Q^4 sites). After reaction with TCS, additional resonances stemming from silylation products can be detected (spectra B and C). It can be observed that primary and secondary products are consumed for the formation of tertiary products at increasing reaction temperature. The formation of tertiary products requires the presence of at least three neighbouring silanol groups. Obviously, silanol groups in ZSM-5 are not isolated or paired but rather clustered. Moreover, the low reaction temperatures required for the formation of tertiary prodocts give evidence of a very

FIG. II.5: Reaction of Silylation Products with the t. Butoxide Ion.

20
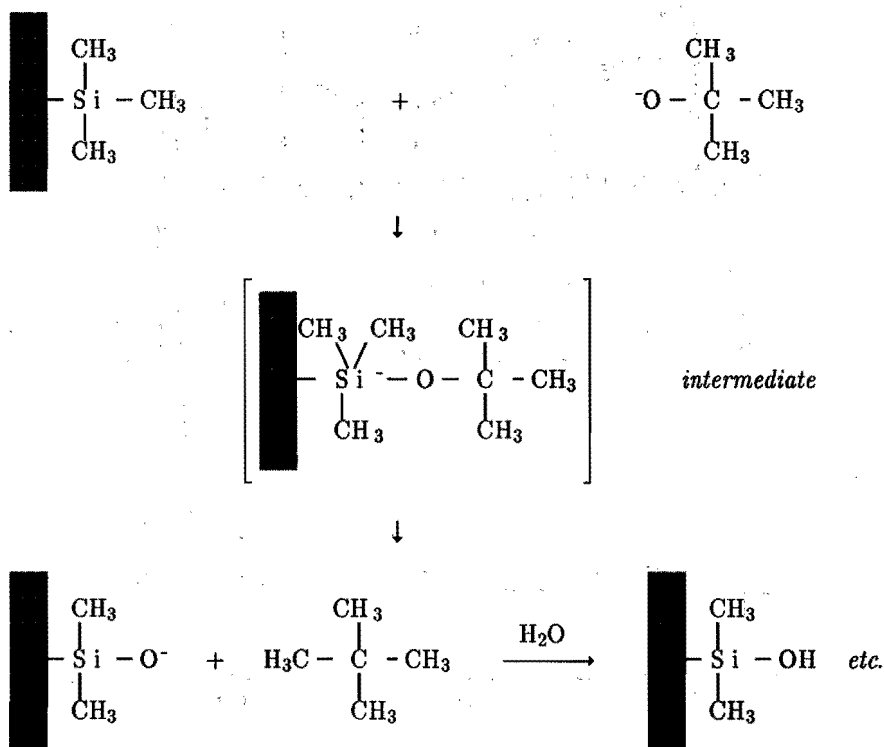
favourable spatial arrangement of the silanol groups in ZSM–5 as compared with silica gels.

Pore volume measurements were performed in order to check whether the silylation really occurred at internal silanol groups. However, the results showed that the accessibility of the threedimensional pore network is hardly affected by the presence of silylation products. A more convincing evidence of internal silylation comprises the detection of remaining silylation products after selective and complete destruction of the silylation products at the external surface. According to Price et al., the cleavage of Si–C bondings in aliphatic organo–silicon compounds and hence the destruction of

Fig. II.6: ^{29}*Si CP MAS NMR Spectra of Silylated Cab–O–Sil.*
(A) before and (B) after reaction with K–t.–butoxide.
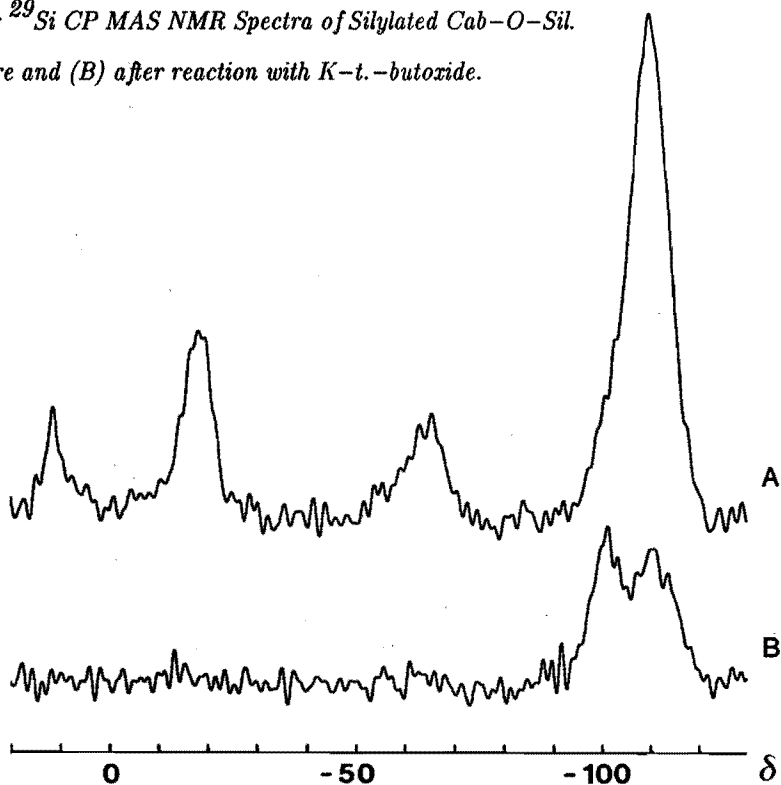
silylation products can be achieved by reaction with strong bases such as the t.–butoxide ion[46]. As shown in Fig. II.5, $\equiv$Si–CH$_3$ groups can be converted into $\equiv$Si–O$^-$ groups, and subsequent hydrolysis yields silanol groups. Although t.–butoxide is a bulky ion, the reaction should proceed easily at accessible surfaces.

The ^{29}Si CP MAS NMR spectrum of silylated Cab–O–Sil, a material that exhibits external silanol groups only, is shown in Fig. II.6. After reaction with K–t.–butoxide, all

Fig. II.7: ^{29}Si CP MAS NMR of ZSM–5 Silylated with TCS at 673 K.
(A) before and (B) after subsequent reaction with K–t.–butoxide.
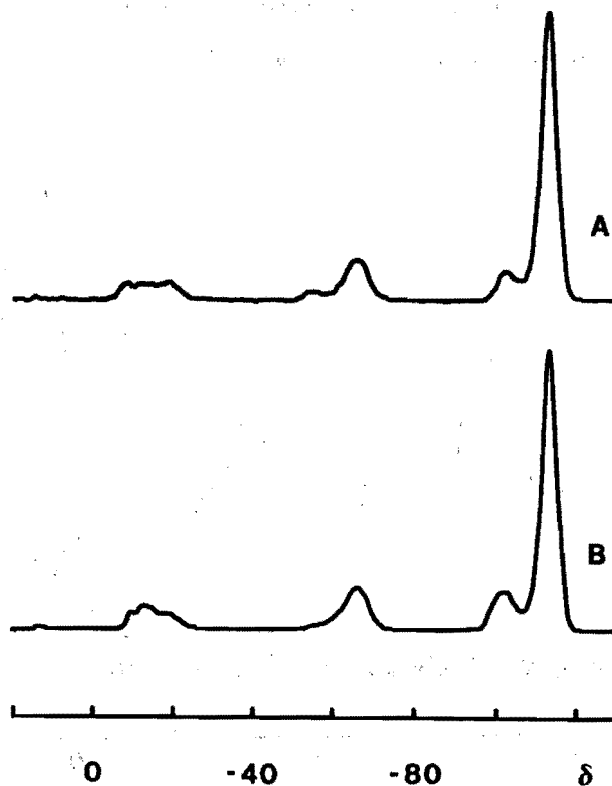
signals due to silylation products disappear while the resonance belonging to silanol groups (−103 ppm) increases. Obviously, the reaction with t.−butoxide is useful for the destruction of silylation products at external surfaces. Moreover, it can be expected that this reaction is selective since the nucleophilic attack under formation of the bulky intermediate (see Fig. II.5) should be sterically hindered inside the channels of ZSM−5.

The ^{29}Si CP MAS NMR spectra of silylated ZSM−5 before and after reaction with t.−butoxide are shown in Fig. II.7. The silylation products on ZSM−5 are hardly affected by the base treatment. It can be concluded that only a minor part of the silylation products was formed at the external surface.

The Figs. II.8, A to E, illustrate how the results can be interpreted: ZSM−5 exhibits external and internal silanol groups. The latter are clustered and surround T−atom vacancies (A). Upon silylation with TCS, trimethylsiloxysilanes are formed as primary products (B). The favourable tetrahedral arrangement of the other silanol groups

Fig. II.8: View into a Straight Channel of ZSM−5.
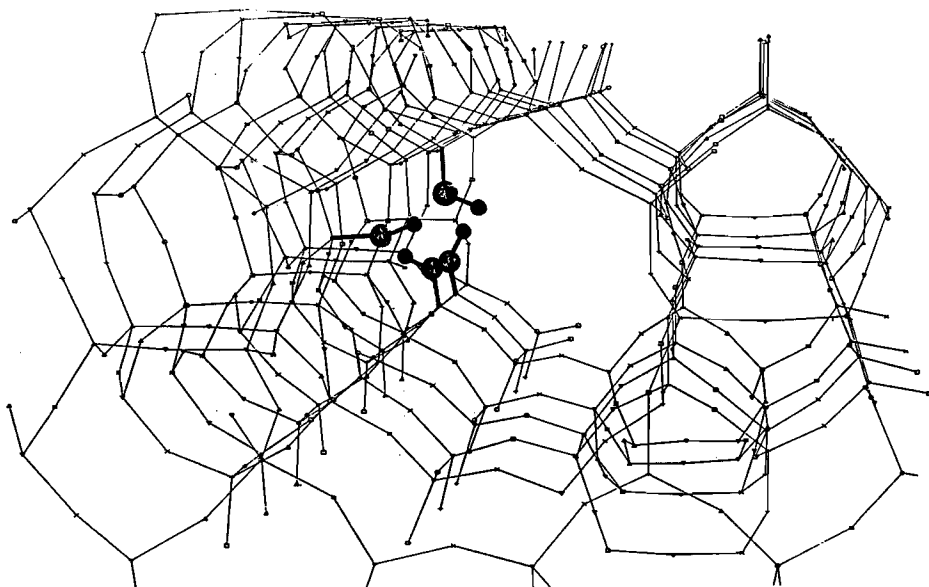
(A) four silanol groups surround a T−atom vacancy;
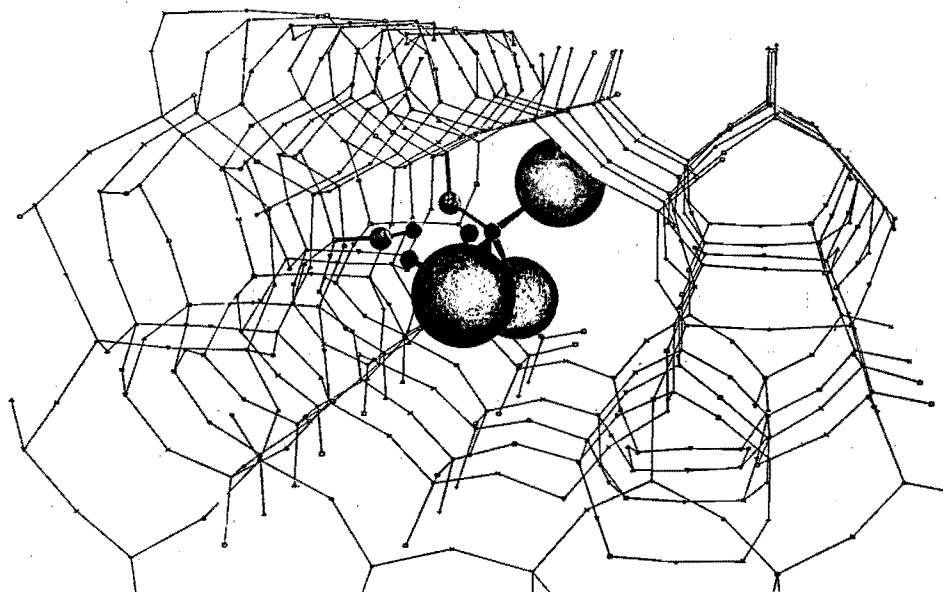
(B) formation of a trimethylsiloxysilane by reaction of TCS with one silanol group;
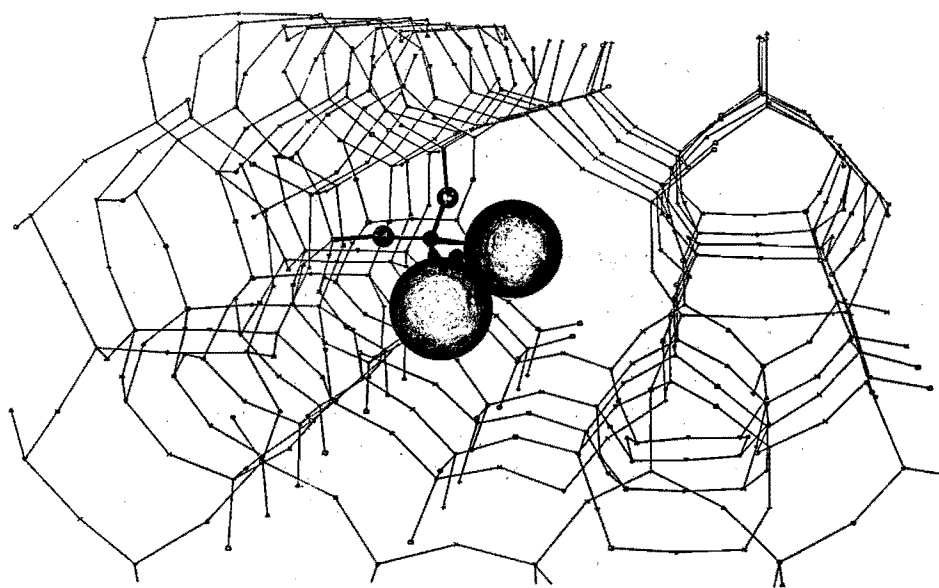
(C) formation of a dimethyldisiloxysilane requiring a second silanol group;

24
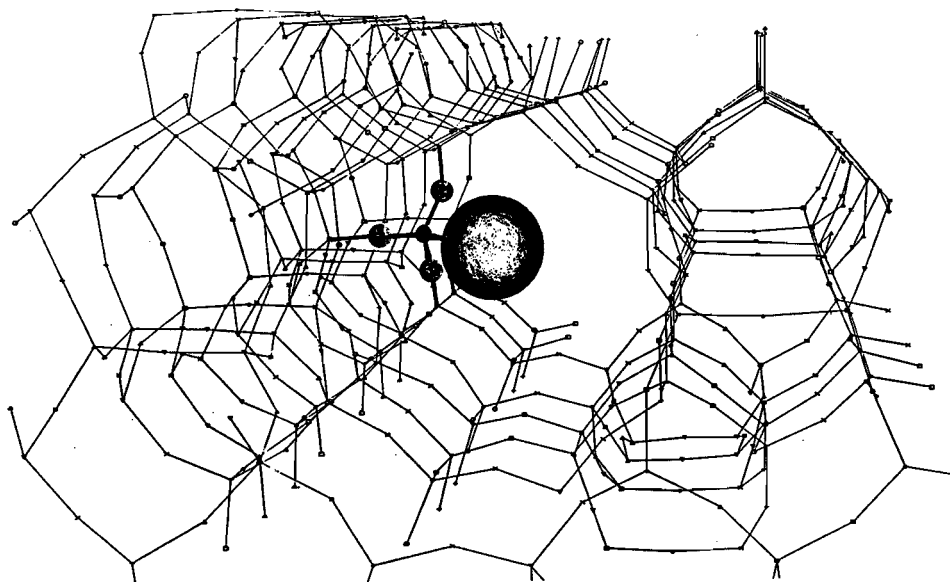
(D) formation of a methyltrisiloxysilane requiring a third silanol group;
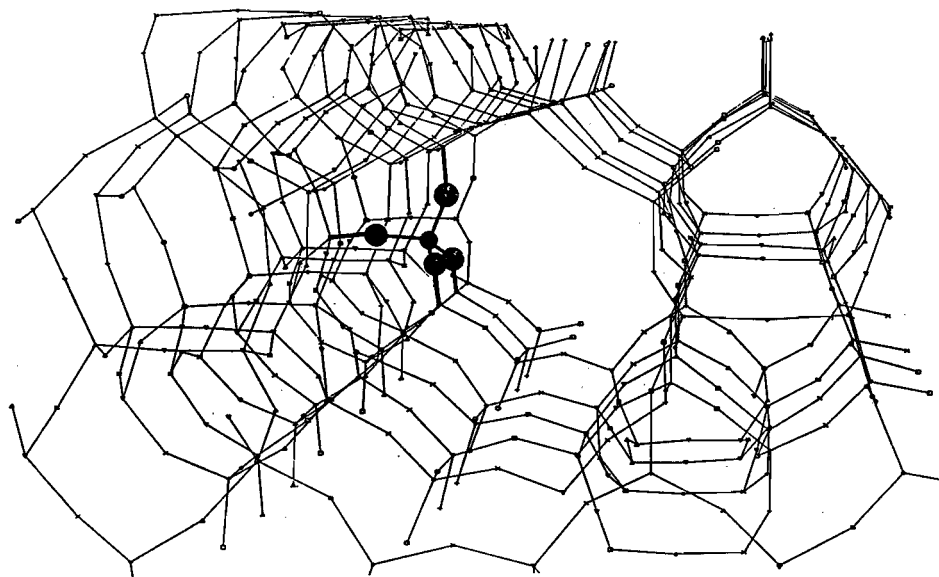
(E) complete insertion of the silicon atom stemming from TCS.

enables the consecutive reactions at relatively low reaction temperatures (C and D) until all methyl groups are cleaved and the T–atom vacancy is filled (E).

Of course, such a T–atom vacancy can also be filled by Al atoms. This would explain why reaction with $AlCl_3$ was found to result in an activation of highly siliceous ZSM–5[49,50]. Infrared investigations also support the idea of T–atom vacancies: A broad band at about 3500 cm^{-1}, typically present in the spectra of highly siliceous ZSM–5, can be ascribed to closely arranged, hydrogen bonded silanol groups[41,43,51]. Moreover, recent ^{1}H MAS NMR studies on ZSM–5 revealed that a part of the internal silanol groups is inaccessible to adsorbed molecules and suggested a vicinal arrangement[51,52].

From the ^{29}Si CP MAS NMR spectra in Figs. II.4 and II.7 even some more conclusions concerning the location of the T–atom vacancies in the lattice of ZSM–5 can be drawn. The signals stemming from dimethyldisiloxysilanes are rather complex and exhibit distinguishable resonances from –8.5 ppm up to –22 ppm. From cyclic dimethyldisiloxysilanes in solution it is known that the [29]Si shielding increases with increasing ring size, i.e. with increasing Si–O–Si bond angle[54]. In fact, the formation of dimethyldisiloxysilanes in ZSM–5 always includes closure of two rings at the same time, whereby the smallest ring can be expected to determine the chemical shift. The complex signal therefore consists of resonances of secondary products incorporated in rings of different sizes. The signal at –9 ppm disappears after reaction with t.–butoxide and can be assigned to 3–rings at the external surface of the ZSM–5 crystals. The resonances at higher fields belong to 4–membered and larger rings formed at internal silanol groups. It should be stressed here that the signal of the dimethyldisiloxysilanes would be much narrower if the internal silanol groups had a preferential position in the lattice, e.g. in interrupted 4–rings.

The formation of tertiary products always includes the closure of 2 x 3 = 6 rings of different sizes. The resulting superposition of the resonances is therefore a broad signal.

26

Conclusions

Internal silanol groups in ZSM–5 can be silylated by reaction with TCS and methyltrisiloxysilanes can be obtained. The formation of these tertiary products at relatively low reaction temperatures requires the presence of at least three neighbouring silanol groups in favourable spatial, i.e. tetrahedral, arrangements. Most probably, the internal silanol groups surround T–atom vacancies in the lattice. Furthermore, it can be excluded from the ^{29}Si CP MAS NMR analyses of the secondary silylation products that the T–atom vacancies have a preferent position in certain rings. The structural defects are rather found to be randomly distributed throughout the lattice.

II.3. MANIPULATING THE AMOUNT OF SILANOL GROUPS IN ZSM–5

Introduction

The discussion about the type of internal silanol groups as described in the previous part cannot be separated from the speculations on the origin and the mechanism of healing of these structural defects. Earlier studies already revealed that the amount of silanol groups can be decreased by heat treatments[38,55]. Recently, it was also found that samples of ZSM–5 with high Si/Al ratios contain more silanol groups than samples with low Si/Al ratios[40,41,43,51].

The model of the paired silanol groups stemming from strained and broken rings gives a simple explanation for the observed effect of heat treatment, namely dehydration and ring closure[38]. It is not obvious, however, why 4–membered rings in high silica ZSM–5 should be more strained than in low silica ZSM–5.

The isolated silanol groups as proposed by Dessau et al. are assumed to stem from $\equiv$Si–O$^-$ groups in the lattice which are required for the charge compensation of the template ions TPA$^+$. The silanol groups are formed upon decomposition of TPA$^+$. Heat treatment in the presence of steam enables structural rearrangements and subsequent

annealing of the silanol groups[43]. This model gives no explanation for the typically high amounts of chemically bound alkaline ions, i.e. sodium ions in $\equiv$Si$-$O$^-$Na$^+$ groups, which cannot be removed by washing but rather by ion exchange[40,55]. Obviously, there can be much more $\equiv$Si$-$O$^-$ groups present than required for charge compensation of template ions. Moreover, Dessau's model includes the assumption that ZSM$-$5 prepared with TPA$^+$ must always contain high amounts of internal terminal groups. It will be shown here that this is not true.

We previously gave evidence of clustered internal terminal groups surrounding T$-$atom vacancies in the lattice. It will be checked here whether this model explains the observed characteristics of differently prepared and treated samples.

Experimental

All samples of ZSM$-$5 were synthesized according to method B described by Derouane et al.[45], but without addition of aluminum. Material I was prepared from Aerosil 200, material II from Aerosil 380 (both Degussa) as silica sources. According to our own chemical analyses, Aerosil 200 contains 0.08 wt.% Al_2O_3, 0.05 wt.% Fe_2O_3, 0.03 wt.% TiO_2, while Aerosil 380 contains 0.05 wt.% Al_2O_3, 0.003 wt.% Fe_2O_3 and 0.02 wt.% TiO_2. Traces of borates, lead and some transition metal ions such as nickel, chromium and copper could be detected in both materials. The recovered crystals of ZSM$-$5 were washed and dried before and after removal of the tetrapropylammonium ions (TPA$^+$). Material I exhibited a Si/Al ratio of 4100 and a Si/Na ratio of 43 (0.86 wt.% Na). In material II, the aluminum content was beyond the limit of detection. The Si/Na ratio of material II was 529 (0.07 wt.% Na).

Ion exchange procedures were performed with 0.1 N HCl, 0.1 N NaOH or 2 N NH_4NO_3, respectively, using typically 100 ml solution per gram zeolite.

Heat or steam treatments were performed in a vertical quartz tube reactor of 3 cm diameter filled with 2 g of zeolite. After heating with a rate of 10 K/min, the samples were exposed to a flow of air (dried or mixed with water vapour) at 823 K.

The reactions with trimethylchlorosilane (TCS) and potassium tert. butoxide as well as the ^{29}Si CP MAS NMR experiments have been described in part II.2.

The FTIR spectra were obtained on a Bruker IFS 113 v spectrometer with wafers from 1 mg zeolite in 200 mg KBr.

Fig. II.9: ^{29}*Si CP MAS NMR Spectra of ZSM-5 (material I).*
(A) starting material; (B) after ion exchange with hydrochloric acid; (C) starting material after heat treatment in air(68 h at 823 K, p(H₂O) ≅ 2 kPa); (D) after heat treatment (see C) and subsequent ion exchange with hydrochloric acid.
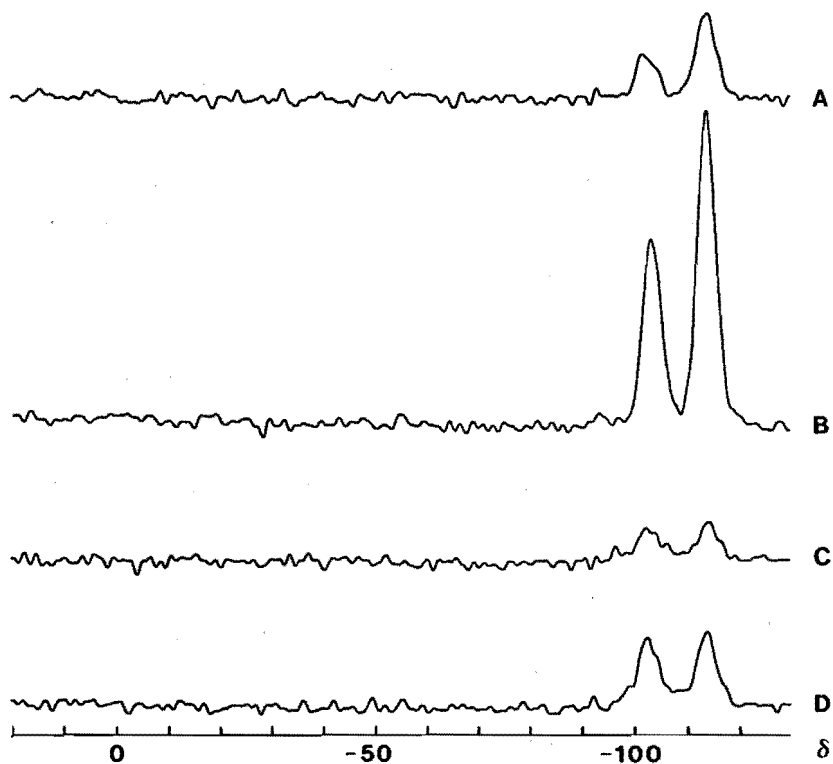
The XPS measurements were recorded on a AEI ES 200 spectrometer equipped with a Mg anode (1254 eV). The samples were deposited on an Ir holder and evacuated at room temperature until a pressure of $0.8 \cdot 10^{-7}$ Pa was attained. The intensities of Na(1s) peaks (binding energy 1074 eV) were related to the intensities of Si(2p) peaks (binding energy 106 eV) as internal standard, assuming that the concentration of Si atoms does not change during heat treatments.

Results and Discussion

The effect of heat treatment and acid ion exchange on the amount of silanol groups can be followed in the ^{29}Si CP MAS NMR spectra of sample I in Fig. II.9. The starting material with 0.86 wt.% of Na exhibits about two $\equiv$Si–O$^-$Na$^+$ groups per unit cell and additionally $\equiv$Si–OH groups which are indicated by the signal at −103 ppm (spectrum A). After ion exchange with hydrochloric acid, the amount of sodium ions is reduced to 0.1 wt.%, and the signals due to silanol groups and Q^4 sites are strongly increased (B). Heat treatment of the starting material results in a nearly complete disappearance of the silanol groups while the sodium content, of course, remains the same (C). Ion exchange of the heated material again reduces the amount of Na$^+$ to 0.1 wt.%, but the increase in silanol groups is now much smaller than before heat treatment (D). The silanol groups in spectrum B are therefore only partly stemming from exchange of sodium ions against protons. A lot of new silanol groups must be formed by hydrolysis of Si–O–Si linkages. Von Ballmoos recently presented an ^{18}O exchange study which gave evidence of cleavage of Si–O–Si bondings in the presence of liquid water. It was suggested that point defects in the lattice can accelerate the process of bond cleavage and oxygen exchange[56,57]. The spectra in Fig. II.9 clearly confirm this: after heat treatment the amount of silanol groups and hence structural defects is decreased, and the whole lattice seems to be more resistant against hydrolysis of Si–O–Si linkages.

Figure II.10 shows the ^{29}Si CP MAS NMR spectra of silylated sample I. The different signal intensities due to silylation products again indicate that the amount of

Fig. II.10: ^{29}Si CP MAS NMR Spectra of ZSM–5 (material I).

(A) starting material after silylation with TCS at 673 K; (B) after heat treatment (68 hours at 823 K, p(H$_2$O) ≅ 2 kPa) and subsequent silylation with TCS at 673 K; (C) after heat treatment, silylation and subsequent reaction with K–t.–butoxide.
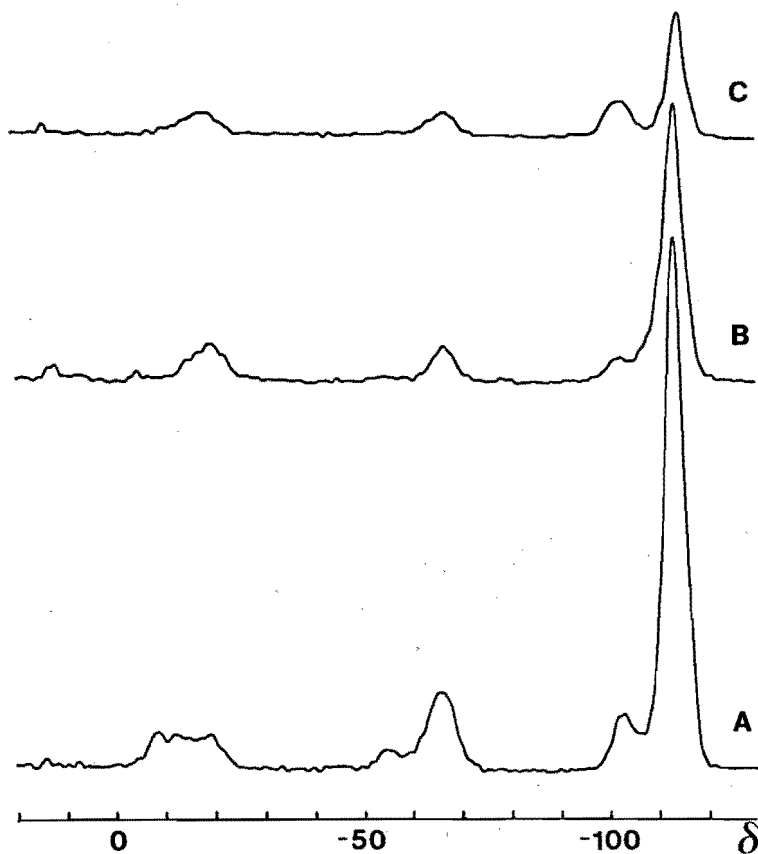
silanol groups has decreased during heat treatment (spectra A and B). The high–field shift of the main signals stemming from secondary and tertiary products moreover show that some structural rearrangement has occurred during heat treatment. After destruction of the external silylation products with t.–butoxide (C), only a few remaining silylation procucts can be detected. Obviously, heat treatment causes a decrease in internal silanol groups whereas the amount of external terminal groups remains the same of even increases.

Fig. II.11: ^{29}*Si MAS NMR Spectra of ZSM–5 (material I).*

(A) starting material; (B) after heat treatment (68 hours at 823 K, p(H$_2$O) $\cong$ 2 kPa).
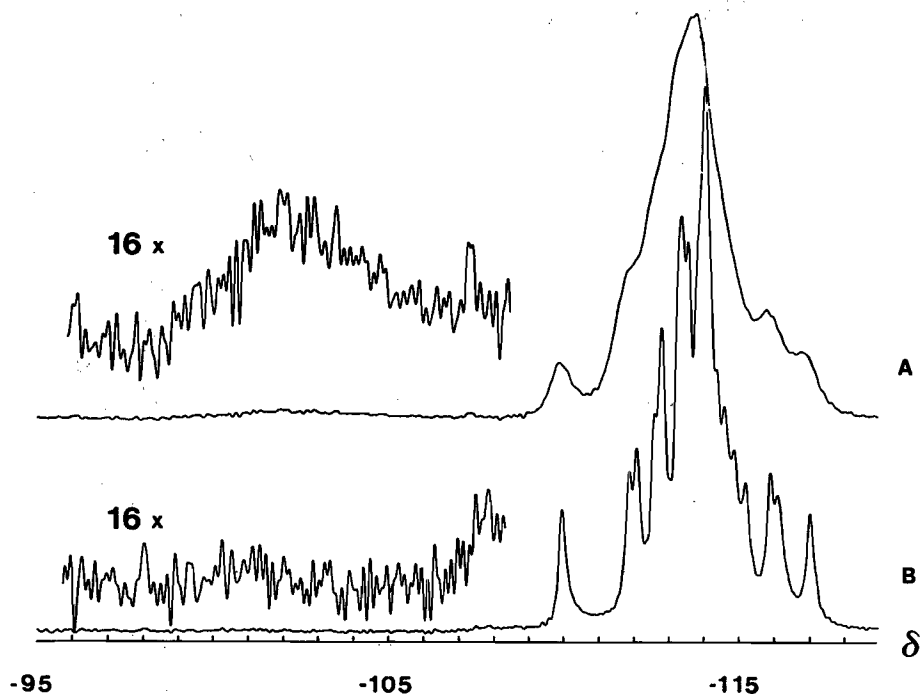
The ^{29}Si MAS NMR and IR spectra of material I before and after heat treatment are shown in Figs. II.11 and II.12. The improvement in spectral resolution after heat treatment can be ascribed to a decrease in structural elements present in the material[57,58]. Lattice defects, i.e. silanol groups, give extra contributions to the number of structural elements and cause a broadening of the spectra, while highly resolved spectra give evidence of highly ordered frameworks with low amounts of silanol groups.

The spectral features of sample I after different ion exchange and heat treatment procedures are shown in Tab. II.1. It seems that sodium ions and water are important factors influencing the process of lattice ordering. The presence of water is an absolute requirement as can be seen from sample 3. At high water vapour pressures, all samples

Fig. II.12: IR Spectra of ZSM–5 (material I).

(A) starting material;

(B) after heat treatment (68 hours at 823 K, $p(H_2O) \cong 2$ kPa).

wavenumber / cm^{-1}
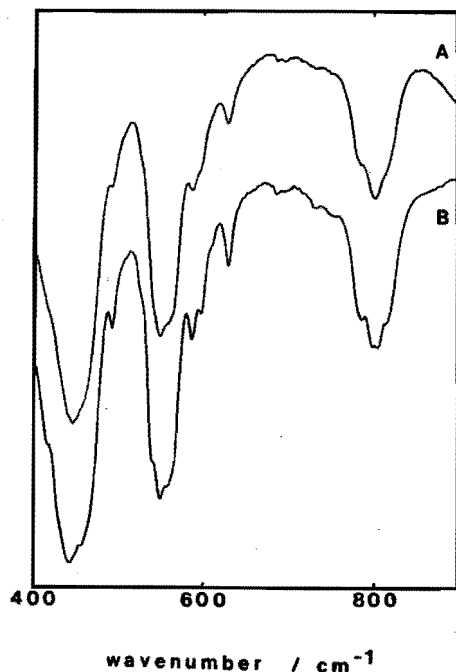
TABLE II.1: Spectral Features of ZSM–5 after Various Treatments.

Sample	Treatment[1]	Na [wt.%]	Spectral Features[2]
1	none, starting material I	0.86	broad
2	sample 1 + HT	0.86	highly resolved
3	sample 1 + DH	0.86	broad
4	sample 2 + HCl	0.10	highly resolved
5	sample 1 + HCl + HT	0.10	broad
6	sample 1 + HCl + ST	0.10	highly resolved
7	sample 1 + HCl + NaOH + HT	0.61	highly resolved
8	sample 1 + NH$_4$NO$_3$ +HT	0.03	broad
9	sample 1 + NH$_4$NO$_3$ + ST	0.03	highly resolved
0	sample 1 + NH$_4$NO$_3$ + NaOH + HT	0.55	highly resolved

[1] *HT = heat treatment (68 hours at 823 K, $p(H_2O) \cong 2$ kPa), DH = heating in dry air (68 hours at 823 K), ST = steam treatment (68 hours at 823 K, $p(H_2O) = 13.5$ kPa), HCl = threefold ion exchange with HCl solution, NaOH = threefold ion exchange with NaOH solution, NH$_4$NO$_3$ = threefold ion exchange with NH$_4$NO$_3$ solution;*

[2] *in ^{29}Si MAS NMR and/or IR spectra.*

did undergo a lattice improvement. But after application of low vapour pressures, only the samples containing considerable amounts of sodium ions gave highly resolved spectra, indicating that the alkaline ion can assist in the reactions occurring during heat treatment.

However, the terminal groups carrying sodium ions ($-Si-O^-Na^+$) cannot diminish since the formation of NaOH aggregates in an open silica structure and in the presence of water is very unlikely. The XPS results in Tab. II.2 clarify the question concerning the whereabouts of the sodium ions. After heat treatment, the sodium ions are enriched at the external surface of the zeolite crystals. Obviously, heat treatment causes rearrangement reactions which are accompanied by a migration of the lattice defects towards the external surface. Movement of point defects in zeolites has already been proposed by von Ballmoos who suggested a T–jump mechanism[56]. The scheme in Fig. II.13 is based on such a T–jump mechanism and illustrates how heat treatment in the presence of water can result in a decrease in T–atom vacancies and a surface enrichment of sodium ions. The favourable role of the alkaline ions may be explained by their high mobility as compared with the covalently bonded hydrogen in silanol groups. They can attack neighbouring siloxane bridges which are then more easily hydrolized. In the absence of sodium ions these consecutive hydration and dehydration reactions of Si–O–Si linkages take much more time or require higher concentrations of water.

There still remains the question concerning the origin of structural defects in ZSM–5.

TABLE II.2: Surface Enrichment of Sodium Ions as Measured by Means of XPS.

Sample	Treatment[1]	Intensity Na(1s)/ Intensity Si(2p)
1	none, starting material I	0.097
2	sample 1 + HT	0.132

[1] *HT = heat treatment (68 hours at 823 K, $p(H_2O) \simeq 2$ kPa).*

Fig. II.13: Migration of T−Atom Vacancies and Sodium Ions towards the External Surface
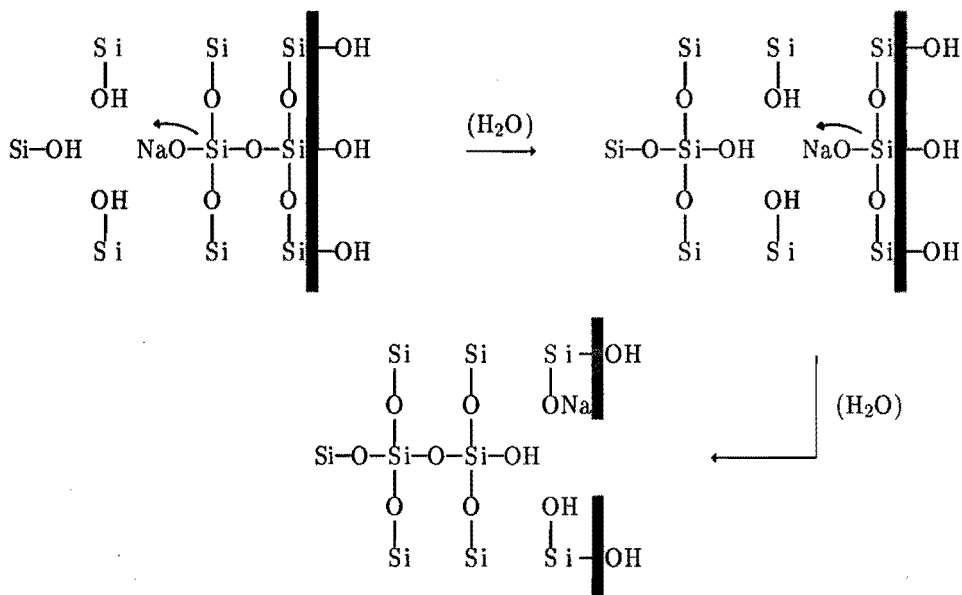
It was suggested that the occurrence of internal silanol groups is related to the type of template used for the preparation[43,52]. We recently prepared several batches of highly siliceous ZSM−5 using TPA$^+$ as template and obtained products with very low amounts of silanol groups and sodium ions. The applied synthesis procedure was exactly the same as for the preparation of material I, but a different silica source was used. An exemplary ^{29}Si MAS NMR spectrum of such a product (material II) is shown in Fig. II.14. Obviously, the template TPA$^+$ is not the reason for the presence of structural defects in some ZSM−5 samples. The difference between the silica sources used for the materials I and II mainly concerns the amount and type of impurities. It should be investigated whether the type of reagents and impurities such as aluminum or transition metal ions can affect the dissolution of silica or the mechanisms of nucleation and particle growth.

T−atom vacancies and other structural defects such as fault planes or twinning of crystals can be the result of subtle changes in the gel composition.

Fig. II.14: ^{29}Si *MAS NMR Spectrum of Material II after Removal of TPA*$^+$.
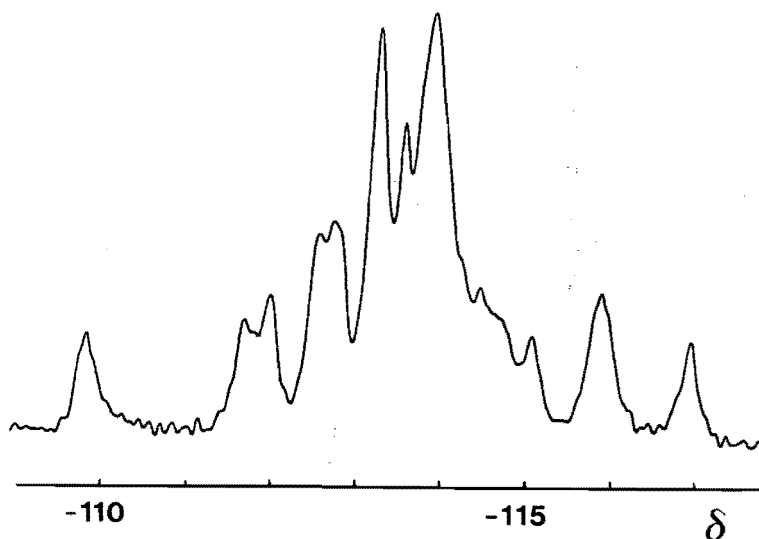
Conclusions

A decrease in the amount of T–atom vacancies and an ordering of the framework of ZSM–5 can be achieved by heat treatments in the presence of water vapour. A reaction scheme can be proposed based on a T–jump mechanism which accounts for the observed structural rearrangements, the favourable role of the sodium ions and their enrichment at the external surface of the zeolite crystals.

The amount of internal silanol groups can be increased by treatment with aqueous solutions of hydrochloric acid which results in hydrolysis of Si–O–Si linkages in the lattice. Highly ordered frameworks, i.e. with low amounts of T–atom vacancies, exhibit improved resistance towards hydrolysis.

There is no connection between the occurrence of T–atom vacancies and the use of TPA$^+$ ions as a template. The formation of structural defects is possibly dependent on the mechanism of crystallization which may be affected by impurities such as aluminum or transition metal cations.

36

II.4. EFFECT OF INTERNAL SILANOL GROUPS ON THE CATALYTIC PROPERTIES OF ZSM–5

Introduction

It is common experience that zeolites of the same type, having the same chemical composition and exhibiting similar morphologies, crystallinities and pore volumes can behave quite differently in catalytic reactions. The "microscopic" differences between those catalysts may concern the distribution of their acid sites which can be more or less homogeneous. However, internal terminal groups are expected to change the surface character, i.e. increase the polarity of the channels. A possible influence of these structural defects on the catalytic properties should therefore be considered.

In the following section, the catalytic cracking of n–hexane and n–butane over ZSM–5 containing different amounts of internal terminal groups will be described. The catalysts under investigation are all stemming from one batch in order to guarantee identical macroscopic features, while the amount of internal silanol groups was manipulated by heat treatment procedures. The presented results will demonstrate that structural defects can considerably affect the intrinsic activity of the catalysts and the rate of deactivation.

Experimental

The synthesis of ZSM–5 was performed with Aerosil 200 (Degussa) as a silica source according to method B described by Derouane et al.[45]. The recovered crystals were washed and dried before and after removal of the template (3 hours calcination at 823 K). The following chemical composition of the dry product was determined by means of chemical analysis: 96.44 wt.% SiO_2, 2.72 wt.% Al_2O_3, 0.72 wt.% Na_2O and 0.12 wt.% K_2O (Si/Al = 30.1 and (Na + K)/Al = 0.86).

Heat treatment as well as ion exchange with aqueous HCl solution has already been described in the previous section.

The temperature programmed desorption of ammonia (NH_3–TPD), as well as the catalytic experiments and the pore volume measurements were performed after in situ activation of the zeolites for about 1 h in a flow of dried and purified helium at 673 K. Instrumentation and procedures for n–butane sorption, NH_3–TPD and the standard n–hexane cracking test (T = 573 K, space velocity = 0.28 $(ks)^{-1}$) have been described in detail by Post[47]. These experiments were reproduced with the exception that the adsorption of ammonia prior to TPD was performed at 353 K and not at 343 K.

Cracking of n–butane was performed in a fixed–bed continuous flow reactor at 673 K. The n–butane (Union Carbide, type HP) was mixed with purified helium as a carrier gas in a volumetric ratio of 1/4 and was led through a catalyst bed of 500 mg zeolite with a space velocity of 0.5 $(ks)^{-1}$. On–line chromatographic analyses were performed every 1 ks of time on stream.

Results and Discussion

The amount of internal silanol groups in highly siliceous ZSM–5 can be decreased by prolonged heat treatment or steaming as has been shown in the previous section. In ZSM–5 with a Si/Al ratio of 30.1, the amount of silanol groups could be somewhat lower than in highly siliceous ZSM–5[40,41,43,51]. Moreover, steam treatments can cause removal of framework aluminum. On the other hand, dealumination by steam is known to occur in the hydrogen form of zeolites while alkaline ions inhibit such a process[60,61]. Therefore, the heat treatments required in order to reduce the amount of structural defects were performed with the starting material containing sodium and potassium ions. After heat treatment at low water vapour pressures, the catalytically active hydrogen form was obtained by ion exchange with hydrochloric acid. The corresponding NH_3–TPD spectra in Fig. II.15 confirm that no or only minor dealumination took place. The integral of the high–temperature peak at about 773 K corresponding to NH_3 sorbed at Brønsted hydroxyl groups remains about the same in all samples. In contrast, the low–temperature peak at about 473 K is decreased with increasing period of heat

38

Fig. II.15: NH₃−TPD Spectra of H−ZSM−5 (Si/Al = 30.1).
——————— = *no heat treatment;* −−−− = *1 day heat treatment;* ······ = *2 days heat treatment;* −·−·− = *3 days heat treatment; heat treatments were performed at 823 K and a water vapour pressure of about 2 kPa.*
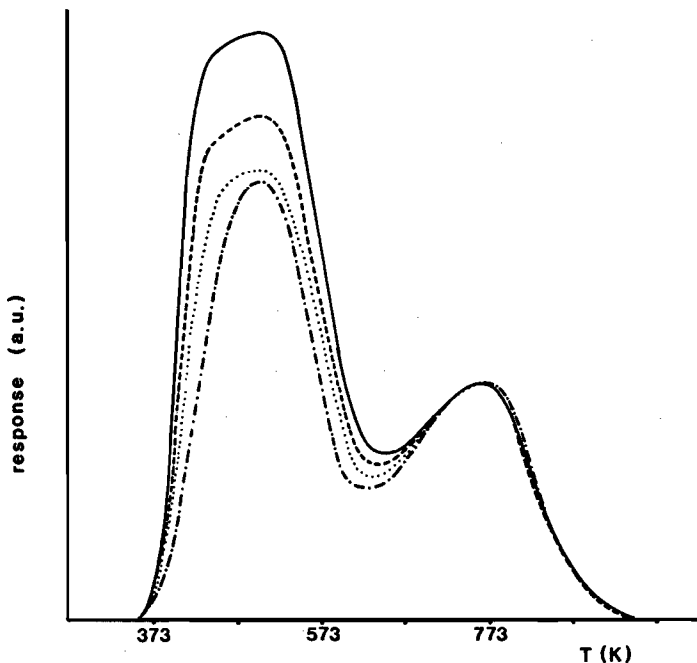
treatment. It stems from a minor part of physisorbed ammonia and a major part of chemisorbed ammonia at weak acidic sites such as external and internal silanol groups. Obviously, the amount of internal silanol groups in ZSM−5 containing aluminum can be manipulated in a similar way as in highly siliceous samples.

Table II.5 shows the relative amounts of ammonia desorbed from the various samples together with the pore volumes as measured by means of n−butane sorption. The differences in pore volumes are within the experimental error, and it can be concluded that the accessible void space does not change very much with the amount of internal silanol groups. Of course, a more bulky sorbate would be a more sensitive tool for subtle changes in pore volume.

TABLE II.3: Pore Volumes of ZSM-5 after Heat Treatments.

Sample	Heat Treatment[1]	Desorbed NH$_3$ [%]	Pore Volume [ml/g][2]
1	none	100	0.156
2	1 day	88	0.161
3	2 days	80	0.160
4	3 days	75	0.160

[1] *Heat treatments were performed at 823 K and a water vapour pressure of about 2 kPa;*
[2] *accuracy ± 0.2 ml/g.*

The conversion of n–hexane over the catalysts containing different amounts of internal silanol groups are shown in Fig. II.16. The differences in activity are quite remarkable: after 7 ks on stream, sample 4 is about 30 % more active than sample 1. Moreover, the rate of deactivation increases with increasing amount of internal silanol groups. It cannot be decided from the graphs in Fig. II. 16 whether the initial activities

Fig. II.16: Conversion of n–Hexane over H–ZSM–5 versus Time on Stream.

H–ZSM–5 catalysts: ——— = no heat treatment; – – – – = 1 day heat treatment;
······ = 2 days heat treatment; –·–·– = 3 days heat treatment; heat treatments were
performed at 823 K and a water vapour pressure of about 2 kPa.
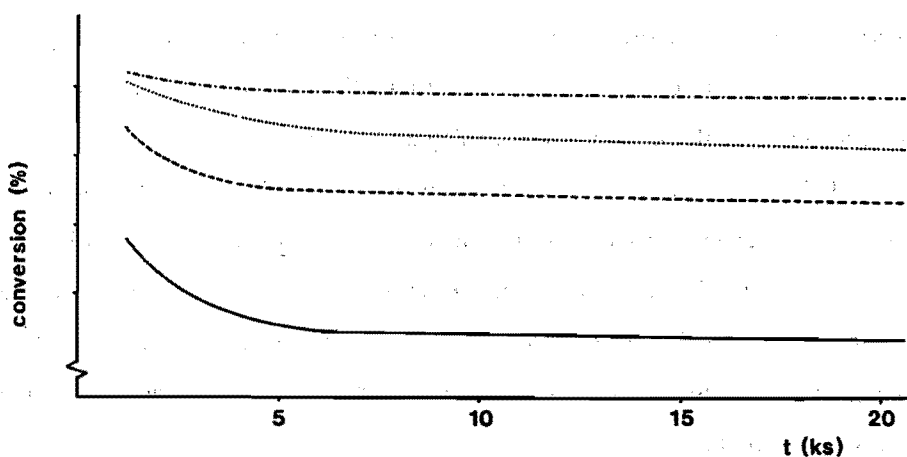
of the samples are the same or not. The first reliable analysis of the products can only be performed after about 1.2 ks on stream. During this time required for the stabilization of the feed, sample deactivation can already take place.

In contrast, cracking of n–butane yields small olefins (C_2 and C_3) which can hardly oligomerize at the applied reaction temperature of 673 K. Formation of coke and hence deactivation should be much less pronounced than in the conversion of n–hexane. The results obtained from the n–butane cracking experiments are depicted in Fig. II.17. The rates of deactivation are now rather low as was expected. The striking differences in activity can therefore not be ascribed to large differences in the extent of deactivation. Furthermore, the amount of Brønsted sites is about the same in all samples as was shown by means of NH$_3$–TPD. Of course, this technique is not a very sensitive tool for the measurement of the amount and strength of acid sites. But a loss of framework aluminum during heat treatment should result in a decrease in activity[62], and the

Fig. II.17: *Conversion of n–Butane over H–ZSM–5 versus Time on Stream.*

H–ZSM–5 catalysts: ——— *= no heat treatment;* – – – – *= 1 day heat treatment;* ...... *= 2 days heat treatment;* –·–·– *= 3 days heat treatment; heat treatments were performed at 823 K and a water vapour pressure of about 2 kPa.*

41
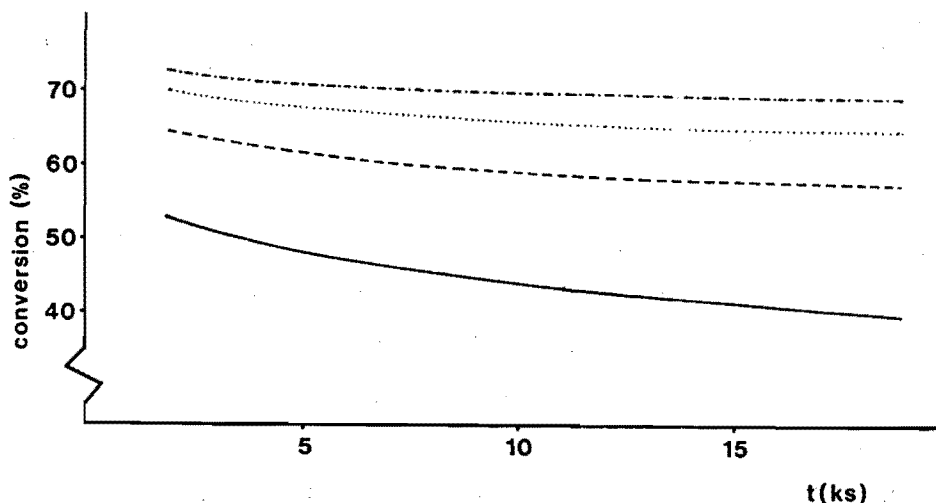
samples with the longest heat treatment (sample 4) should therefore be the least active. In fact, the inverse trend is observed. Our experiments show that the intrinsic activities of the zeolites increase with decreasing amount of internal silanol groups.

This remarkable effect may be interpreted in terms of changes in framework–sorbate interactions. Recently, Derouane postulated the concept of confinement effects which includes a formalism for the quantification of sorbate–framework interaction energies. In part I of this thesis, this novel concept has been introduced shortly. The sorption measurements showed that the void volume accessible for n–butane molecules is not affected by the presence of internal silanol groups. But the polarity of the surface and possibly also the surface curvature change which must have consequences for the interaction between the zeolite framework and the sorbate. Regrettably, the concept of confinement effect does not account for changes in the polarity, and the results presented here may indicate that this is a serious deficiency in Derouane's formalism.

However, the interaction between the frameworks of molecular sieves and sorbate molecules can be described qualitatively in terms of solvatation. From homogeneous systems it is known that the interaction between solvents and reagents, products and intermediates has a tremendous influence on the reaction pathway and the kinetics of the reaction. Evidence of remarkable interaction between the framework of highly siliceous ZSM–5 and sorbed molecules has recently been obtained by means of XRD and ^{29}Si MAS NMR measurements: even low amounts of sorbates in the channels cause a reversible perturbation of the zeolite lattice accompanied by a phase transition from monoclinic to orthorhombic framework symmetry[27,28]. On the other hand, ^{1}H NMR pulsed field gradient measurements and ^{13}C NMR studies on the sorbed molecules revealed increasing molecular mobilities of the sorbates in the channels with increasing amount of internal silanol groups[53]. The increase in sorbate mobility can be ascribed to a loss of framework–sorbate interaction. However, much more experimental data are required in order to describe the effect of structural defects on the solvatation of sorbates. This effect may change with the type of molecule and its coverage.

A further effect of internal silanol groups concerned the rate of deactivation. Structural defects obviously favour the formation of coke. As an explanation it can be considered that radical and/or charged coke precursors can be better stabilized at structural defects than at a rather homogeneous and apolar surface.

Conclusions

Internal silanol groups can considerably affect the catalytic properties of ZSM–5. The intrinsic activity in cracking of n–butane and n–hexane strongly decreases with increasing amount of internal silanol groups. This effect can be interpreted in terms of a decrease in framework–paraffin interaction. It should be the subject of further investigations in which way such an interaction can contribute to the activation of sorbed hydrocarbons. Caloric effects, i.e. high heats of sorption, can be considered as well as steric effects. Moreover, internal silanol groups were found to favour the formation of coke, possibly because of a stabilization of radical and/or charged precursors at polar terminal groups.

II.5. REFERENCES

1   G.T. Kerr and G.T. Kokotailo, J. Am. Chem. Soc. 83, 4675 (1961).
2   R.L. Wadlinger, G.T. Kerr and E.J. Rosinski, U.S. Patent 3.308.069 (1967).
3   R.J. Argauer and G.R. Landolt, U.S. Patent 3.702.868 (1972).
4   J.L. Casci, B.M. Lowenand T.V. Whittam, Eur. Pat. Appl. 0.042.225 (1981).
5   H. Hagiwara, Y. Kiyozumi, M. Kurita, T. Sato, H. Shimada, K. Suzuki, S. Shin, A. Nishijima and N. Todo, Chem Letters 1653 (1981).
6   H. Nakamoto and H. Takahashi, Chem. Letters 169 (1981).
7   T. Mole and J.A. Whiteside, J. catal. 75, 284 (1982).
8   E. Narita, K. Sato and T. Okabe, Chem. Letters 1055 (1984).
9   E.W. Valyocsik and L.D. Rollmann, Zeolites 5, 123 (1985).

10 E. Costa, M.A. Uguina, A. De Lucas and J. Blanes, J. Catal. 107, 317 (1987).

11 R.W. Grose and E.M. Flanigen, U.S. Patent 4.257.885 (1981).

12 E. Narita, K. Sato, N. Yatabe and T. Okabe, Ind. Eng. Chem. Prod. Res. Dev. 24, 507 (1985).

13 D.M. Bibby, N.B. Milestone and L.P. Aldridge, Nature 285, 30 (1980).

14 G.T. Kokotailo, S.L. Lawton, D.H. Olson and W.M. Meier, Nature 272, 437 (1978).

15 E.M. Flanigen, J.M. Bennett, R.W. Grose, J.P. Cohen, R.L. Patton and R.M. Kirchner, Nature 271, 512 (1978).

16 C.D. Chang and A.J. Silvestri, J. Catal. 47, 249 (1977).

17 N.Y. Chen, J. Phys. Chem. 80, 60 (1976).

18 D.H. Olson, W.O. Haag and R.M. Lago, J. Catal. 61, 390 (1980).

19 E.L. Wu, S.L. Lawton, D.H. Olson, A.C. Rohrman and G.T. Kokotailo, J. Phys. Chem. 83, 2777 (1979).

20 C.A. Fyfe, G.C. Gobbi, J. Klinowski, J.M. Thomas and S. Ramdas, Nature 296, 530 (1982).

21 J.M. Thomas, J. Klinowski and M.W. Anderson, Chem. Letters 1555 (1983).

22 C.A. Fyfe, G.C. Gobbi, W.J. Murphy, R.S. Ozubko and W.J. Slack, Chem. Letters 1547 (1983).

23 D.G. Hay and H. Jaeger, J. Chem. Soc., Chem. Commun. 1433 (1984).

24 D.G. Hay, H. Jaeger and G.W. West, J. Phys. Chem. 89, 1070 (1985).

25 C.A. Fyfe, G.J. Kennedy, G.T. Kokotailo, J.R. Lyerla and W.W. Fleming, J. Chem. Soc., Chem. Commun. 740 (1985).

26 J. Klinowski, T.A. Carpenter and L.F. Gladden, Zeolites 7, 73 (1987).

27 G.W. West, Aust. J. Chem. 37, 455 (1984).

28 C.A. Fyfe, G.J. Kennedy, C.T. De Schutter and G.T. Kokotailo, J. Chem. Soc., Chem. Commun. 541 (1984).

29 S.M. Csicsery, in "Zeolite Chemistry and Catalysis" (J.A. Rabo, Ed.), ACS, vol. 171, Washington 1976, p. 680.

30 N.Y. Chen and W.E. Garwood, J. Catal. 52, 453 (1978).

31 N.Y. Chen, R.L. Garring, H.R. Ireland and T.R. Stein, Oil Gas J. 75 (23), 165 (1977).

32 W.W. Kaeding, C.C. Chu, L.B. Young, B. Weinstein and S.A. Butter, J. Catal. 67, 159 (1981).

33 D.H. Olson and W.O. Haag, U.S. Patent 4.159.282 (1979).

34   W.O. Haag and T.J. Huang, U.S. Patent 4.157.338 (1979).

35   A.W. Chester and Y.F. Chu, U.S. Patent 4.283.584 (1981).

36   S.L. Meisel, J.P. McCullough, C.H. Lechthaler and P.B. Weisz, Chem. Tech. 6, 86 (1976).

37   C.W.R. Engelen, Thesis, Eindhoven University of Technology 1986, p. 46.

38   G. Boxhoorn, A.G.T.G. Kortbeek, G.R. Hays and N.C.M. Alma, Zeolites 4, 15 (1984).

39   S.G. Fegan and B.M. Lowe, J. Chem. Soc., Chem. Commun. 437 (1984).

40   A.W. Chester, Y.F. Chu, R.M. Dessau, G.T. Kerr and C.T. Kresge, J. Chem. Soc. Chem. Commun. 289 (1985).

41   G.L. Woolery, L.B. Alemany, R.M. Dessau and A.W. Chester, Zeolites 6, 14 (1986).

42   J.B. Nagy, Z. Gabelica and E.G. Derouane, Chem. Letters 1105 (1982).

43   R.M. Dessau, K.D. Schmitt, G.T. Kerr, G.L. Woolery and L.B. Alemany, J. Catal. 104, 484 (1987).

44   B. Kraushaar, L.J.M. van de Ven, J.W. de Haan and J.H.V. van Hooff, Stud. Surf. Sci. Catal., vol. 37, Elsevier Amsterdam 1988, p. 167.

45   E.G. Derouane, S. Detremmerie, Z. Gabelica and N. Blom, Appl. Catal. 1, 201 (1981).

46   C.C. Price and J.R. Sowa, J. Am. Chem. Soc. 32, 4126 (1967).

47   J.G. Post, Thesis, Eindhoven University of Technology 1984, p. 20.

48   G. Rutten, A. van de Ven, J.W. de Haan, L.J.M. van de Ven and J. Rijks, J. High Res., Chrom. Commun. 7, 607 (1984).

49   R.M. Dessau and G.T. Kerr, Zeolites 4, 315 (1984).

50   C.D. Chang, C.T.–W. Chu, J.N. Miale, R.F. Bridger and R.B. Calvert, J. Am. Chem. Soc. 106, 8143 (1984).

51   G.O. Brunner, Zeolites 7, 9 (1987).

52   M. Hunger, D. Freude, T. Fröhlich, H. Pfeifer and W. Schwieger, Zeolites 7, 108 (1987).

53   M. Hunger, J. Kärger, H. Pfeifer, J. Caro, B. Zibrowius, M. Bülow and R. Mostowicz, J. Chem. Soc., Faraday Trans. I, 83, 3459 (1987).

54   R.K. Harris, C.T.G. Knight and W.E. Hull, J. Am. Chem. Soc. 103, 1577 (1981).

55   B. Kraushaar, J.W. de Haan, L.J.M. van de Ven and J.H.C. van Hooff, Chem. Letters 1523 (1986).

56   R. von Ballmoos, "The ^{18}O–Exchange Method in Zeolite Chemistry: Synthesis, Characterization and Dealumination of High Silica Zeolites", Salle and Sauerländer, Frankfurt 1981.

57   R. von Ballmoos and W.M. Meier, J. Phys. Chem. 86, 2698 (1982).

58   J.M. Thomas and J. Klinowski, "Advances in Catalysis" (D.D. Eley et al., Eds.), vol. 33, Academic Press, London 1985, p. 200.

59   G.T. Kerr, J. Catal. 15, 200 (1969).

60   G. Engelhardt, U. Lohse, V. Patzelová, M. Mägi and E. Lippmaa, Zeolites 3, 233 (1983).

61   K. Suzuki, T. Sano, H. Shoji, T. Murakami, S. Ikai, S. Shin, H. Hagiwara and H. Takaya, Chem. Letters 1507 (1987).

62   D.H. Olson, W.O. Haag and R.M. Lago, J. Catal. 61, 390 (1980).

III. MODIFICATION OF ZSM-5: CHANGING FROM ACIDIC TO OXIDATION CATALYSIS

III.1. GENERAL INTRODUCTION

Modification of Acid Strength by Isomorphous Substitution of Trivalent Elements

Isomorphous substitution of other elements for silicon and aluminum in the frameworks of zeolites became a subject of great interest in zeolite chemistry[1]. Especially in the case of ZSM-5, much efforts were made in order to modify the strength of the acid Brønsted sites. The strong intrinsic acidity of [Al]ZSM-5 causes high protolytic activity, which is not required and/or desired in some catalytic reactions. Isomorphous substitution of trivalent elements for aluminum has therefore been investigated with the aim to combine the well documented shape selective properties of ZSM-5[2-6] with moderate acidity. Meanwhile, the hydrothermal syntheses of boron-, iron- and gallium-substituted ZSM-5 have been reported[7-14] and the incorporation of these elements into the framework could be established. The acidity of the Brønsted sites was found to increase in the order: H[B]ZSM-5 << H[Fe]ZSM-5 < H[Ga]ZSM-5 < H[Al]ZSM-5[15-19]. But it was also found that the thermal and hydrothermal stability of these derivatives is low as compared with [Al]ZSM-5. Ione et al. proposed that the probability of isomorphous substitution and hence the stability of a substituted element in the tetrahedral oxygen environment of the framework depends on the radius of the corresponding cation $r(El^{n+})$ relative to the radius of the oxygen ions $r(O^{2-})$. Unfavourable ratios $r(El^{n+})/r(O^{2-})$ can cause large distortions in the framework which restrict the amount of incorporated cations El^{n+} to a very low number or which make isomorphous substitution impossible[20].

47

Changing from Acidic to Oxidation Catalysis by Incorporation of Titanium Atoms

In 1983, Taramasso et al. awarded a patent on the hydrothermal preparation of the titanium containing derivative of high silica ZSM–5 which was denoted as titanium silicalite or TS–1[21]. Evidence of the incorporation of the titanium atoms into the framework of ZSM–5 was given by means of X–ray data. The mean Ti–O distance in tetrahedrally coordinated titanium(IV) compounds is known to be longer than the Si–O distance in high silica ZSM–5, and the expected regular increase in unit cell parameters with increasing titanium content could be observed. Moreover, it was found that the symmetry of the framework changes from monoclinic to orthorhombic upon incorporation of about one titanium atom per unit cell. In the case of [Al]ZSM–5 this change occurs at about 0.2 Al/unit cell. Remarkably, titanium silicalite containing more than 2.5 titanium atoms per unit cell was not yet reported. According to Ione et al., this may indicate distortion of the silica framework and low stability of tetrahedrally coordinated titanium atoms therein[20].

TABLE III.1: Oxidation Reactions Catalyzed by Titanium Silicalite.

Reactants[1]	Products	Product Selectivity	Conversion H_2O_2	References
$R-C_6H_5$	$R-C_6H_4-OH$	> 85 %	70–88 %	22
$R-C_6H_4-OH$	$R-C_6H_3(OH)_2$	> 87 %	70–88 %	22, 23
$R-CH=CH-R'$	$R-CH\overset{O}{-}CH-R'$	> 85 %	> 90 %	24, 25
$R-CH=CH-R' + CH_3OH$	$R-CH(OH)-C(OCH_3)-R'$	> 95 %	> 70 %	24
$R-CH=CH-CH=CH-R'$	$R-CH\overset{O}{-}CH-CH=CH-R'$	> 85 %	> 90 %	26
$R-CH_2OH$	$R-CHO$	> 90 %	60–95 %	27
$R-CHOH-R'$	$R-CO-R'$	> 90 %	90–96 %	27
⬡=O + NH_3	⬡=NOH	80 %	92 %	28

[1] *Oxidant in all reactions is hydrogen peroxide; methanol, tert. butanol, acetone or water are used as solvents.*

48

The incorporation of titanium as a tetravalent element does not induce any charge in the framework and therefore no Brønsted acidity can be generated. The novel titanium silicalite was rather reported to be an active catalyst in oxidation reactions involving hydrogen peroxide as an oxidant. Some of the oxidation reactions claimed to be catalyzed by TS–1 are listed in Tab. III.1.

A common feature of the listed reactions is that they can be carried out at rather mild conditions. Diluted aqueous solutions (40 wt.%) of hydrogen peroxide can be used, and most of the reactions take place at normal pressure and temperatures below 377 K. The tendency towards para selectivity in the hydroxylation of aromatic hydrocarbons has been reported[22,23], showing the similarity with the shape selective poperties of the isostructural [Al]ZSM–5 catalysts. The remarkable selectivities in the epoxidation of dienes and in the oxidation of primary alcohols, i.e. the absence of secondary oxidations, were explained with the high dispersion of active sites in TS–1 catalysts. The low number of incorporated titanium atoms, which were found to be homogeneously distributed throughout the crystals, enable isolation of the Ti atoms from each other by long sequences of SiO_4 tetrahedra[29,30].

Until now, however, very little is known about the nature of the active sites in TS–1 and the mechanisms of the catalytic oxidations. The presence of titanium(IV) in tetrahedral $(\equiv SiO)_4Ti$ units has been considered. On the other hand, an infrared absorption band at about 960 cm^{-1}, characteristic of titanium silicalite, gives indication of titanium atoms in trigonal titanyl groups $(\equiv SiO)_2Ti=O$[29,30]. Addition of hydrogen peroxide is assumed to result in the formation of a framework–immobilized peroxotitanate which can act as the actual oxidant in the conversions of organic compounds[30].

It is obvious that the characterization of TS–1 by means of X–ray diffraction and infrared spectroscopy is insufficient. The increase in unit cell volume is very small and can also be caused by incorporation of other elements than titanium or by sorbed molecules such as water. The origin of the infrared absorption band has not yet been

eludicated. The novel titanium silicalite is therefore a promising subject of spectroscopic and other physico–chemical studies. Moreover, the reactions listed in Tab. III.1 are of considerable scientific and industrial interest. In spite of the potential importance of titanium silicalite in the field of fine chemicals, the knowledge and the number of publications is, nearly 6 years after discovery, remarkably low. The main reason for this apparently low response most probably concerns the difficulties in reproducing the synthesis of TS–1 according to the patent procedure.

In the following part, two alternative routes for the preparation of titanium silicalite will be described. The first route concerns hydrothermal synthesis according to the patent procedure which is slightly modified. The other route comprises incorporation of titanium in an already synthesized ZSM–5, demonstrating how internal silanol groups can be used for the modification of zeolites. The preliminary results presented here will show that both methods can yield active and highly selective oxidation catalysts.

III.2.   HYDROTHERMAL SYNTHESIS OF TS–1

Introduction

Taramasso, Perego and Notari described two methods for the hydrothermal synthesis of TS–1[21]. Both recipees include the preparation of a gel containing silicon and titanium compounds, tetrapropylammonium hydroxide (TPAOH) and water, followed by crystallization under autogeneous pressure at about 450 K. The first method, example 1, starts from the tereaethanolates of silicon and titanium which are hydrolyzed prior to crystallization. In example 2, the gel precursor is prepared from colloidal silica and tetrapropylammonium peroxotitanate. Example 1 was reported to be more simple and effective[30], and the experiments described in this section are therefore essentially based on this procedure.

Starting point of the experiments performed was the proposal that hydrolysis of the

50

highly reactive tetraethyltitanate in the relatively stable silicate can cause precipitation of titania. The titanium consumed for the formation of the quite indissoluble titania is no longer available for incorporation into the framework. Moreover, the stability of titanium in the tetrahedral oxygen environment of the silica framework was assumed to be lower than the stability of aluminum in the corresponding [Al]ZSM−5 framework. The following results, indeed, will show that hydrolysis of the tetraethanolates is one of the most critical steps in the hydrothermal preparation of TS−1 and that incorporated titanium can easily be removed from the framework upon calcination.

Experimental

All samples have been synthesized from varying amounts of tetraethylsilicate (Selectipur, Merck), tetraethyltitanate (pro synthesis, Merck), tetrapropylammonium hydroxide (Aldrich, 1.0 M aqueous solution) and bidest water. The gel precursors were prepared in an atmosphere of nitrogen by mixing the silicon and titanium compounds followed by slow addition of TPAOH solution. After about 1 hour, the mixtures were slowly heated at 353 K and kept stirring at this temperature until all ethanol was removed. The mixtures were then diluted with water and transferred to a teflon−lined autoclave equipped with a stirrer. Crystallizations were performed at 448 K under autogeneous pressure. The recovered crystals were washed several times with hot water, filtered and dried. If not otherwise indicated, removal of TPAOH was performed by heating the samples with 5 K/min at 773 K and calcination for 6 h in a flow of dried air.

X−ray diffraction patterns of the dried samples were recorded in the presence of dehydrated zeolite A on a Philips PW 7200 spectrometer using Cu Kα radiation. The unit cell parameters were obtained by a least−squares fit to the interplanar spacings of 10 strong reflections. The infrared spectra were measured on a Hitachi 270−30 spectrometer using wafers of 0.6 mg sample in 200 mg KBr. The scanning electron micropraph was taken on a Cambridge Stereoscan 200 electron microscope.

Results and Discussion

It is well known from the literature that the titanium atoms in titanium(IV) compounds preferentially exhibit octahedral coordination. The tetrahedral compounds are known to be strong Lewis acids which can easily be hydrolyzed, forming octahedrally coordinated species with –OH– or –O– bridges[31]. The pure tetraethyltitanate, which is used for the synthesis of TS–1, consists of oligomers (see Fig. III.1) in which the titanium atoms are in a nearly octahedral coordination provided by threefold bridging μ_3–OC$_2$H$_5$ groups[31].

Fig. III.1: Tetraethyltitanate Oligomer.
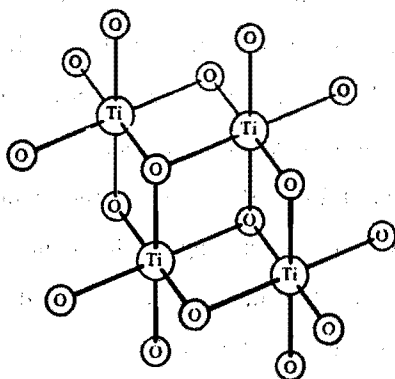
The first step in the preparation of TS–1 comprises dilution of tetraethyltitanate in tetraethylsilicate. Most probably, the oligomers of the titanate are then split into monomers, or they form mixed oligomers with the tetraethylsilicate molecules. However, subsequent hydrolysis of the mixed ethylates must provide formation of Si–O–Ti–O–Si sequences instead of Ti–O–Ti bondings. Titanium oxides are very stable compounds. Once formed, they probably do not dissolve again at the conditions of crystallization.

Some preliminary tests were performed in order to examine the behaviour of the ethanolates of silicon and titanium during addition of TPAOH solution. The results are

TABLE III.2: Hydrolysis of Tetraethyltitanate and −silicate.

Ethanolates[1]	Added TPAOH[2]	T [K]	Remarks
10 ml Ti(OEt)$_4$	1 ml	293	precipitation
10 ml Si(OEt)$_4$	1 ml	293	remains clear
29 ml Si(OEt)$_4$ + 1 ml Ti(OEt)$_4$	3 ml	293	precipitation
29 ml Si(OEt)$_4$ + 1 ml Ti(OEt)$_4$[3]	3 ml	273	remains clear
29 ml Si(OEt)$_4$ + 1 ml Ti(OEt)$_4$[4]	3 ml	273	slow precipitation

[1] *Ti(OEt)$_4$ = tetraethyltitanate, Si(OEt)$_4$ = tetraethylsilicate;*

[2] *dropwise addition of aqueous 1.0 M TPAOH solution;*

[3] *the ethanolates were mixed at room temperature and then cooled at 273 K;*

[4] *the ethanolates were mixed at 273 K.*

shown in Tab. III.2. As was expected, the titanium compound is much more sensitive towards hydrolysis than the corresponding silicon compound. The mixture of both ethanolates, however, responds very differently to the addition of aqueous TPAOH. At ambient temperature, the first drops of TPAOH solution already cause formation of a white precipitate which is assumed to be titania. In contrast, the mixture remains clear if the ethanolates are cooled at 273 K prior to addition of TPAOH. If the tetraethylsilicate and −titanate are already cooled during mixing with each other, precipitation upon addition of TPAOH is again observed. In the latter case it can be assumed that the oligomeric tetraethyltitanate does not dissolve readily in the silicate at low temperatures. Hydrolysis and subsequent condensation of these oligomeric titanium species, which already contain coordinative Ti−O→Ti bondings, can easily yield titania with stable Ti−O−Ti bondings. This is less probable if the tetraethyltitanate is monomeric or formes mixed oligomers with the corresponding silicate. A high dispersion of the teraethyltitanate molecules in the silicate can apparently be provided by carefully mixing the two compounds at ambient or elevated temperatures. Subsequent addition of

TPAOH solution should then be performed at low temperatures in order to retard the hydrolysis reaction and provide slow and controlled build–up of mixed silica–titania polymers.

In the following, samples of TS–1 will be denoted with P if the gel precursors have been prepared at ambient temperatures and contained precipitate. Samples with the designation C (for clear) have been prepared from clear, opalescent solutions obtained by addition of TPAOH at 273 K. Table III.3 shows the XRD results of some products yielded after different periods of crystallization. The crystallization of TS–1 at 448 K

TABLE III.3: XRD Results after Different Periods of Crystallization.

Gel composition: 1.0 $Si(OC_2H_5)_4$ · 0.025 $Ti(OC_2H_5)_4$ · 0.4 TPAOH · ≅ 80 H_2O; crystallization temperature: 448 K

Sample[1]	Time [d]	Crystallinity [%][2]	Symmetry[3]
P1	7	70 – 80	M
C1	7	70 – 80	M → O
P2	9	90 – 100	M → O
C2	9	90 – 100	O
P3	10	100	M → O
C3	10	100	O
P4	13	100	M → O
C4	13	100	O

[1] *P = gel precursor contained precipitate or C = clear gel precursor;*
[2] *as compared with highly siliceous ZSM–5;*
[3] *framework symmetry after removal of the template; M = monoclinic, O = orthorhombic, M → O = between M and O.*

takes at least 9 days which is a quite long period as compared with the crystallization of ZSM–5. The crystallinities of the corresponding P and C samples are almost the same, indicating that the presence of precipitate in the starting mixtures does not affect the rate of crystallization. However, the structures of the crystals obtained after removal of the template are slightly different with respect to their framework symmetry. The

54

highly crystalline C samples are all orthorhombic while the corresponding P samples are in a state inbetween monoclinic and orthorhombic framework symmetry. The monoclinic lattice symmetry is characteristic of highly siliceous ZSM–5. According to the literature, the change to orthorhombic symmetry is observed after incorporation of 1 mol–% titania which is equivalent to about 1 titanium atom per unit cell[21,29,30]. This means that the P samples contain less framework titanium than the C samples.

The IR spectra of the samples P4 and C4 in Fig. III.2 confirm this conclusion. The absorption band at about 960 cm^{-1}, which was reported to increase in intensity with increasing content of framework titanium[21,29,30], is obviously more pronounced in the spectrum of sample C4. The presented results agree with the initially proposed

Fig. III.2: Mid–infrared Spectra of Calcined Samples P4 and C4.
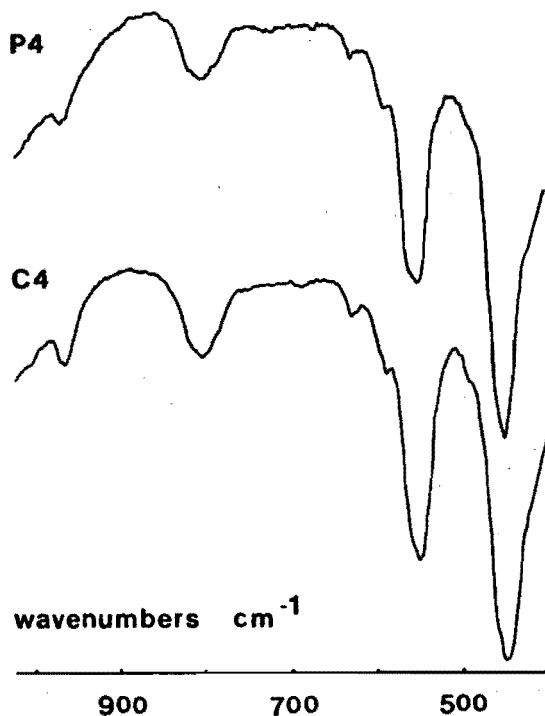
statement that titania particles, once formed upon careless mixing of the components, do not dissolve again, but rather remain as an impurity in the crystallization product.

Some syntheses of TS–1 have been performed with gels of different compositions in order to achieve incorporation of more titanium into the framework. The results are listed in Tab. III.4 and III.5.

TABLE III.4: Variation of the Titanium Concentration.

Gel composition: 1.0 Si$(OC_2H_5)_4$ · x Ti$(OC_2H_5)_4$ · 0.4 TPAOH · $\cong$ 80 H_2O; crystallization temperature: 448 K; crystallization time: 10 days.

Sample	x	Crystallinity [%]	Symmetry	Si/Ti (framework)[1]
C3	0.025	100	orthorhombic	80
C5	0.03	100	orthorhombic	75
C6	0.033	100	orthorhombic	75

[1] *Determined from the unit cell parameters according to ref. 21.*

TABLE III.5: Variation of the Template Concentration.

Gel composition: 1.0 Si$(OC_2H_5)_4$ · 0.033 Ti$(OC_2H_5)_4$ · x TPAOH · $\cong$ 80 H_2O; crystallization temperature: 448 K; crystallization time: 10 days.

Sample	x	Crystallinity [%]	Symmetry	Si/Ti (framework)[1]
C6	0.4	100	orthorhombic	75
C7	0.45	100	orthorhombic	50
C8	0.75	50	orthorhombic	about 50
C9	1	20	n.d.	n.d.

[1] *Determined from the unit cell parameters according to ref. 21; n.d. = not determined.*

It seems that the amount of titanium that can be incorporated increases with increasing template concentration. On the other hand, the high pH values resulting from high concentrations of TPAOH can prevent complete crystallization. A more detailed

56

interpretation of these preliminary experiments would be speculative. After all, sample C7 exhibits a relatively high amount of incorporated titanium. The highest titania content reported in the literature[21,29,30] is 2.5 mol–% which is equivalent to a Si/Ti ratio of 39, and sample C7 contains about 2 mol–%. A scanning electron micrograph is shown in Fig. III.3. The sample consists of single crystals which are 1 to 10 μm long and 0.1 to 5 μm across.

Fig. III.3: Scanning Electron Micrograph of Sample C7 (bar indicates 10 μm).
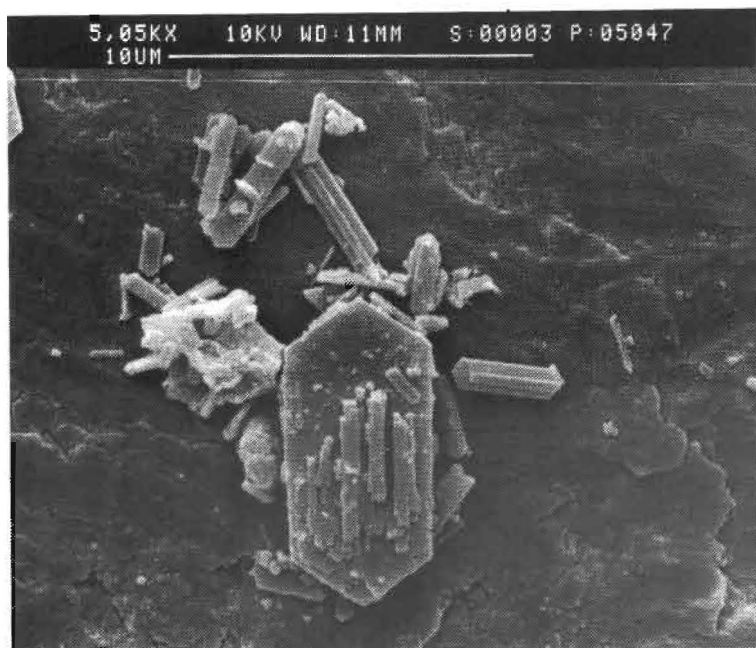
Finally, the conditions for the removal of the template from the channel system were examined. The infrared spectra depicted in Fig. III.4 have been obtained from TS–1 before and calcination. Strikingly, the frequency of the typical absorption band of TS–1 changes from 980 cm^{-1} to 960 cm^{-1} upon removal of TPAOH. Similar and reversible frequency shifts were observed upon ad– and desorption of polar sorbates such as
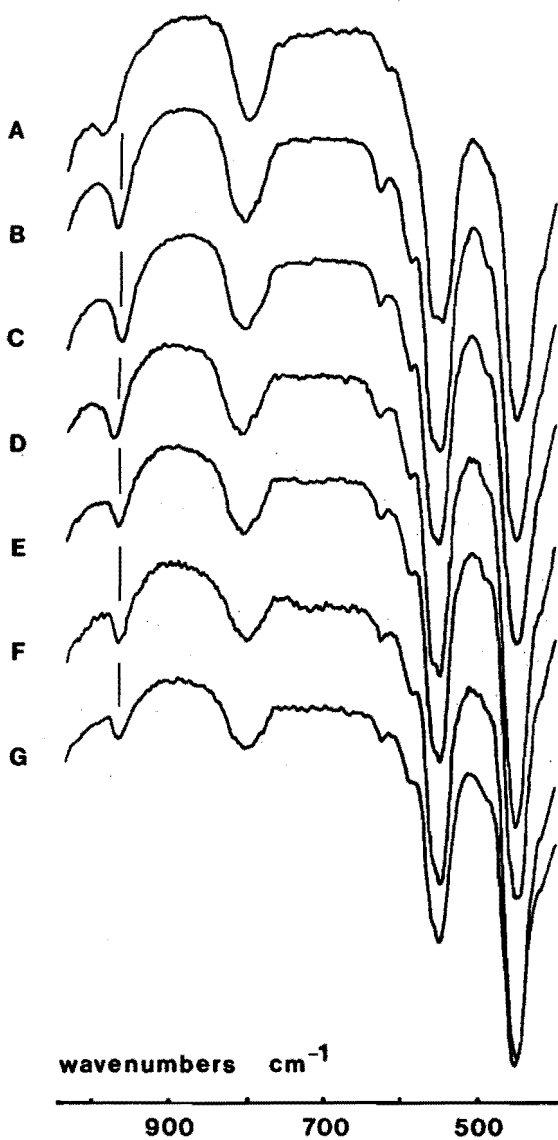
Fig. III.4: *Effect of the Calcination Conditions on the IR Spectra of TS-1.*

Infrared spectra of titanium silicalite before removal of TPAOH (A); after 3 hours calcination at 773 K in dried air (B) and in moist air (C); after 3 hours calcination at 823 K in dried air (D) and in moist air (E); after 3 hours calcination at 873 K in dried air (F) and in moist air (G).

methanol, ethanol, hexanol and acetone, while apolar sorbates such as pentane, hexane or cyclohexane did not cause any changes. Regrettably, these remarkable effects can not yet be interpreted since the coordination of the titanium atoms in as–synthesized as well as in calcined TS–1 is still unknown. However, the intensity of the absorption band at about 960 cm^{-1} was reported to be a measure for the estimation of the amount of incorporated titanium. The series of infrared spectra in Fig. III.4 show that the relative intensity of this band decreases with increasing calcination temperature. Moreover, the decrease is more pronounced if the calcinations are performed in usual laboratory air instead of dried air. The patent literature recommends 6 h calcination in air at 823 K[21]. Obviously, removal of TPAOH at these conditions would result in concomitant removal of titanium atoms from framework positions and formation of titania deposits in the channels. The low thermal and hydrothermal stability of framework titanium in TS–1 as has been documented here is in agreement with the considerations by Ione et al.[20].

Conclusions

One of the critical steps in the hydrothermal synthesis of titanium silicalite from the ethanolates of titanium and silicon is the hydrolysis of this compounds upon addition of the aqueous template solution. Titania can be formed if the hydrolysis proceeds too fast and if the tetraethyltitanate is not sufficiently dispersed in the silicate. Most probably, the titania present in the gel precursor does not dissolve again and is therefore not incorporated into the framework but rather remains as an impurity in the crystallization product. Nevertheless, the patent procedure for the synthesis of TS–1 is reproducible if the preparation of the gel precursor occurs at carefully controlled conditions.

A further critical step in the preparation concerns removal of the template TPAOH from the channels of TS–1 since the stability of the titanium atoms in the framework is low. Concerning this point, the patent clearly recommends unfavourable experimental conditions causing partial removal of titanium atoms from framework positions.

III.3.   PREPARATION OF TS–1 FROM ZEOLITE ZSM–5

Introduction

It has been shown in part II of this thesis that zeolite ZSM–5 can contain internal silanol groups which surround vacant T–atom positions in the framework. The reaction with trimethylchlorosilane was used in order to characterize these internal silanol groups since ^{29}Si MAS NMR analyses of the silylated derivatives can reveal information about their spatial arrangement and location in the framework.

At the same time, the study on structural defects in ZSM–5 lead to the conclusion that internal silanol groups can be considered as functional groups which enable modification reactions. Defective samples exhibiting T–atom vacancies should be particularly useful starting materials for the preparation of derivatives. Therefore, the reaction of highly siliceous ZSM–5 with titaniumtetrachloride has been examined. The results presented here will show that the products of this modification reaction have the same properties as hydrothermally prepared TS–1.

Experimental

Highly crystalline zeolite ZSM–5 with a Si/Al ratio of 50 was used as a starting material. The zeolite was three times treated with 1 N aqueous HCl solution (100 ml/g sample) at 353 K and subsequently washed and dried. Chemical analysis of the product revealed a Si/Al ratio of about 2000.

The reaction with titaniumtetrachloride (TiCl$_4$) was performed in a vertical quartz tube reactor of 3 cm diameter. Prior to the reaction, typically 2 g of sample were dried overnight at 723 K in a flow of purified and dried nitrogen. Then, nitrogen was saturated with TiCl$_4$ vapour at room temperature and passed through the quartz reactor (100 ml/min) at temperatures between 673 and 773 K. After two hours, the TiCl$_4$ supply was stopped, and the products were purged with pure nitrogen at 773 K overnight in order to remove excess chloride.

60

X–ray diffraction and infrared measurements have been explained in the previous section (III.2). The ^{29}Si MAS NMR experiments were already described in part II.2.

Results and Discussion

Dealumination of zeolites by means of acid leaching is a well known method. It is assumed that this reaction causes the formation of T–atom vacancies in the lattice which are surrounded by four silanol groups[32]. In dealuminated zeolite Y, these T–atom vacancies, also called hydroxyl nests, could be identified[33]. The studies described in part II of this thesis revealed that T–atom vacancies in the lattice of zeolite ZSM–5 can be present even if no dealumination was performed before. However, acid leaching of ZSM–5 containing about 2 Al/unit cell must result in the formation of additional T–atom vacancies. In principle, two potential lattice positions per unit cell can be provided for the incorporation of titanium atoms.

The results of the XRD analyses of ZSM–5 before and after reactions with TiCl$_4$ are listed in Tab. III.6. Upon acid leaching, the unit cell constants slightly decrease, and the framework undergoes a transition from orthorhombic to monoclinic symmetry. These changes are remarkable since shrinkage of the unit cell is typically a result of substitutions of Si–O bondings for the relatively longer Al–O bondings. In the present

TABLE III.6: Crystal Data of ZSM–5 and Modified Products.

	Sample	Framework Symmetry[1]	Unit Cell Parameters [nm]
1:	[Al]ZSM–5	O	a = 2.0131, b = 1.9922, c = 1.3410
2:	1 after acid leaching	M	a = 2.0110, b = 1.9890, c = 1.3386
3:	2 after reaction with TiCl$_4$ at 673 K	O	a = 2.0125, b = 1.9912, c = 1.3401
4:	2 after reaction with TiCl$_4$ at 773 K	O	a = 2.0127, b = 1.9916, c = 1.3407

[1] *O = orthorhombic, M = monoclinic.*

61

case, the decrease in unit cell constants upon acid extraction of aluminum may indicate some structural rearrangements in the framework, which were reported to be typical of ZSM–5 in aqueous acid medium[34]. Nevertheless, the unit cell parameters of the sample 2 are still larger than those of corresponding as–synthesized samples, showing that the structure is still defective[35]. Reaction of the dealuminated sample with $TiCl_4$ yields products with slightly expanded unit cells of orthorhombic symmetry. According to the literature, the lattice parameters of sample 4 can be related to the incorporation of about 1 titanium atom per unit cell[21,29,30].

The infrared spectra obtained from samples treated with $TiCl_4$ exhibit the typical absorption band at about 960 cm^{-1} which is absent in ZSM–5 (Fig. III.5). The increase in intensity of this band shows the same trend as the increase in unit cell parameters.

Fig. III.5: IR Spectra of Modified ZSM–5.

(A) sample 2 = ZSM–5 after dealumination;

(B) sample 3 = dealuminated ZSM–5 after subsequent reaction with $TiCl_4$ at 673 K;

(C) sample 4 = dealuminated ZSM–5 after subsequent reaction with $TiCl_4$ at 773 K.
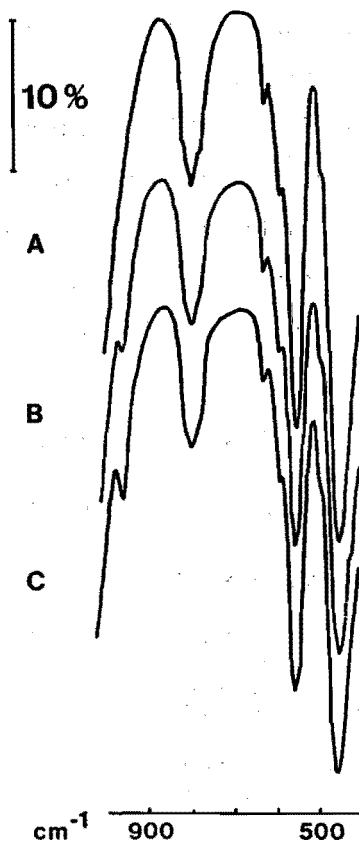
The ^{29}Si MAS NMR spectra of all samples, shown in Fig. III.6 exhibit a broad signal at -113 ppm due to Q^4 silicon atoms. Moreover, the starting material and the dealuminated sample contain Q^3 silicon atoms in Si(3Si, 1Al) or Si(3Si, 1OH) structural units which resonate at -106 ppm. In the samples treated with TiCl$_4$, the intensity of this signal is decreased. Instead, the spectrum of the relatively titanium–rich sample 4 exhibits a weak resonance at about -103 ppm, possibly due to Si(3Si, 1Ti) structural units, and a strong shoulder at about -115 ppm. According to the literature, the presence of the shoulder at -115 ppm is characteristic of TS–1[29], but an interpretation was not yet presented. This example again shows that, at least until now, the character-

Fig. III.6: ^{29}*Si MAS NMR Spectra of ZSM−5 and Modified Products.*

(A) sample 1 = [Al]ZSM−5;

(B) sample 2 = ZSM−5 after dealumination;

(C) sample 3 = dealuminated ZSM−5 after
    subsequent reaction with TiCl$_4$ at 673 K;

(D) sample 4 = dealuminated ZSM−5 after
    subsequent reaction with TiCl$_4$ at 773 K.
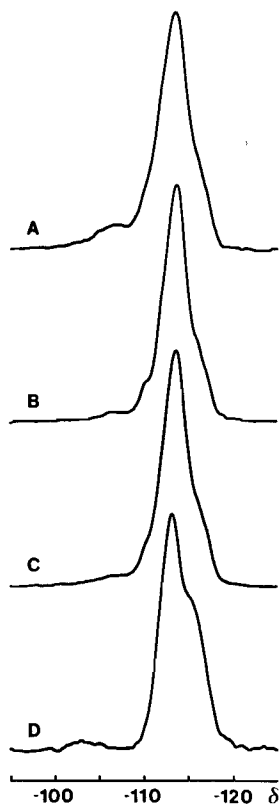
ization of titanium silicalite is reduced to the observation of some changes in the XRD, IR and ^{29}Si MAS NMR spectra, which are partly not yet understood. This is, of course, not satisfactory.

However, it can be claimed here that dealumination of ZSM–5 and subsequent reaction with $TiCl_4$ yields products which exhibit the same spectroscopic properties as the reported TS–1. The reaction of silanes with the internal silanol groups in ZSM–5 has been well documented. A similar reaction with the even more reactive $TiCl_4$ can therefore be assumed. At least, substitution of Ti for Al or Si in the framework can be excluded since $TiCl_4$ treatments with [Al]ZSM–5 or highly ordered silicalite did not have any effect. The number of incorporated Ti atoms is restricted to the number of T–atom vacancies in the lattice. Moreover, the extent of incorporation of titanium depends on the reaction temperature and, most probably, on the vapour pressure of $TiCl_4$ and the reaction time. However, it should be mentioned that, starting from sample 2, no higher titanium contents could be achieved even when more drastical reaction conditions were applied. It is possible that the number of T–atom vacancies generated by dealumination has been reduced by structural rearrangements which can occur during acid treatments or during subsequent drying and heating procedures.

Conclusions

The acid extraction of framework aluminum from zeolite ZSM–5 and the subsequent reaction with $TiCl_4$ vapour yield materials which exhibit the same spectroscopic features as TS–1. It is assumed that T–atom vacancies obtained by removal of aluminum can be refilled by titanium atoms. Similar modification reactions should, in principle, be possible with other zeolites. Therefore, the method described for the incorporation of titanium in microporous silica frameworks enables the preparation of new titanium silicalites while the hydrothermal method is still restricted to materials with the structure of ZSM–5.

64

III.4. CATALYTIC CHARACTERIZATION OF TITANIUM SILICALITES

Introduction

Previously, it was shown that the spectroscopic characterization of titanium silicalites by means of XRD, IR and ^{29}Si MAS NMR gives little more than indication of incorporation of titanium atoms into the lattice of high silica ZSM–5. However, a further indispensible characterization of titanium silicalites comprises a catalytic test since TS–1 was reported to exhibit remarkable catalytic properties in the oxidations of organic compounds involving hydrogen peroxide as an oxidant[22-28].

The catalytic behaviour of some differently prepared samples of TS–1 exhibiting similar spectroscopic features will be described in this section. It will be shown that the catalytic hydroxylation of phenol is a useful test reaction since the activities and selectivities of the catalysts involved depend strongly on the presence of small amounts of non–framework titania which is a typical impurity in hydrothermally prepared TS–1.

Experimental

The preparation of the TS–1 catalysts used in the catalytic oxidation of phenol has already been reported: Sample 1 has been obtained from dealuminated ZSM–5 by reaction with TiCl$_4$ and is identical with sample 4 described in part III.3. The catalysts 2 and 3 are identical with the samples C4 and P4 described in part III.2. Samples 4 and 5 are physical mixtures of 1 part titania with 99 parts of sample 2 or high silica ZSM–5 (Si/Al = 4000), respectively. The titania, obtained from tetraethyltitanate by precipitation in water and subsequent washing and drying, was found to be XRD–amorphous. The characterization by means of XRD, IR and ^{29}Si MAS NMR has already been described in the previous sections.

The catalytic oxidation of phenol with hydrogen peroxide was performed according to the patent literature, example 1[23], using a round–bottom flask equipped with condenser and stirrer as a reactor. Instead of acetone, the "UV–transparent" methanol was used as

a solvent. Typically, 1 g of catalyst was suspended in a solution of 20 g phenol in 15.6 g methanol. Heating of this mixture at about 353 K (refluxing) was followed by dropwise addition of 4 ml of aqueous hydrogen peroxide solution (36 %). Sampling was performed by taking about 1 ml of the hot reaction mixture, cooling rapidly at room temperature and diluting 250 μl of the cooled liquid in 25 ml methanol. The excess sample was immediately restored to the reaction mixture. The diluted samples were allowed to stand about 1 h in the dark in order to provide sedimentation of catalyst particles. The samples were then analyzed by means of high pressure liquid chromatography (HPLC) using a 100 mm polygosil 60–5C8 colomn and a UV detection system operating at a wavelength of 280 nm. Calibration experiments made sure that the integrated signals of the compounds phenol, hydroquinone, catechol and resorcinol increase linearly with increasing concentration in the range of interest. The consumption of hydrogen peroxide was measured by means of iodometric titration.

Results and Discussion

The spectroscopic features with respect to XRD, IR and ^{29}Si MAS NMR and hence the amounts of incorporated titanium were about the same in the samples 1,2,3 and 4, while non–framework titanium, as e.g. added to the samples 4 and 5, was not detectable. Nevertheless, the differences in catalytic behaviour of the samples were obvious and could already be observed without extensive product analyses (Tab. III.7): The reaction mixtures containing methanol, phenol and hydrogen peroxide remained yellow–orange in the presence of the samples 1 or 2, whereas the colour changed rapidly to deep brown if the samples 3, 4 or 5 were used as catalysts.

The analyses depicted in Fig. III.7 show that the samples 1 and 2 catalyze the conversion of phenol (left side) to hydroquinone and catechol (right side) with high selectivity. These two products were obtained in a molar ratio of 1, whereas resorcinol was not formed. The activities, however, were still 40–50 % lower than those reported in the literature[23]. According to Bellussi, this difference can be explained by the higher

66

TABLE III.7: *Differently Prepared Catalysts in the Conversion of Phenol.*

Sample	Preparation	Ti/u.c.[1]	Reaction Mixture[2]
1	from [Al]ZSM–5, see sample 4 in part III.3	1.1 – 1.3	yellow–orange
2	hydrothermal synthesis, see sample C4 in part III.2	1.1 – 1.3	yellow–orange
3	hydrothermal synthesis, see sample P4 in part III.2	0.9 – 1.2	brown
4	sample 2 + TiO_2	1.1 – 1.3	brown
5	high silica ZSM–5 + TiO_2	0	brown

[1] *Number of framework Ti atoms per unit cell as calculated from XRD data;*
[2] *methanol + phenol + H_2O_2 + catalyst at 353 K after 15 min reaction time.*

titanium content of the catalysts reported in the patent (2 Ti/u.c.) as compared with the titanium content of the present samples 1 and 2 (about 1 Ti/u.c.)[36].

In contrast, only traces of hydroquinone and catechol were yielded if the samples 3, 4 and 5 were used as catalysts. Moreover, the conversion of phenol was found to be lower, and the main part being was consumed for the formation of unidentified tar species.

The conversion of hydrogen peroxide could not be related quantitatively to the formation of products. Especially in the presence of the samples 4 and 5, the peroxide was decomposed rapidly, and evolution of a gas (probably oxygen) could be observed.

Considering the common features of the catalysts 3, 4 and 5 exhibiting low activities and selectivities in the oxidation of phenol, it becomes clear that the presence of impurities of titania must play a major role. Sample 4, for instance, has been prepared by mixing the highly selective catalyst 2 with a small amount of amorphous titania, indicating that impurities of titania can, in fact, dominate the catalytic behaviour. In sample 3, the titania was formed during preparation of the gel precursor. On the other hand, the highly selective catalyst 2 was obtained from the same compounds as sample 3, but precipitation of titania was prevented by carefully controlled hydrolysis of the tetraethanolates of titanium and silicon in the gel precursor.
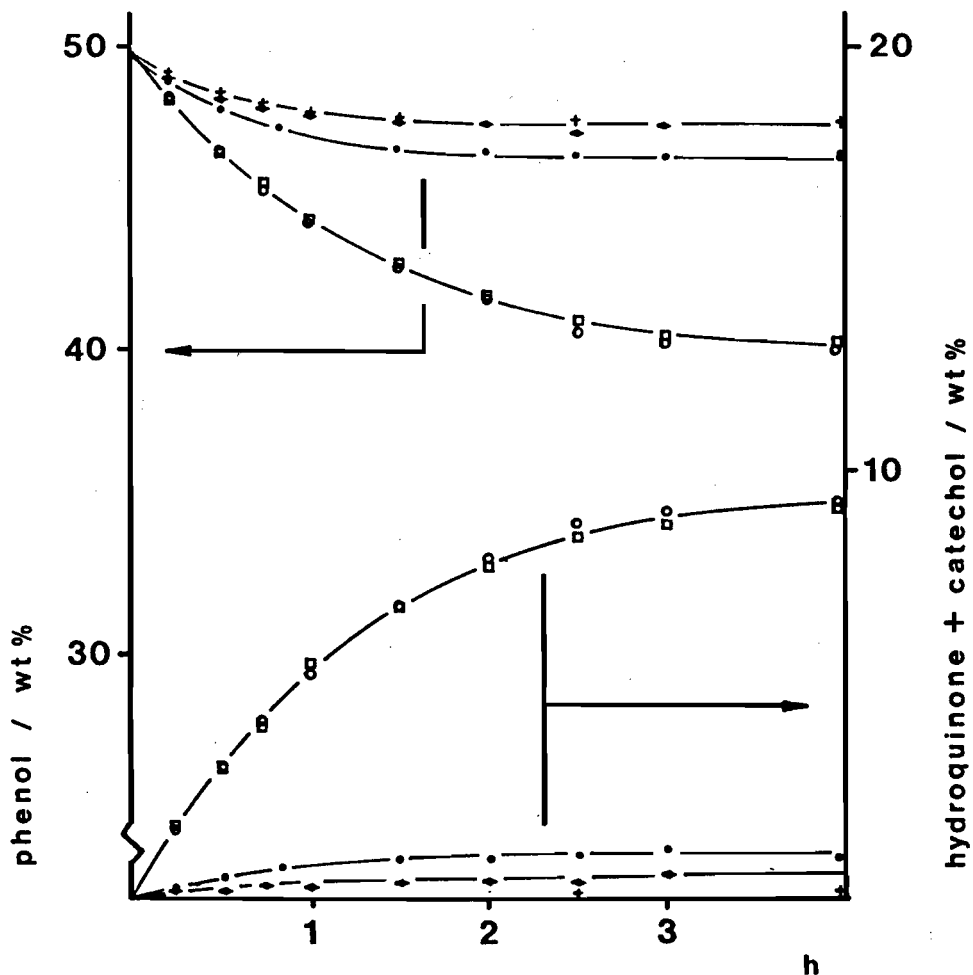
The most interesting result of the catalytic test reactions possibly concerns the performance of sample 1, which was prepared by modification of a ZSM–5 zeolite. Obviously, this sample behaves as a hydrothermally prepared titanium silicalite of high

purity. The incorporation of titanium atoms via reaction with titaniumtetrachloride is, of course, less relevant for the preparation of TS–1 which can also be synthesized directly. But titanium silicalites with other framework structures cannot yet be synthesized hydrothermally. In these cases, the modification route may be a promising alternative. Especially, the preparation of large–pore titanium silicalites, e.g. from zeolite beta, can be of importance for the catalytic oxidations of more bulky compounds which cannot be converted on the medium–pore TS–1.

Conclusions

The catalytic oxidation of phenol with hydrogen peroxide is an appropriate test reaction for titanium silicalites and a necessary completion to conventional spectroscopic characterization. Impurities of titania considerably affect the activities and the selectivities of the catalysts and can therefore be detected. Impure catalysts favour the rapid decomposition of the oxidant hydrogen peroxide and the conversion of phenol into brown tar species, while titania–free samples catalyze selectively the formation of hydroquinone and catechol. In the absence of non–framework titania, the activity in phenol conversion may be a measure for the number of incorporated (framework) titanium atoms.

Highly active and selective TS–1 can be obtained by direct hydrothermal synthesis as well as by modification of already synthesized ZSM–5. The modification of zeolites may be an important route for the preparation of novel titanium silicalites, e.g. with large pores, that can not yet be synthesized directly.

III.5. REFERENCES

1   M. Tielen, M. Geelen and P.A. Jacobs, Acta Phys. Chem. 31, 1 (1985).
2   N.Y. Chen and W.E. Garwood, J. Catal. 52, 453 (1978).
3   N.Y. Chen, R.L. Garring, H.R. Ireland and T.R. Stein, Oil Gas J. 75 (23), 165 (1977).

4   D.H. Olson and W.O. Haag, U.S. Patent 4.159.282 (1979).

5   W.O. Haag and T.J. Huang, U.S. Patent 4.157.338 (1979).

6   S.L. Meisel, J.P. McCullough, C.H. Lechthaler and P.B. Weisz, Chem. Tech. 6, 86 (1976).

7   M.R. Klotz, Belgian Patent 859.656 (1978).

8   M. Taramasso, G. Manara, V. Fattore and B. Notari, French Patent 2.429.182 (1979).

9   M. Taramasso, G. Perego and B. Notari, in "Proc. 5th Int. Conf. on Zeolites, Naples, 1980" (L.V.C. Rees, Ed.), Heyden London 1980, p.40.

10   L. Marosi, J. Stabenow and M. Schwarzmann, German Patent 2.909.929 (1980).

11   H.W. Kouwenhoven and W.H.J. Stork, U.S. Patent 4.208.305 (1984).

12   M.A.M. Boersma, J.M. Janne and M.F.M. Post, U.S. Patent 4.337.176 (1982).

13   W.J. Ball, K.W. Palmer and D.G. Stewart, U.S. Patent 4.346.021 (1982).

14   A.W. Chester and Y.F. Chu, U.S. Patent 4.350.835 (1982).

15   K.F.M.G.J. Scholle, A.P.M. Kentgens, W.S. Veeman, P. Frenken and G.P.M. van der Velden, J. Phys. Chem. 88, 5 (1984).

16   C. T.–W. Chu and C.D. Chang, J. Phys. Chem. 89, 1569 (1985).

17   G. Coudurier, A. Auroux, J.C. Vedrine, R.D. Farlee, L. Abrams and R.D. Shannon, J. Catal. 108, 1 (1987).

18   R. Szostak, V. Nair and T.L. Thomas, J. Chem. Soc., Faraday Trans. I, 83, 487 (1987).

19   D.K. Simmons, R. Szostak, P.K. Agrawal and T.L. Thomas, J. Catal. 106, 287 (1987).

20   K.G. Ione, L.A. Vostrikova and V.M. Mastikhin, J. Mol. Catal. 31, 355 (1985).

21   M. Taramasso, G. Perego and B. Notari, U.S. Patent 4.410.501 (1983).

22   A. Esposito, M. Taramasso, C. Neri and F. Buonomo, U.K. Patent 2.116.974 (1985).

23   A. Esposito, C. Neri and F. Buonomo, German Patent 3.309.669 (1983).

24   C. Neri, B. Anfossi and F. Buonomo, Eur. Pat. Appl. 100.118 (1984).

25   C. Neri, A. Esposito, B. Anfossi and F. Buonomo, Eur. Pat. Appl. 100.119 (1984).

26   F. Maspero and U. Romano, Pat. Pend.

70

27   A. Esposito, C. Neri and F. Buonomo, Eur. Pat. Appl. 102.655 (1984).

28   P. Roffia, M. Padovan, E. Moretti and G. De Alberti, Eur. Pat. Appl. 208.311 (1987).

29   G. Perego, G. Belussi, C. Corno, M. Taramasso, F. Buonomo and A. Esposito, in "Proc. 7th Int. Conf. on Zeolites, Tokyo, 1986" (Y. Murakami et al., Eds.), Elsevier Tokyo 1986, p. 129.

30   B. Notari, Stud. Surf. Sci. Catal., vol. 37, Elsevier Amsterdam 1988, p. 413.

31   Gmelin Handbuch der Anorganischen Chemie, vol. 40, Springer–Verlag, Berlin 1977.

32   D.W. Breck, "Zeolite Molecular Sieves", John Wiley & Sons, New York 1974, p. 95.

33   B. Kraushaar, J.W. de Haan, L.J.M. van de Ven and J.H.C. van Hooff, Z. anorg. allg. Chem. 564, 72 (1988).

34   R. von Ballmoos, "The ^{18}O–Exchange Method in Zeolite Chemistry: Synthesis, Characterization and Dealumination of High Silica Zeolites", Salle und Sauerländer, Frankfurt 1981.

35   E.L. Wu, S.L. Lawton, D.H. Olson, A.C. Rohrman and G.T. Kokotailo, J. Phys. Chem, 83, 2777 (1979).

36   G. Bellussi, personal communication.

IV.1.   GENERAL INTRODUCTION

Basic Features of Zeolite Y

Zeolite Y is a synthetic aluminosilicate that is structurally equivalent to the natural faujasite. The hydrothermal synthesis of zeolite Y has been described by Breck in 1964[1] and involves preparation of a gel from silica sol, alumina, sodium hydroxide and water. In general, zeolite Y requires excess silica and sodium hydroxide which remain in the crystallization mother liquor. The reaction mixture is first aged for about 24 h and then heated at the crystallization temperature which is typically 373 K. Zeolite Y exhibits Si/Al ratios between 1.5 and 3, and attempts to synthesize zeolite Y with higher ratios have not been successful.

The framework of zeolite Y can be described in a very convenient and illustrative way by using Smith's topological concept (see part I of this thesis). The truncated octahedron, also called sodalite cage or β–cage, can be considered as a building unit. The truncated octahedra are arranged in a tetrahedral diamond–type array, joined to each other through double 6–rings or hexagonal prisms. The crystallographically equivalent T–atom positions are occupied by Si or Al atoms which are randomly distributed throughout the framework with the restriction of the Löwenstein rule.

It can be seen from Fig. IV.1 that the faujasite structure provides a large– and a small–pore system. The former comprises the spherical large cavities, also called supercages or α–cages, which are accessible via the 12–ring windows of about 0.72 nm diameter, enabling sorption of organic molecules such as gas–oil components. The small–pore system is provided by the internal voids of the truncated octahedra and

hexagonal prisms and can be entered via 6–rings of about 0.25 nm diameter. It is generally inaccessible to organic molecules but permits sorption of water or ammonia, and can be involved in cation sieving. The positions of cations in zeolite Y are strongly dependent on the valency of the ions and on the amount of adsorbed water. A detailed description of the positions of different cations in faujasites has been given by Breck[2].

Fig. IV.1: Model of the Faujasite Framework.
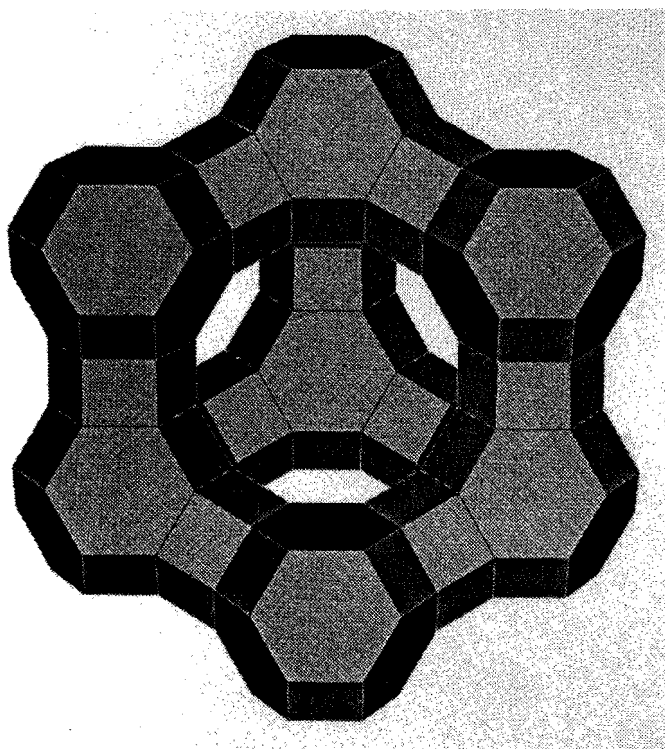
Zeolite Y as Fluid Cracking Catalyst

In the early 1960s, zeolites and particularly the synthetic faujasites were introduced as cracking catalysts. It was found that the rare earth–exchanged zeolite X, a synthetic faujasite having a Si/Al ratio between 1 and 1.5, exhibits 100 times higher activity combined with high selectivity and reduced sensitivity to coke as compared with

conventional silica–alumina cracking catalysts[3-6]. Incorporating these zeolites in a matrix of silica, silica–alumina or clay produces a catalyst in which the relatively small amount of zeolite (3–25%) dominates the catalytic behaviour while the matrix provides excellent mechanical strength[6-9]. The yields in Tab. IV.1 from pioneering work of Plank and Rosinski[9] are representative, showing the superior selectivity of zeolites over pure silica–alumina. At the expense of dry gas, C_4's and coke, the faujasite favours the cleavage of higher hydrocarbons to the C_5 to C_{12} range.

TABLE IV.1: Selectivity Advantage of REHX over Silica–Alumina

| | Δ Advantage over Silica–Alumina[1] | |
	REHX	10% REHX in Matrix[2]
C_{5+} Gasoline [vol%]	+ 7.1	+ 5.9
C_4 [vol%]	− 3.5	− 1.3
Dry Gas [wt%]	− 2.1	− 1.5
Coke [wt%]	− 2.1	− 2.2

[1] *At same conversion level, fixed bed cracking, mid–continent gas–oil;*
[2] *REHX = rare earth and hydrogen exchanged zeolite X; matrix = silica–alumina.*

As the zeolite development progressed, the Y zeolite having a higher Si/Al ratio than the X zeolite was found to be more active, selective and particularly more stable[10]. The thermal and hydrothermal stability, which is of great importance for the FCC (fluid catalytic cracking) processing, as well as the resistance against acids depends on the composition of the zeolite and increases with increasing framework Si/Al ratio[11]. As a consequence, rare earth–exchanged zeolite Y (REY) displaced the REX catalyst in FCC processes. But even the REY suffers from irreversible deactivation due to partial damage of the framework during carbon burnoff in commercial regenerators[12-14]. The process occurring in a regenerator is, in fact, a hydrothermal treatment at elevated

temperature. Under controlled conditions, hydrothermal treatment can achieve removal of some framework aluminum without loss of crystallinity. Such a hydrothermal dealumination has first been described by McDaniel and Maher[15]. The procedure was called "ultrastabilization" since the product, the so–called ultrastable Y or USY, exhibits superior thermal and hydrothermal stability[11,15]. However, in spite of the great thermal resistance, the commercial importance of USY as compared with REY was quite poor because of its relatively low activity and high manufactoring costs.

Meanwhile, the pollution by exhaust gases of cars and the increasing common awareness of environmental problems caused demand of a lower gasoline lead level. Renouncing the addition of tetra–ethyl lead to gasoline requires a FCC octane enhancement which can be achieved operationally and catalytically. In contrast to NH_4Y and REY, dealuminated zeolites are, in general, high octane catalysts and this is the reason why USY again attracts special attention today.

Octane Enhancement by Dealuminated Zeolite Y

The chemistry of catalytic cracking has been described in detailed reviews by Poutsma[16] and by Venuto and Habib[17]. Only a summary of the most important reaction steps will be given here.

It is generally accepted that cracking over silica–alumina, zeolites or other acidic materials proceeds via the same mechanistic pathways involving carbenium ions. Different possibilities for the initiation of the catalytic cracking process can be considered. A trace amount of highly reactive olefin in the feed might yield a carbenium ion upon protonation by the Brønsted site of the catalyst, thereby setting up the reaction chain. Another possibility is the abstraction of a hydride ion from a paraffin molecule after attack of a proton, resulting in the formation of a carbenium ion and H_2 gas. A further initiation route involves the protonation of a paraffin and the formation of a pentacoordinated carbonium ion that subsequently decomposes into a smaller paraffin and a carbenium ion.

Once formed, a carbenium ion can undergo β–scission which is, in fact, splitting of C–C bonds with generation of smaller olefin molecules. Isomerization is an other important carbenium ion reaction involving 1,2–shifts of hydride or alkyl groups. Propagation of the cracking process via chain transfer is provided by hydride transfer reactions which are also responsible for the hydrogen redistribution typically observed with zeolites. Termination of the cracking process is achieved by deprotonation and subsequent desorption of the olefin.

The superior activities of zeolites as compared with amorphous catalysts can be explained by the higher site density, the higher concentration of reactants inside the micropores and an additional polarization and hence activation due to the presence of electrostatic fields in the pores.

Fig. IV.2: *Comparison of Gasoline Compositions Yielded from Zeolitic and Amorphous Cracking*

(A) = California virgin gas–oil, (B) = California coker gas–oil, (C) = Gachsaran virgin gas–oil; left bars reflect zeolitic, right bars reflect amorphous cracking; from ref. (18).

$P = Paraffins$

$O = Olefins$

$N = Naphthenes$

$A = Aromatics$
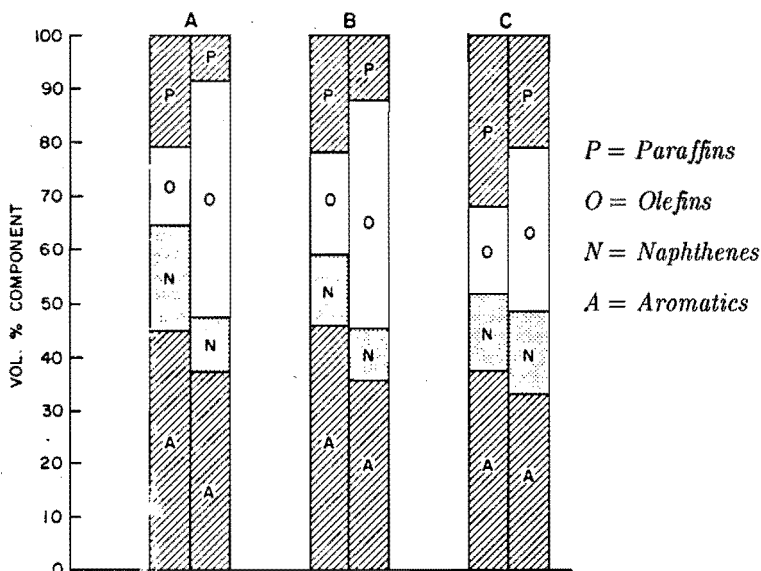
The high selectivity of zeolites for the gasoline cracking fraction has already been demonstrated with the data in Tab. IV.1. But within this fraction, there is also remarkable difference in the product distribution (Fig. IV.2): Zeolite catalysts yield more paraffins (P) and aromatics (A) at the expense of olefins (O) as compared with silica–alumina. The widely accepted explanation for these differences in product distribution is the higher rate of hydrogen transfer reactions in zeolites. As is shown in the following scheme, the hydrogen transfer is a bimolecular reaction wich is favoured over β–scission at high hydrocarbon concentrations.

$$R(1)^+ \left\{ \begin{array}{l} \xrightarrow[k_H]{R(2)H} R(1)H + R(2)^+ \\ \\ \xrightarrow[k_\beta]{} olefin + R(3)^+ \end{array} \right.$$

$$\frac{(Hydride\ Transfer)}{(\beta-Scission)} = \frac{(k_H)}{(k_\beta)} \cdot [R(2)H]$$
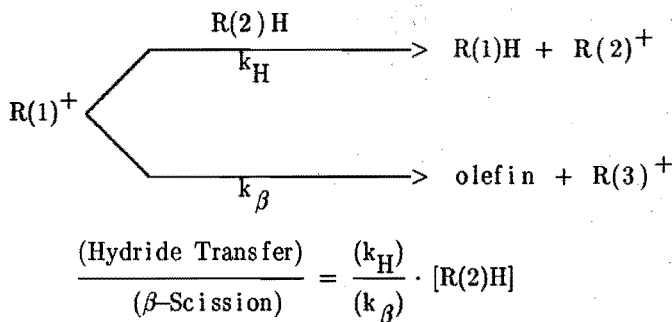
In contrast to amorphous catalysts, microporous zeolites sorb and concentrate hydrocarbons in the pores close to the active sites[16]. Therefore, hydrogen transfer is much more pronounced on zeolites than on silica–alumina. Less splitting of C–C bonds and more chain transfer reactions yield less dry gas and more gasoline. In the gasoline fraction, olefins and particularly tertiary olefins are the most reactive components. They are easily protonated and can act as hydride acceptors. The reactions listed in Fig. IV.3 show how olefins are converted to paraffins, aromatics and naphthenes by means of hydrogen transfer reactions. Olefins exhibit a lower octane number than aromatics and a higher octane number than n–paraffins and naphthenes. However, the high consumption of olefin molecules causes a strong decrease in octane number that can not be

77

Fig. IV.3: Olefins as Acceptors in Hydrogen Transfer Reactions.

3 Olefins   +   Naphthene   ⟶   3 Paraffins   +   Aromatic

4 Olefins   ⟶   3 Paraffins   +   Aromatic

3 Cyclo—Olefins   ⟶   2 Naphthenes + Aromatic
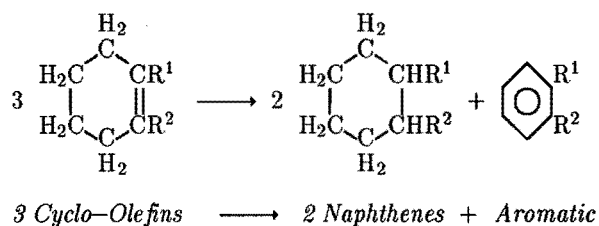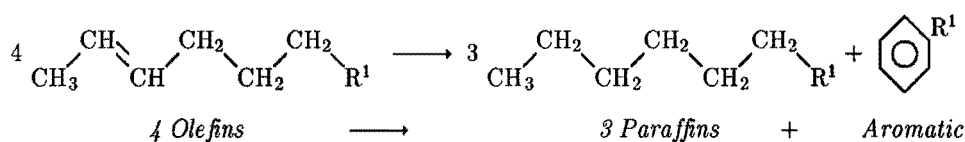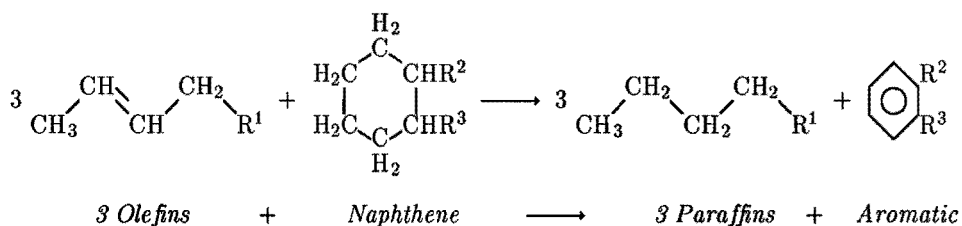
compensated by the formation of aromatics. Hydrogen transfer therefore decreases the overall octane number.

It has already been mentioned before that zeolites are highly active in hydrogen transfer reactions because the reactants can be concentrated in the micropores. Moreover, there is a quantitative relationship between hydrogen transfer and the site density in the zeolite[19,20], suggesting that this bimolecular reaction requires two sites close to each other. These neighbouring sites are not necessarily two Brønsted hydroxyl groups. The hydrogen transfer activity even reaches a maximum if any next nearest neighbour of a Brønsted site is neutralized by a sodium ion[19]. Possibly, the hydride donor must be polarized and hence activated by sorption at a negatively charged

framework site (AlO$_4$ tetrahedron) close to the sorbed carbenium ion. However, hydrogen transfer activity is not decreased by ion exchange with metal ions. The alternative possibility comprises the reduction of sites by dealumination, which has the additional advantage of improving the stability of the zeolite[11,15,17].

As a first approximation, one might expect that the reduction of active sites also results in a decrease in catalytic activity. But the framework electronegativity and hence the partial charges of the hydrogens in Brønsted sites increase with increasing framework Si/Al ratios (see part I). The more isolated sites therefore exhibit a higher acidity and activity which can compensate to some extent for the decrease in the amount of sites[22,23]. However, the increase in acid site strength with increasing framework Si/Al ratio is still a point of discussion. According to Haag et al.[24] the maximum strength of acid sites in zeolite ZSM–5 is reached at Si/Al = 20. For other zeolites such as faujasites this value is supposed to be lower[22,25-27]. At a certain degree of dealumination, however, the activity will drop. The decrease in yield caused by overcracking and loss of activity must be compensated by the improvement of product quality due to octane enhancement of the C$_{5+}$ fraction. Preparation of zeolites with the optimum acid site density that provides a good balance between the positive and negative effects is therefore of great commercial importance.

But the situation is even more complicated because more things are changed in a dealuminated zeolite apart from the acid site density: non–framework aluminum, structural defects and inhomogeneous distributions of the remaining framework aluminum can also influence the activities and selectivities of dealuminated zeolites. The following arbitrary examples will illustrate this: Beyerlein and coworkers found, for instance, that the balance between framework and non–framework aluminum affects the catalytic behaviour of hydrothermally dealuminated zeolite Y. At an optimum ratio of these two aluminum species ($Al_{NF}/Al_F \simeq 0.4$) the acidity was found to be strongly enhanced[28]. Other authors stress the fact that the coke selectivity and hence the activity of dealuminated Y depends on the amount and location of non–framework aluminum

species[29-31]. Acid site gradients throughout the zeolite crystals can be the result of inhomogeneous dealumination and were also found to affect the activities and selectivities of the catalysts[32].

It is obvious that apart from changes in the amount and strength of acid sites, dealuminations can have a lot of other effects, and some of them will be discussed in more detail in part IV.3 of this thesis. It should be emphasized here, that the compositional and structural changes in the zeolite are dependent on the dealumination procedure and conditions. Refined characterization of dealuminated zeolites is required in order to find correlations between the dealumination conditions, physico–chemical properties and catalytic behaviour. The increasing amount of publications on the characterization of dealuminated zeolites as well as the following sections of this thesis account for the importance of this subject.

IV.2.   PROCEDURES FOR THE DEALUMINATION OF ZEOLITE Y

Introduction

Zeolite Y possesses one of the most open structures, and any aluminum atom in the framework is, in fact, an accessible surface atom. The Al–O–Si linkages can easily be attacked by protons, water molecules or other sorbed reagents.

Proton attack can result in opening of these linkages even at room temperature, and therefore dealumination can be achieved by treatment with aqueous acid solutions. Certain zeolite structures such as clinoptilolite, mordenite, erionite and zeolite L can stand severe acid leaching without gross structural collapse[11,33-35]. But the faujasite is rather sensitive towards acids. This is the reason why the hydrogen forms of the former zeolites can be prepared by ion exchange with acid solutions while HY can only be obtained by careful calcination of NH_4Y[2]. Lee and Rees found that dealumination and concommitant loss of crystallinity begins at pH < 2.3[36]. Framework aluminum can also

80

be removed by chelating agents such as EDTA[37,38].

The most prominent and industrially applied dealumination procedure comprises hydrolysis of Al—O—Si bondings at elevated temperatures and is called hydrothermal treatment. Hereby, the ammonium or hydrogen form of the zeolite is treated with steam at temperatures above 773 K. The first who reported this dealumination reaction were McDaniel and Maher[15]. Meanwhile, numerous variations of this reaction have been published, e.g. dealumination under self—steaming conditions by "deep—bed" calcination[39] or exposure to a flow of steam in a fixed—bed tube reactor[40]. Hydrothermal treatments remove tetrahedral aluminum from the framework but not from the zeolite channels or cages. The total Si/Al ratio remains therefore constant while the framework Si/Al ratio is increased. The combinations of hydrothermal dealuminations with EDTA—treatments[41] or acid leaching[42,43] usually enable the increase in framework as well as total Si/Al ratios.

Dealuminations with volatile halides, usually chlorides, have been introduced recently. These reactions yield zeolites with relatively low contents of non—framework aluminum because the framework aluminum is converted to halides which are volatile as well. Beyer and Belenykaja reported the reaction with silicontetrachloride vapour which comprises not only dealumination but also silicon—enrichment of the zeolite since the silicon provided by the chloride is incorporated into the framework[44,45]. Reactions with other halides such as phosgene only result in removal of aluminum[46].

Substitution of framework aluminum by silicon can also be achieved by treatments with aqueous solutions of ammonium hexafluorosilicate. But the amount of aluminum removed from the zeolite is proposed to exceed the silicon uptake because some framework Al can be extracted by hydrofluoric acid evolved during the course of the reaction[47]. A number of dealumination reactions are listed in Tab. IV.2. It is obvious that the type of reaction determines whether and to which extent the removal of framework aluminum is accompanied by an increase in total Si/Al ratio. It must be assumed that dealuminated zeolites can, in principle, contain non—framework aluminum.

TABLE IV.2: Reactions for the Dealumination of Zeolite Y.

Reactant	Reference	Total Si/Al	Non–framework Al[1]
HCl	36	increases	(charge compensating) cations
EDTA	37, 38	increases	(charge compensating) cations
Steam	11, 15, 39, 40	not affected	hydroxide/oxide
Steam + EDTA	41	increases	hydroxide/oxide + cations
Steam + HCl	43	increases	hydroxide/oxide + cations
$SiCl_4$	44, 45	increases	Al_2Cl_6 and/or $NaAlCl_4$
$COCl_2$	46	increases	Al_2Cl_6 and/or $NaAlCl_4$
$(NH_4)_2SiF_6$	47	increases	$(NH_4)_2AlF_5$ and/or AlF_3

[1] *Formed upon dealumination and may remain in the channels and cages.*

In this section, the two most prominent dealumination reactions, the hydrothermal treatment and the reaction with $SiCl_4$, will be described in more detail. Due to the probable differences in total and framework Si/Al ratios of the products these values have been determined separately. Total Si/Al ratios are usually measured by means of wet–chemical analyses in combination with atomic adsorption spectroscopy. For the determination of framework Si/Al ratios, several spectroscopic techniques have been developed during the last years. These techniques and their reliability will be discussed in detail in part IV.4. For the present, it should be noted that an exact determination of the amount of framework Al in dealuminated zeolites is very difficult. As far as framework compositions are concerned, the quantitative results presented in this part are therefore objectionable and should be considered as a first approximation. However, the technique applied here, namely measurement of the mid–infrared absorption frequencies, is widely accepted as a tool for the determination of framework aluminum.

Experimental

Faujasite NaY (Akzochemie, Ketjen Catalysts) exhibiting 56 aluminum atoms per unit cell (56 Al/u.c.) was used as starting material. The ammonium form of this material was prepared by fivefold ion exchange with 1.5 M aqueous solution of NH_4NO_3

at room temperature, using about 50 ml solution per gram zeolite. In the final product, 85 % of the sodium ions were exchanged by ammonium ions.

The hydrothermal dealuminations were performed with 2 g of the ammonium form of zeolite Y placed in a vertical quartz tube reactor of 3 cm diameter. The water vapour was generated by passing a flow of dried air through a saturator filled with distilled water. In the stream of air with water vapour (150 ml/min), the zeolite was heated with a rate of 5 K/min and kept at the final temperature for various periods. During cooling, the samples were purged with dry air.

Acid leaching of the samples was performed by threefold exposure to 0.01 M HCl (about 20 ml aqueous solution per gram zeolite) for 0.5 h at room temperature.

Usually, the sodium form of zeolite Y was used for the reaction with $SiCl_4$ vapour. 2 g of zeolite were placed in a vertical quartz tube reactor and were carefully dried in two steps (5 h at 393 K and about 10 h at 723 K) in a flow of dried nitrogen. At the desired reaction temperature, the zeolite was exposed to a flow of nitrogen (100 ml/min) saturated with $SiCl_4$ vapour at 273 K. After completion of the reaction, the products were flushed in pure nitrogen at 723 K overnight in order to remove $AlCl_3$ and excess $SiCl_4$. The zeolites were cooled down and washed several times with water (about 100 ml per gram zeolite) until no more chloride ions were detectable in the washing liquor. A couple of samples were not washed with water but were treated with refluxing tetrachloromethane which is known to be a good solvent for Al_2Cl_6. Subsequently, these samples were filtered and dried in a stream of nitrogen at 393 K overnight.

The total Si/Al ratios have been determined by means of wet—chemical analyses and atomic absorption spectroscopy (AAS). The framework ratios were measured by means of IR spectroscopy. The spectra were obtained on a Hitachi 270—30 spectrometer, using wafers of 0.6 mg sample in 200 mg KBr. Among the different empirical correlationships between absorption frequencies and the amount of framework Al in zeolite Y, the correlationships proposed by Flanigen et al. were preferred, using the frequencies of the so—called symmetric and asymmetric O—T—O stretching bands for the calculations[48].

The scanning electron micrograph of the starting material was obtained on a Cambridge Stereoscan 200 electron microscope. The crystallinities of the samples have been checked by means of X—ray diffraction on a Philips PW 7200 spectrometer.

XPS measurements were recorded on a AEI ES 200 spectrometer equipped with a Mg anode (1254 eV). Samples were deposited on an iridium holder and evacuated at room temperature until a pressure of $0.8 \cdot 10^{-7}$ Pa was reached. The Si/Al ratios were calculated from the areas of Si(2p) and Al(2p) peaks using photo—ionization cross sections reported by Scofield[49].

Results and Discussion

The scanning electron micrograph in Fig. IV.4 shows that the samle of zeolite Y consists of intergrowths of octahedral crystals with a size of about 1 μm. The XRD patterns of this sample as well as products of the reaction with $SiCl_4$ revealed excellent

Fig. IV.4: Scanning Electron Micrograph of NaY (Bar indicates 10 μm).
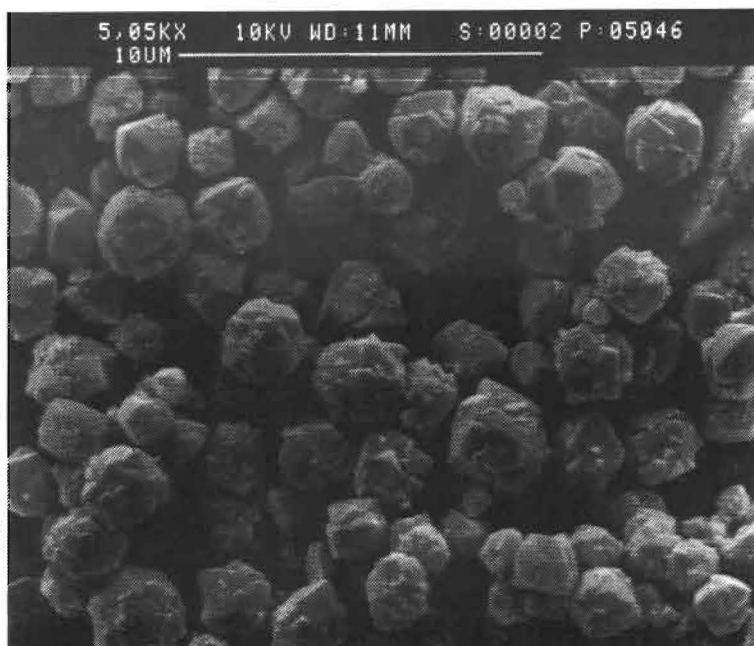
crystallinities. Only in the diffraction patterns of hydrothermally dealuminated zeolites, a slight decrease in intensities was observed.

The changes in framework aluminum content during various hydrothermal dealumination reactions are shown in Fig. IV.5. The initial rates of these reactions differ considerably and increase with increasing temperature and water vapour pressure. But after long times on stream, all reactions proceed to almost the same level at which about 68 % of the framework aluminum has been removed. There, the dealumination reactions seem to stop. It is well known from the literature that the maximum amount of removable Al atoms corresponds to the amount of charge compensating ammonium ions or protons[2,15,50,51]. In the present case, 85 % of the sodium ions were exchanged for ammonium ions, but only 68 % of the framework Al could be removed.

Fig. IV.5: Dealumination by Hydrothermal Treatment.
Number of framework aluminum atoms as measured by means of IR versus reaction time.

$\square : T = 923\ K$ and $p(H_2O) = 20\ kPa$
$\times : T = 973\ K$ and $p(H_2O) = 26.6\ kPa$
$\odot : T = 1023\ K$ and $p(H_2O) = 20\ kPa$
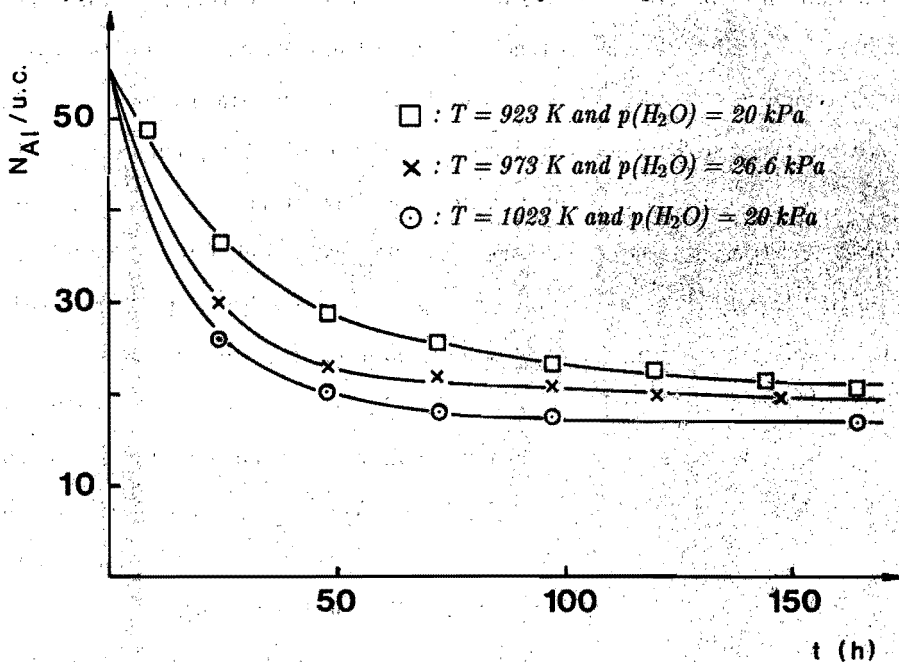
As a reason for this discrepancy it can be assumed that removal and reincorporation of Al are competing reactions in a hypothetical equilibrium. At high concentrations of non–framework Al, the reincorporation reaction may become as fast as the removal reaction, and dealumination apparently stops. However, changes in the reaction parameters temperature and vapour pressure should result in a shift of the equilibrium amounts of framework and non–framework Al. But in the present case, the final degrees of dealumination do not differ very much although the reaction temperature is varied over a range of 100 K. Kinetic constraints are not probable either, since water molecules are small enough to reach any framework Al atom even when the pores are partly blocked by non–framework species.

However, it was already mentioned that the quantitative determination of framework Al by means of IR is problematic. Flanigen et al. found that the absorption bands of some lattice vibrations shift towards higher frequencies with increasing framework Si/Al ratios or decreasing content of framework Al, respectively, and the shifts were ascribed to the differences in force constants of Si–O–Al bondings as compared with Si–O–Si bondings[48]. Actually, there are still no profound calculations on zeolite lattice dynamics which account for the influence of framework Al on the spectral features, and a linear correlation between the amount of framework Al and the absorption frequency is not obvious. Nevertheless, it is widely accepted that substitution of the weaker Si–O–Al bondings by stronger Si–O–Si bondings causes the observed high–frequency shifts. This means that IR may be a sensitive tool for the amount of Si substituting for removed Al.

In hydrothermal dealumination reactions, however, the only silicon source is the zeolite framework itself, and it is obvious that the formation of new Si–O–Si bondings due to substitution by silicon from the framework cannot compensate for the removal of Al. Therefore, the measured values for framework Al as depicted in Fig. IV.5 are higher than the real values. It is possible that the real final level of framework Al is close to the theoretical maximum value of about 9 Al/u.c. (85 % dealumination).

In Fig. IV.6 it is shown how the dealumination can proceed if steaming is interrupted

86

Fig. IV.6: Effect of Acid Leaching on the Course of the Steaming Reaction.

Number of framework aluminum atoms as measured by means of IR versus reaction time; bifurcations indicate interruptions of the steaming reactions (T = 1023 K and p(H₂O) = 20 kPa) in order to perform acid leachings.

$\odot$: no acid leaching;

$\square$: 1 x acid leaching (after 24 h);

$\times$: 2 x acid leaching (after 24 h and 48 h).
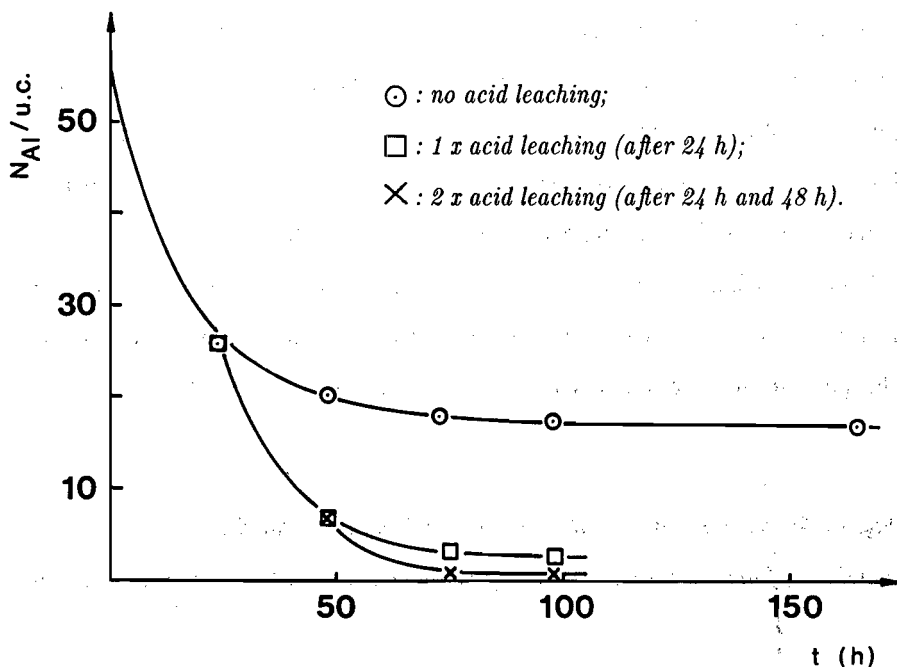
TABLE IV.3: Chemical Compositions of Hydrothermally Dealuminated Y before and after Acid Leaching

Sample	F[1] Al/u.c.	NF[2] Al/u.c.	NF[2] Al/u.c.	Extracted NF[2] Al [%]
	before acid leaching		after acid leaching	
1	30	26	17	36
2	26	30	20	35
3	21	35	31	11
4	18	38	36	4

[1] F = framework Al, as determined by means of infrared spectroscopy;

[2] NF = non–framework Al, obtained by substraction of framework Al from total amount Al as measured by wet–chemical analyses.

by acid leaching. The acid is partly consumed for the exchange of residual sodium ions, enabling further hydrothermal removal of Al from the framework. The data in Tab. IV.3 show that another part of the acid is consumed for the dissolution of non–framework Al species. It seems that the solubility of these species in hydrochloric acid decreases with increasing steaming periods, giving evidence of concentration of non–framework Al and formation of a stable phase. According to Shannon et al., the non–framework Al forms boehmite–like clusters in the supercages of the zeolite[52]. But also concentration on the external surface of the zeolite crystals could be established[53,54]. However, the decrease in solubility makes it difficult to prepare a "clean" sample without deposits of non–framework Al species. Acid solutions of higher concentrations must be applied for this purpose with the consequence that framework Al is extracted at the same time.

Fig. IV.7: Dealumination by Reaction with Silicontetrachloride.
Number of framework Al atoms as measured by means of IR versus reaction time.
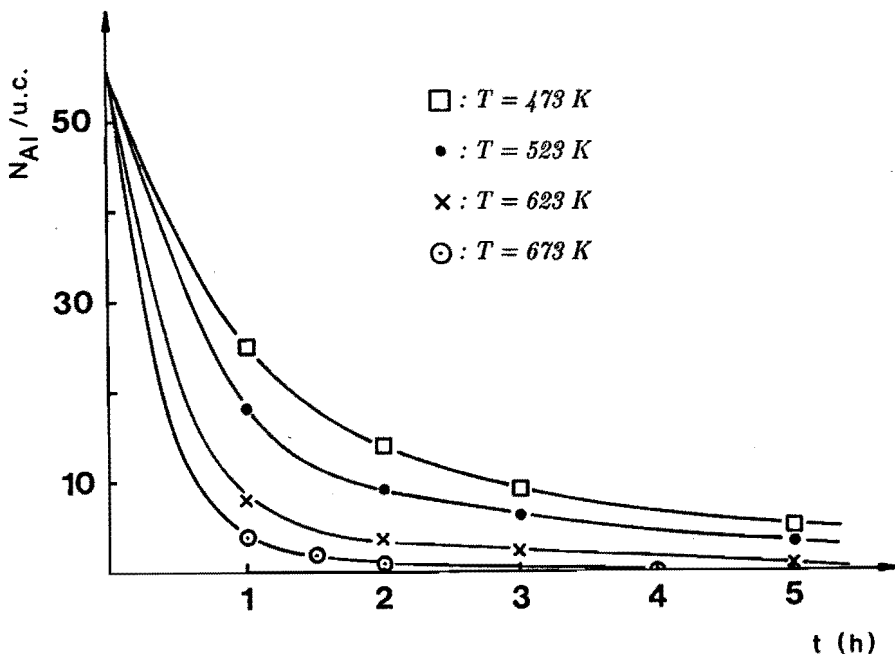
The reaction with $SiCl_4$ vapour is completely different in character. Silicon atoms stemming from $SiCl_4$ can replace Al atoms in the framework. Some results are shown in Fig. IV.7, demonstrating that this replacement proceeds very fast. At sufficiently high reaction temperatures (above 673 K), nearly all framework Al can be substituted by Si within 4 hours. Due to this substitution by an external silicon source it can be proposed that the measured amounts of framework Al are closer to the real values than in the case of hydrothermally dealuminated zeolites.

The total amounts of framework Al of selected samples after washing and drying are shown in Tab. IV.4. Obviously, these samples contain non–framework Al stemming from Al_2Cl_6 or $NaAlCl_4$ that could not readily be removed by stripping. By means of ^{27}Al MAS NMR, Klinowski et al. detected $AlCl_4^-$ complexes in comparable samples obtained from NaY. After hydration, these species were found to be converted in octahedrically coordinated aluminum[55]. In our own experiments, the presence and hydrolysis of residual aluminum chlorides was indicated during washing of the products with water: the washing liquor became acidic, and chloride ions were detectable. Uptake of the dealuminated zeolites in tetrachloromethane instead of water did not have any effect. The amount of non–framework Al remained the same (Tab. IV.4). Only when

TABLE IV.4: *Chemical Compositions after Dealumination with SiCl₄.*

Starting Material	Framework[1] Al/u.c.	Total Al/u.c.[2]	
		uptake in H_2O	uptake in CCl_4
NaY	19	39	39
NH_4Y	17	35	34
NaY	13	18.9	18.9
NH_4Y	12	14.8	14.7
NaY	3.4	4.8	4.7
NH_4Y	3.4	4	4

[1] *As determined by means of IR;*
[2] *obtained from wet–chemical analyses.*

NH_4Y was used as starting material instead of NaY, the amount of non–framework Al was found to be somewhat lower at the same degree of dealumination.

The results presented indicate that the non–framework Al is partly entrapped inside the small–pore system of the faujasite, i.e. inside the sodalite cages. These cages are accesible for water molecules but not for tetrachloromethane. Therefore, hydrolysis of the entrapped Al_2Cl_6 and/or $NaAlCl_4$ is possible, but dissolution in CCl_4 cannot be achieved. The aluminum hexaquocomplex formed is still too large to pass the 6–rings and remains therefore inside the sodalite cages.

Some authors found that NaY dealuminated with $SiCl_4$ exhibits a higher concentration of Al in the surface layers than in the bulk of the zeolite crystals. This surface enrichment is explained by migration of $NaAlCl_4$ towards the external surface[54,56]. Our XPS measurements (Tab. IV.5) partly confirm this idea: With NaY as starting material, products with aluminum–rich surfaces were obtained. But dealumination of NH_4Y yielded products with less surface enrichment of Al, indicating that Al_2Cl_6 can sublimate more easily than $NaAlCl_4$.

TABLE IV.5: *Surface and Bulk Si/Al Ratio after Dealumination with SiCl₄.*

Starting Material	Si/Al^1 Framework	Si/Al^2 Total	Si/Al^3 Surface
NaY	15	9.14	4.1
NH_4Y	16	12	10
NaY	55	39	19.9
NH_4Y	55	47	37

[1] *As measured by means of IR;*
[2] *obtained from wet–chemical analyses;*
[3] *as measured by means of XPS.*

Conclusions

The rate of a hydrothermal dealumination can be controlled by the reaction parameters temperature and vapour pressure of water. The extent of dealumination corresponds to the degree of ion exchange NH_4^+ or H^+ versus Na^+. The non–framework Al can concentrate inside the cages and on the external surfaces of the zeolite crystals. This concentration in combination with the formation of dense–phase clusters, e.g. boehmite, lowers the solubility of these species in diluted mineralic acids. Cleaning of hydrothermally dealuminated zeolites by means of selective extraction of non–framework Al is therefore difficult or even impossible.

The reaction with $SiCl_4$ comprises a rapid substitution of framework Al by Si atoms. Starting from NH_4Y (85 % NH_4^+, 15 % Na^+), the main non–framework Al species is Al_2Cl_6, whereas only $NaAlCl_4$ is formed upon reaction with NaY. These chlorides are partly entrapped inside the sodalite cages of the zeolite and cannot be removed by washing. Those species, which are not entrapped, can sublimate or migrate towards the external surface of the zeolite particles. Since Al_2Cl_6 is more volatile than $NaAlCl_4$, lower amounts and more homogeneous distributions of non–framework Al can be achieved, if NH_4Y is used as starting material instead of NaY.

IV.3. STRUCTURAL CHANGES UPON DEALUMINATION

Introduction

It follows from simple stoichiometric considerations that removal of aluminum atoms from the framework of a zeolite must result in structural changes if no external silicon is provided in order to fill up the vacant lattice positions. These vacant lattice positions, also called T–atom vacancies or hydroxyl nests, consist of four surrounding silanol groups as shown in the following scheme:

```
        Si                          S i
        |                           |
        O                           OH
        |      dealumination        |
Si – O – Al – O – Si  ───────────▶  Si – OH      HO – Si  +  non–framework Al
        |                           |
        O                           OH
        |                           |
        Si                          S i
```
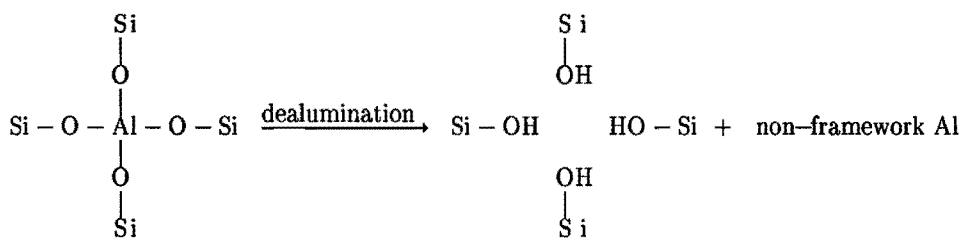
Hydroxyl nests were proposed to be present in zeolites dealuminated with acids[2,33], with EDTA[15,37], with steam[11,15] and with phosgene or nitrosyl chloride[46]. But even in the case of dealuminations with reagents containing silicon such as $SiCl_4$ or $(NH_4)_2SiF_6$, the formation of hydroxyl nests was discussed. The reason is that the non–framework Al species are easily hydrolyzed, yielding acids (hydrochloric or hydrofluoric acid) which can cause additional extraction of framework Al[45,47].

The increase in silanol groups in dealuminated zeolites was detected by means of infrared measurements in the hydroxyl stretching region $(3000–4000\ cm^{-1})$[51,57-60], ^{29}Si MAS NMR measurements in combination with ^{1}H $–^{29}$Si cross polarization[59-61] and ^{1}H MAS NMR measurements[62,63]. These investigations confirmed, indeed, that any of the mentioned dealumination reactions affects the framework. However, the detected silanol groups are not necessarily part of isolated hydroxyl nests. At the conditions of hydrothermal treatment, for instance, hydroxyl nests are not stable. Early XRD investigations on steamed zeolite Y suggested the occurrence of rearrangement reactions in the framework, resulting in some replacement of Al vacancies by Si atoms provided from other parts of the framework[64,65]. Adsorption data gave evidence of secondary pores in hydrothermally dealuminated zeolites, demonstrating that healing of the hydroxyl nests occurs at the expense of large holes in the framework[66,67]. In strongly dealuminated zeolites, these holes are large enough to be visible in transmission electron micrographs[68]. Engelhardt was the first who succeeded in observing structural rearrangements, i.e. the formation of new Si–O–Si bondings in the framework, by means

92

of ^{29}Si MAS NMR[61]. Some months later, similar results were presented by Maxwell et al.[69] and by Klinowski et al.[70].

There is, of course, a missing link between detection of silanol groups as such and evidence of rearrangement reactions including formation of secondary pores. The missing link comprises the direct detection of hydroxyl nests or small clusters of silanol groups, which requires the characterization of the silanol groups with respect to their position and spatial arrangement in the lattice. It has been shown in part II of this thesis that silylation of silanol groups and subsequent ^{29}Si (CP) MAS NMR analyses of the products enables the identification of isolated, paired and clustered silanol groups inside the lattice and the discrimination from terminal silanol groups at the external surface of the crystals. In zeolite frameworks consisting of crystallographically different T–atoms such as ZSM–5, additional information about the position of internal silanol groups is available[71,72]. It will be shown in the following part that silylation in combination with ^{29}Si (CP) MAS NMR can also be used in order to characterize subtle structural defects such as hydroxyl nests and small secondary pores in dealuminated zeolite Y[73].

Experimental

A sample of zeolite Y with 52.6 framework Al per unit cell was prepared by threefold acid leaching, using each time 100 ml of 0.033 N aqueous hydrochloric acid per gram zeolite. A second sample was prepared by hydrothermal treatment of NH$_4$Y, exhibiting 50 Al/u.c.. A third sample with 18 Al/u.c. was obtained by dealumination of NaY with SiCl$_4$ vapour. Starting material and dealumination procedures have already been described in part IV.3.

Silylated zeolite Y was obtained from reactions of 40 μl trimethylchlorosilane (TCS) with 500 mg dried sample. The procedure of silylation as well as the ^{29}Si (CP) MAS NMR measurements are described in part II.2. Control measurements after some months made sure that the silylation products are stable in air. XRD measurements revealed that the reaction with TCS does not affect the crystallinity of the zeolites.

Results and Discussion

The reaction between trimethylchlorosilane (TCS) and the silanol groups of Cab–O–Sil and ZSM–5 has already been described in part II of this thesis. The mechanism will not be discussed again since it does not matter whether the silanol groups are stemming from silica, ZSM–5 or faujasite. Of course, the reaction conditions,

TABLE IV.6: Products formed upon Reaction of TCS with Silanol Groups.

Reaction Step		Product	δ [ppm][1]
$(CH_3)_3SiCl$	$+ HO–Si \rightarrow (CH_3)_3\underline{Si}–OSi + HCl$	primary	$+12$
	$+ HO–Si \rightarrow (CH_3)_2\underline{Si}(–OSi)_2 + CH_4$	secondary	$ca.\ -18$
	$+ HO–Si \rightarrow (CH_3)\underline{Si}(–OSi)_3 + CH_4$	tertiary	$ca.\ -66$
	$+ HO–Si \rightarrow \underline{Si}(–OSi)_4 + CH_4$	quarternary	> -104[2]

[1] *Chemical shifts of underlined Si atoms relative to TMS;*
[2] *value depends on the structure and the Si/Al ratio of the silylated material.*

Fig. IV.8: ^{29}Si MAS NMR Spectrum of the Starting Material NaY.
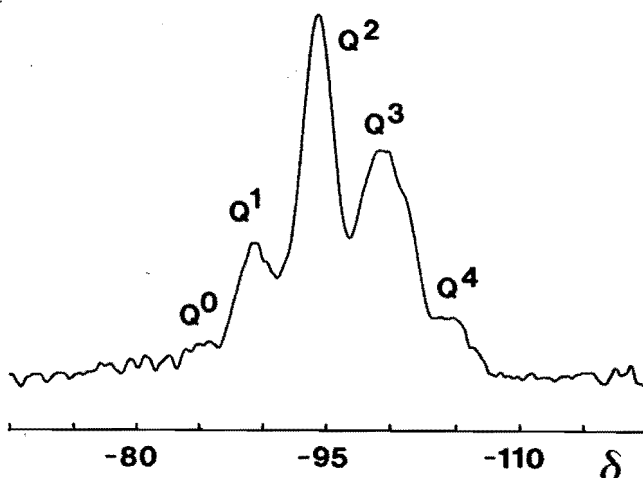
i.e. the temperature, required for the formation certain products can differ depending on the accessibility and the spatial arrangement of the silanol groups. The reaction steps together with the chemical shifts of the products are therefore only summarized in Tab. IV.6. Apart from the resonances of possible silylation products, the ^{29}Si (CP) MAS NMR spectra of zeolite Y will, of course, exhibit signals stemming from original framework silicon atoms.

Fig. IV.9: ^{29}Si (CP) MAS NMR Spectra of Zeolite Y after Acid Leaching.

(A): before reaction with TCS, (A1) CP excited, (A2) single pulse exitation;
(B): after 16 h reaction with TCS at 473 K, CP excited;
(C): after 16 h reaction with TCS at 573 K, (C1) CP excited, (C2) single pulse exitation.
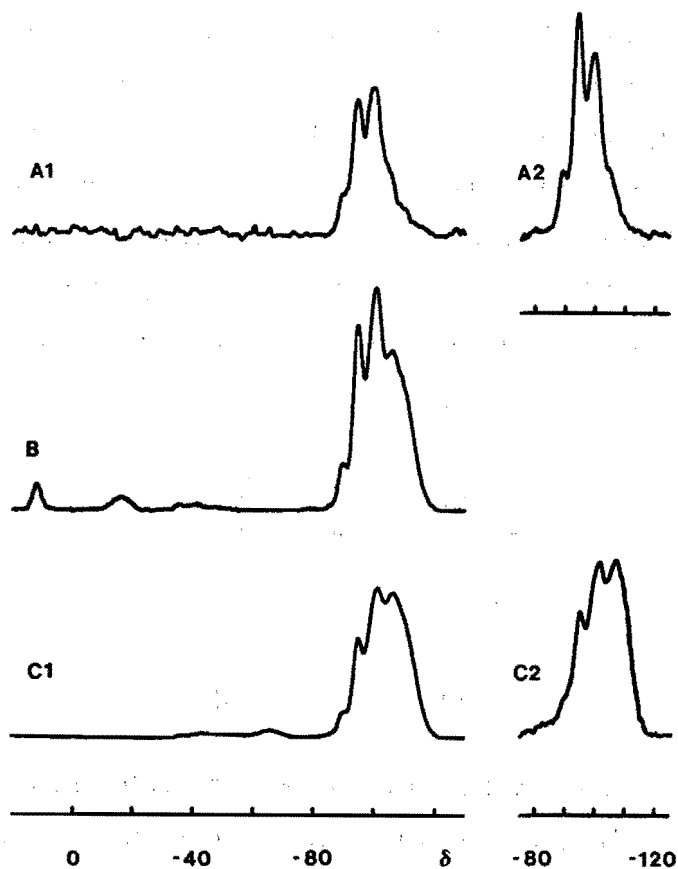
The ^{29}Si MAS NMR spectrum of the starting material NaY is shown in Fig. IV.8. The spectrum consists of five resonances belonging to Q^4, Q^3, Q^2, Q^1 and Q^0 silicon atoms in the framework. The number in the superscript accounts for the amount of silicon neighbours in the first coordination shell. A Q^3 silicon atom, for instance, is via oxygen atoms connected to three neighbouring silicon atoms, while the fourth neighbour is aluminum or a hydroxyl group. The Q^3 signal at -103 ppm may therefore consist of $(SiO)_3\underline{Si}OAl$ and/or $(SiO)_3\underline{Si}OH$ sites. But the parent NaY has not yet been dealuminated and the amount of silanol groups is expected to be very low.

Figure IV.9 shows a series of ^{29}Si (CP) MAS NMR spectra of zeolite Y after acid leaching. The spectra A1 and A2 have been obtained with and without ^{1}H–^{29}Si cross polarization (CP), respectively. The comparison of these spectra enables the detection of silanol groups, since CP causes enhancement of signals stemming from silicon atoms connected to OH groups. Obviously, most of the silanol groups formed upon acid leaching are Q^3 sites. After reaction with TCS, signals at $+12$, -18 and -66 ppm indicate the subsequent formation of primary, secondary and tertiary products (spectra B and C1). The comparison of the spectra A2 and C2 shows that the intensity of the signal at about -107 ppm belonging to Q^4 sites is strongly increased. The following scheme may illustrate how new Q^4 sites are formed at the expense of e.g. Q^3 sites:

$$
\begin{array}{ccc}
\begin{array}{c} \text{S i} \\ | \\ \text{OH} \\ \\ \text{Si} - \text{OH} \qquad \text{HO} - \text{Si} \\ \\ \text{OH} \\ | \\ \text{S i} \end{array}
&
\xrightarrow{+ \ (CH_3)_3SiCl}
&
\begin{array}{c} \text{Si} \\ | \\ \text{O} \\ | \\ \text{Si} - \text{O} - \text{Si} - \text{O} - \text{Si} \ + \ HCl \ + \ 3\ CH_4 \\ | \\ \text{O} \\ | \\ \text{Si} \end{array}
\end{array}
$$

$$
4 \times Q^3 \qquad\qquad \longrightarrow \qquad\qquad 5 \times Q^4
$$

Bein et al. reported that the reaction between TCS and HY can also result in the silylation of Brønsted hydroxyl groups yielding the primary trimethyl

monosiloxysilanes[74]. But the formation of secondary, tertiary and quarternary silylation products would require the presence of neighbouring Brønsted hydroxyls, which is in conflict with Löwenstein's rule. Moreover, the ^{29}Si NMR signals of methylsiloxysilanes connected to aluminum atoms should shift towards lower fields. But a comparison of the spectra in Fig. IV.9 with those of silylated silica or silicalite (e.g. Fig. II.3) shows that the signals of the methylsiloxysilanes appear at the same chemical shift. If primary products have initially been formed at Brønsted hydroxyl groups, it must be assumed that these species are not stable, probably because of the high temperature and the presence of HCl. They may split up again and react subsequently with silanol groups stemming from hydroxyl nests. The stabilization of the silylation products at hydroxyl nests is achieved by the evolution of methane since this is an irreversible reaction.

The dealumination of zeolite Y by acid leaching is depicted schematically in Fig. IV.10. Removal of framework Al yields hydroxyl nests which could be detected via formation of tertiary and quarternary silylation products.

Fig. IV.10: Formation of Hydroxyl Nests upon Acid Leaching.

■ = *framework Al atoms*,   o = *OH at silanol groups*
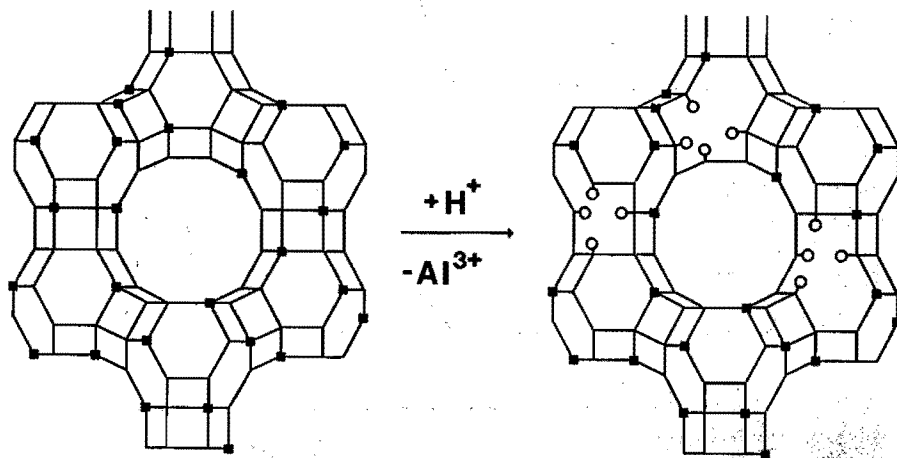
The ^{29}Si (CP) MAS NMR spectra in Fig. IV.11 have been obtained from hydrothermally dealuminated zeolite Y with about 50 framework Al per unit cell. The strong Q^4 signal in spectrum A2 indicates that rearrangement reactions under formation of new Si–O–Si bondings already occurred during steaming. Cross polarization, however
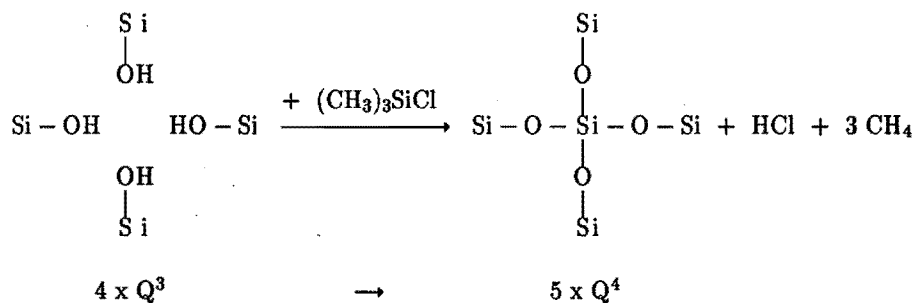
Fig. IV.11: ^{29}*Si (CP) MAS NMR Spectra of Zeolite Y after Steaming.*

(A): before reaction with TCS, (A1) CP excited, (A2) single pulse exitation;
(B): after 1 h reaction with TCS at 573 K, CP excited;
(C): after 16 h reaction with TCS at 573 K, (C1) CP excited, (C2) single pulse exitation.
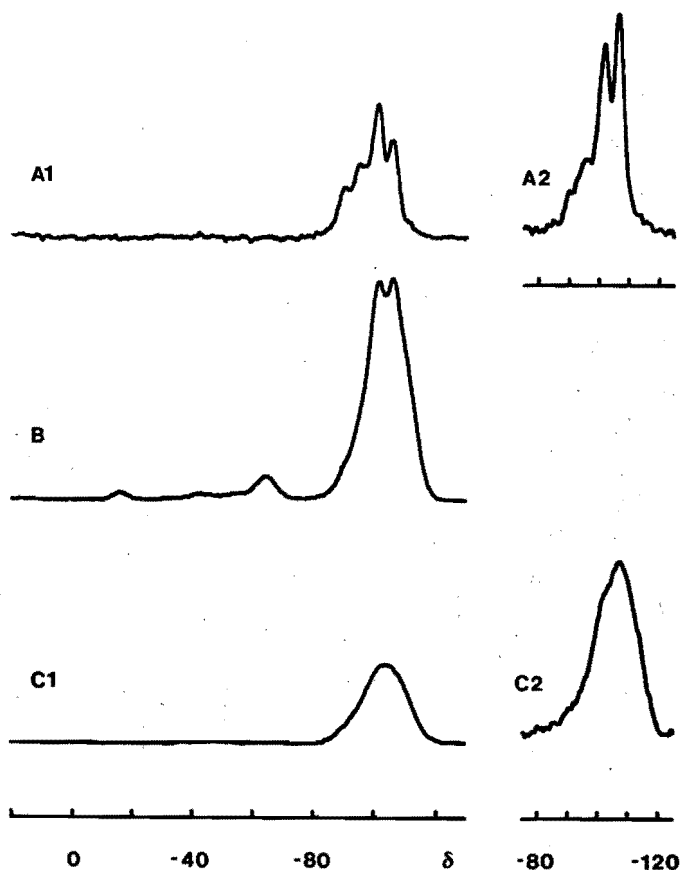
results in an enhancement of the Q^3 signal (spectrum A1), clearly demonstrating that still a lot of silanol groups are present. Silylation of the silanol groups can be followed in spectra B and C1: At 573 K, secondary and tertiary products are completely converted into quarternary products. This is accompanied by a dramatic loss in spectral resolution. The expected increase in Q^4 signal intensity at the expense of Q^3, Q^2 and Q^1 cannot be observed since the ^{29}Si MAS NMR spectrum (C2) apparently consists only of one broad signal. In fact, it is misleading to say that the spectrum consists of one signal since this suggests that it belongs to one kind of silicon site, only. In contrast, such a spectral broadening should be considered in terms of disorder or increase in variety of silicon sites. How can magnetically new types of silicon atoms be created in the framework of zeolite Y? In order to answer this question we first imagine the insertion of TCS into isolated hydroxyl nests. The four silanol groups forming each nest restrict the possibilities of incorporation to exactly one. The new silicon atoms stemming from TCS must occupy original T–atom positions. In this case, the ^{29}Si MAS NMR spectrum must exhibit the same distinct signals as before silylation, but the intensity of the Q^4 signal must be increased at the expense of the other signals. The situation becomes completely different if more than four silanol groups are located together, forming ensembles e.g. at the walls of secondary pores. The TCS molecules have various possibilities to form quarternary products with bonding distances and angels not typical of T–atoms in the framework of zeolite Y. These new Q^4 silicon atoms as well as their next neighbours in the framework exhibit therefore chemical shifts different from those of regular T–atoms. The superposition of the various signals causes the observed broadening in the ^{29}Si MAS NMR spectra.

The widely accepted mechanism of hydrothermal dealumination is depicted in Fig. IV.12. Hydrolysis of Si–O–Al bondings results in the removal of Al from framework positions and the formation of hydroxyl nests. Rapid rearrangement reactions cause healing of these isolated T–atom vacancies at the expense of larger defect sites or mesopores, respectively, surrounded by ensembles of silanol groups. Silylation

experiments and subsequent analyses by means of ^{29}Si MAS NMR have confirmed this proposed mechanism. Moreover, the presented results show that defect sites in dealuminated zeolites can be characterized in an early stage. It is possible to detect secondary pores in the lattice which are just larger than hydroxyl nests but still too small to influence the adsorption properties.

Fig. IV.12: Formation of Silanol Ensembles upon Hydrothermal Dealumination.
■ *= framework Al atoms,* ○ *= OH at silanol groups.*
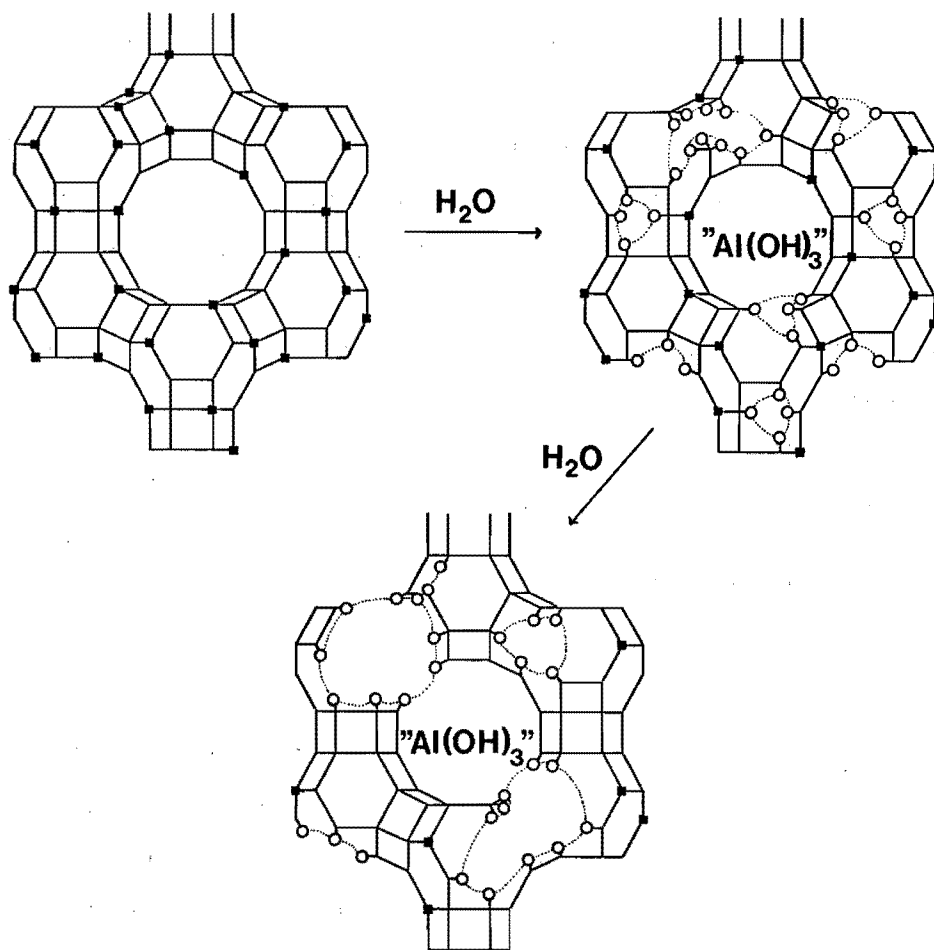
The series of ^{29}Si (CP) MAS NMR spectra in Fig. IV.13 has been obtained from zeolite Y after dealumination with SiCl$_4$ vapour. The presence of silanol groups in this material is clearly indicated by the Q^3 signal enhancement upon cross polarization (spectrum A1 as compared with spectrum A2). Reaction of these silanol groups with TCS again results in the stepwise incorporation of silicon via primary, secondary and

Fig. IV.13: ^{29}*Si (CP) MAS NMR Spectra of Zeolite Y after Reaction with SiCl$_4$.*
(A): before reaction with TCS, (A1) CP excited, (A2) single pulse exitation;
(B): after 16 h reaction with TCS at 473 K, CP excited;
(C): after 16 h reaction with TCS at 573 K, (C1) CP excited, (C2) single pulse exitation.
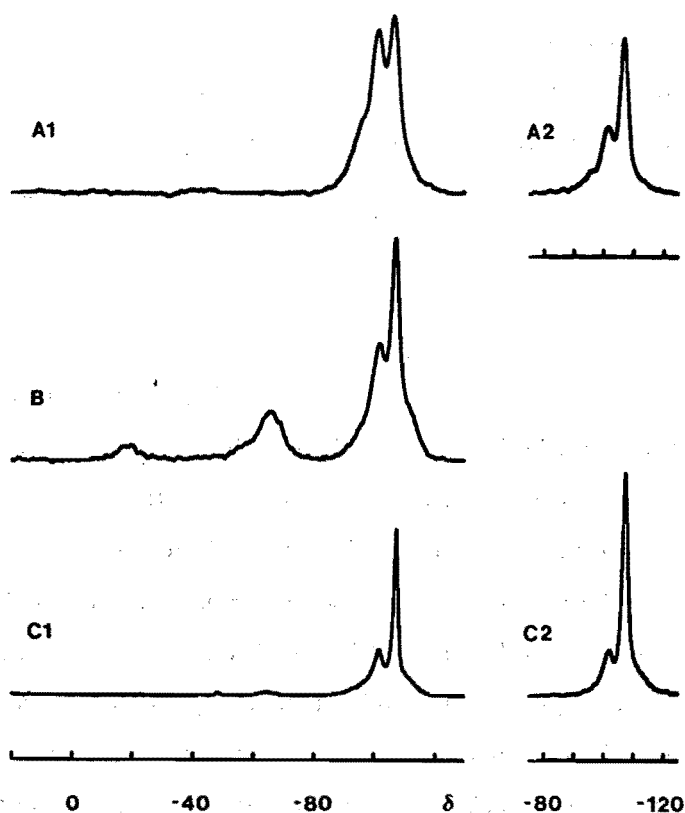
tertiary products (spectra B and C1). In contrast to the hydrothermally dealuminated zeolite, the formation of quarternary products is here accompanied by an increase in relative intensity of the Q^4 signal and an improvement of the spectral resolution. It must be assumed that the silanol groups in this zeolite belong to isolated hydroxyl nests. The scheme in Fig. IV.14 illustrates the dealumination with $SiCl_4$: Replacement of framework Al by silicon stemming from $SiCl_4$ yields a silicon–rich faujasite in which some of the formed $NaAlCl_4$ is still occluded. Washing or exposure to (moist) air results in hydrolysis of these species and evolution of hydrochloric acid, which is, finally, responsible for a kind of secondary dealumination. The hydroxyl nests are therefore formed during an undesired acid leaching procedure. In samples prepared from NH_4Y, the amount of hydroxyl nests is generally lower than in products obtained from NaY because less aluminum chloride species remain in the cages and hence less hydrochloric acid can be formed. On the other hand, strongly dealuminated faujasites contain only a few framework Al atoms that can be removed by secondary dealumination. Consequently, most hydroxyl nests were found to be formed in poor and medium dealuminated zeolites.

Conclusions

The study of the recent literature reveals that any known dealumination reaction is assumed to cause defects in the framework of the zeolite. Generally, this is ascribed to a higher extent of Al removal than of replacement. For the three most prominent dealumination procedures acid leaching, hydrothermal treatment and reaction with $SiCl_4$, the structural defects have been studied and characterized. It could be shown that acid leaching results in the formation of isolated hydroxyl nests in the framework of zeolite Y. Acid leaching is also an unavoidable secondary reaction occurring in zeolites which have been dealuminated with $SiCl_4$. The acid is formed upon hydrolysis of occluded non–framework aluminum chloride species. The resulting isolated hydroxyl nests consisting of four silanol groups could be well characterized by silylation of the

Fig. IV.14: Formation of Isolated Hydroxyl Nests after Reaction with SiCl₄.

■ = *framework Al atoms*, ○ = *OH at silanol groups.*
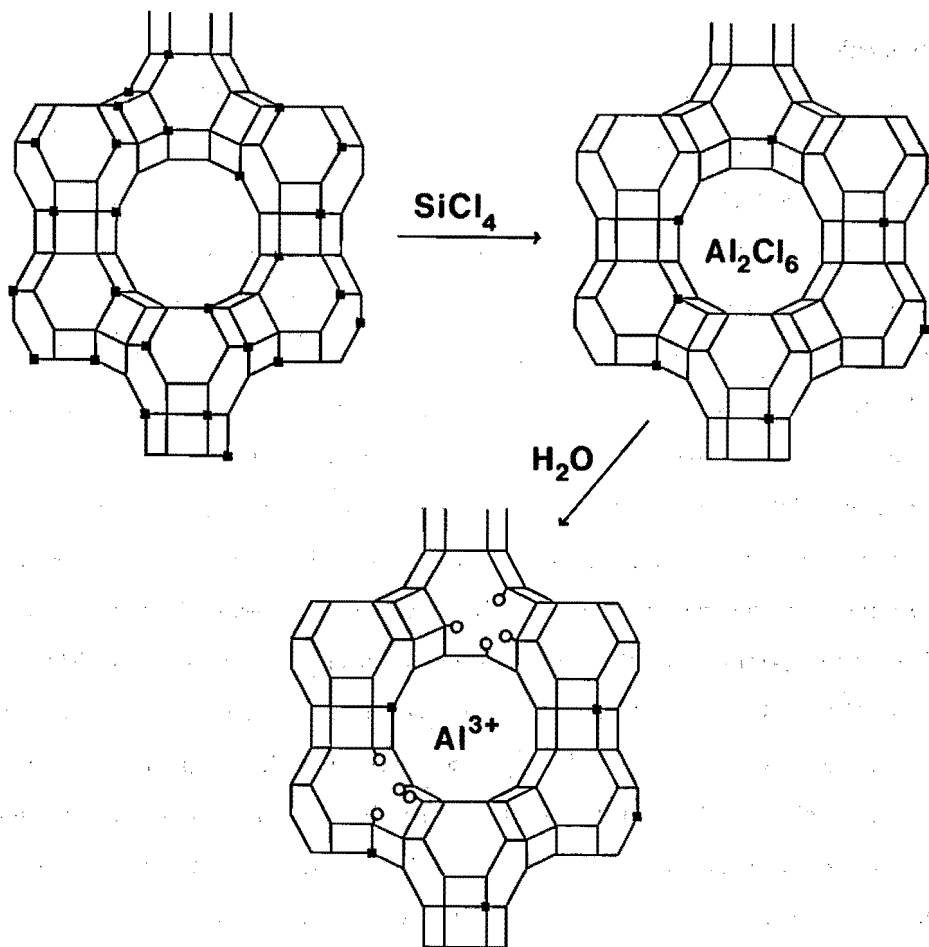
silanol groups with TCS and subsequent ^{29}Si (CP) MAS NMR analyses of the products. This technique moreover enables to distinguish between isolated hydroxyl nests and ensembles of silanol groups, i.e. surrounding holes or secondary pores in the framework. Ensembles of silanol groups were found to be present in hydrothermally dealuminated zeolite, which gives further evidence of rearrangement reactions occurring in the presence of steam.

IV.4. ON THE DETERMINATION OF FRAMEWORK Si/Al RATIOS IN DEALUMINATED ZEOLITES: A CRITICAL EVALUATION OF METHODS

Introduction

Previously, it was pointed out that the modification of zeolite Y by dealumination is of great commercial interest because highly siliceous FCC catalysts exhibit improved selectivity towards olefinic gasoline fractions. The main selectivity—determining factor is the hydrogen transfer activity which decreases with increasing framework Si/Al ratio of the catalyst. The determination and control of framework Si/Al ratios in dealuminated zeolites is therefore of great importance.

The total amounts of Si and Al can be measured by means of wet—chemical methods or by energy—dispersive analyses of X—rays (EDAX). But the total ratios can considerably differ from the framework ratios due to the presence of non—framework Al species in the channels and/or at the external surface of the dealuminated zeolites. The Si/Al ratios in the framework are usually determined by X—ray diffraction (XRD), mid—infrared spectroscopy (IR), solid—state nuclear magnetic resonance (MAS NMR) of ^{29}Si or ^{27}Al nuclei or by combination of these spectroscopic techniques. The mentioned methods are widely accepted although they include typical experimental errors. Structural defects in dealuminated zeolites such as hydroxyl nests or secondary pores, for instance, can impair the accuracy of some of these measurements, which are often not taken into consideration. In the following, the most important techniques used for the determination of framework Si/Al ratios will be subjected to a critical evaluation.

Measurement of the Unit Cell Size

The replacement of Al—O linkages (bond length 0.169 nm) in the framework by Si—O linkages (0.161 nm) causes a contraction of the unit cell which can be measured by means of XRD. If the framework Al is not effectively replaced by Si but just removed under formation of structural defects, no such contraction of the unit cell can be

104

expected although the framework Si/Al ratio is increased. Moreover, the size of the unit cell depends on the extend of hydration and on the amount and kind of charge compensating cations[2]. Both factors change, in their turn, with the framework Si/Al ratio[75,76]. Until now, the probable influence of non—framework Al species inside the channels and cages has not even been investigated. Summing up the possible error sources it must be concluded that XRD is no sensitive tool for the measurement of framework Si/Al ratios in dealuminated zeolites.

Measurements of IR Frequency Shifts

The determination of framework Si/Al ratios by means of IR has already been problemized in part IV.2. This technique is based on the measurement of absorption bands in the mid—infrared region which shift towards higher frequencies if the weaker Al—O linkages are replaced by the stronger Si—O linkages. Figure IV.15 shows a series of IR spectra obtained from zeolite Y. Spectrum A belongs to the starting material NaY with 56 framework Al atoms per unit cell. Spectrum B has been measured after acid leaching of NaY and removal of 4 Al atoms per unit cell. In spite of the increase in framework Si/Al ratio, no high—frequency shift of the absorption bands can be detected. Only after subsequent incorporation of silicon atoms by reaction of TCS with hydroxyl nests in the framework a slight increase in absorption frequencies can be observed (spectrum C).

These results clearly demonstrate that the position of the absorption bands is not affected by removal of framework Al but rather by formation of new Si—O—Si linkages. Obviously, IR enables to follow the course of structural rearrangements or silicon enrichment, but the changes in framework Si/Al ratios during dealumination cannot be measured.

It is interesting to compare the empirical correlations between IR data and amount of framework Al in faujasites published during the last years[48,75-78]. The discrepancies must partly be ascribed to differences in the quality of the samples with respect to

Fig. IV.15: Changes in IR Band Positions in Zeolite Y after Removal of Al and Subsequent Incorporation of Si.

(A) starting material NaY with 56 Al/u.c.; (B) after acid extraction of 4 Al/u.c.; (C) after subsequent reaction with TCS (16 h at 623 K) under formation of quarternary products.
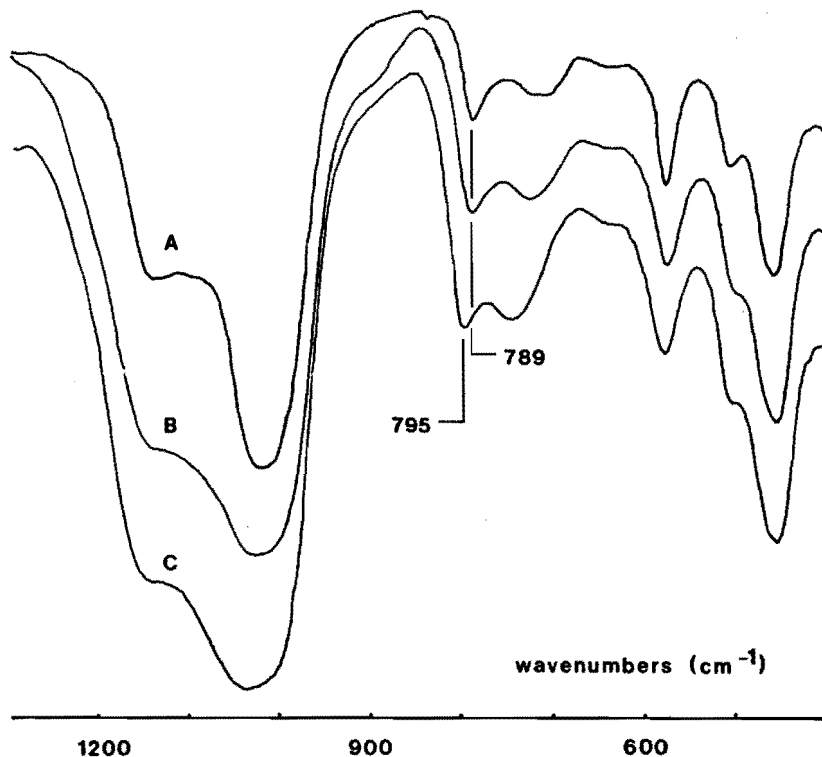
structural defects. Moreover, the IR data are relative and the proposal of a correlation with the content of framework Al requires calibration by means of other methods. Most of the published IR correlations are obtained from dealuminated samples of zeolite Y and the determination of framework Si/Al ratios is based on chemical analyses, XRD or ^{29}Si MAS NMR. This means, in fact, that two methods of unknown and varying accuracy are related to each other.

Flanigen et al. investigated as–synthesized faujasites in which the total Si/Al ratios

106

as measured by means of chemical analyses are almost identical with the framework ratios[48]. The resulting correlations between IR absorption frequencies and framework compositions are therefore reliable. However, faujasites with Si/Al > 3 cannot be synthesized directly. The question arises whether extrapolation of Flanigen's correlation to higher Si/Al ratios is useful since structural defects in dealuminated zeolites always hamper the accuracy.

^{29}Si MAS NMR

Structural studies on aluminosilicates in general and zeolites in particular proceeded rapidly since ^{29}Si MAS NMR was introduced by Lippmaa et al.[79,80]. It was found that the spectra of zeolites exhibit up to five distinct signals which were ascribed to SiO_4 tetrahedra connected to different numbers of AlO_4 neighbours (see e.g. Fig. IV.9). The five types of silicon atoms were designated as Si(nAl) with n equal to 0 — 4. If Löwenstein's rule is valid, the framework Si/Al ratio of zeolites can be determined from the intensities of the ^{29}Si MAS NMR signals according to Engelhardt's formula[81]:

$$(Si/Al)_{NMR} = \frac{\sum\limits_{n=0}^{4} I_{Si(nAl)}}{\sum\limits_{n=0}^{4} \frac{n}{4} I_{Si(nAl)}}$$

Engelhardt and coworkers were also the first who noticed that the signal of the silanol groups $(SiO)_3SiOH$ coincides with the signal of the Si(1Al) units[61]. The ^{29}Si MAS NMR spectrum of dealuminated zeolites therefore contains contributions originating from silanol groups which are hidden under the Si(1Al) signal while still belonging to the Si(0Al) units. Silanol groups can be indicated by means of ^1H–^{29}Si cross polarization, but there is still no method to quantify their contribution on the spectra. Engelhardt et al. therefore warned of application of ^{29}Si MAS NMR as far as dealuminated zeolites are concerned because the measured framework Si/Al ratios are lower than the true ratios[61].

^{27}Al MAS NMR

From the first ^{27}Al MAS NMR studies on different zeolite structures it was concluded that the ^{27}Al chemical shift only depends on the coordination of the Al atoms. Tetrahedrally coordinated framework Al could easily be distinguished from octahedrally bound non–framework Al species[55,70,82]. No or only little variation of the ^{27}Al chemical shift was observed for framework Al in different zeolite lattices[82,83], and it was concluded that ^{27}Al MAS NMR provides only little structural information. Recently, Lippmaa et al. showed that most of the published conclusions were incorrect because second–order quadrupolar line shifts precluded the accurate determination of the ^{27}Al chemical shifts by simple inspection of line positions. However, isotropic chemical shifts can be obtained if very high spinning frequencies are used, preferably at high field strengths. The data obtained by Lippmaa et al.[85] show a clear dependence of ^{27}Al chemical shifts on the first and second coordination shell and on the mean Si–O–Al angles in aluminosilicate frameworks, confirming earlier assumptions of Müller et al.[84]. Other recent investigations revealed that also the variety of non–framework Al species present in dealuminated zeolites is much greater than initially assumed. Mobile, hydrated Al complexes were detected by Freude et al.[86], Gilson et al.[87] reported penta–coordinated Al, Corbin et al.[88] and Samoson et al.[89] gave evidence of tetrahedrally bound non–framework species and Ray et al.[90] showed that some tetrahedrally bound non–framework Al has the same chemical shift than framework Al. An accurate quantitative determination of framework and non–framework Al in dealuminated zeolites therefore requires correct assignments of the observed signals, and this may be difficult due to the variety in species. Moreover, it is possible that some highly unsymmetric Al species are present which are not detected because of the large quadropular interaction with the electric field gradient at the nucleus. Particularly in dehydrated samples, the symmetry of the local environment of Al atoms may be low, and the pronounced quadrupolar broadening makes the Al species NMR–invisible[91,92]. Two–dimensional NMR nutation experiments enable to determine the quadrupolar

interaction parameters and hence separation and asignment of overlapping lines[89,93-96]. However, in the case of strong quadrupolar interactions, the line integrals cannot be interpreted quantitatively even when selective central $(+1/2 \leftrightarrow -1/2)$ transitions are achieved. Chemical treatments can yield Al species of higher symmetry, giving sharper ^{27}Al resonances. Ethanolic acetylacetone solutions, for instance, can be used to improve the detection of octahedrally coordinated non–framework Al[86]. But the Al species in zeolites respond differently to sample treatments: Acac mainly narrows the octahedral resonance while hydration has most effect on the tetrahedral resonance[90].

Summing up, it becomes clear that ^{27}Al MAS NMR is still far from standard. The accurate determination of ^{27}Al chemical shifts and the detection of all aluminum species possibly present already require most modern instrumentation. For the quantitative determination of aluminum, additional chemical treatments are necessary which must provide formation of highly symmetric Al species in order to decrease the second–order quadrupolar broadening. Since chemical reagents such as acetylacetone can cause further dealumination and favour only the detection of certain Al species, there always remains some uncertainty concerning the fullfilling of this requirement.

^{1}H MAS NMR

The first proton magnetic resonance studies revealed the presence of acidic and non–acidic hydroxyl groups in zeolites[97,98]. The ^{1}H chemical shift of the protons belonging to so–called bridging (Brønsted) hydroxyl groups was found to increase with increasing acid strength[99-101]. Apart from these bridging hydroxyl groups, dealuminated zeolites also contain AlOH hydroxyl groups at non–framework Al species and silanol groups stemming from structural defects and external surfaces[62,63,101,102]. It was found that the relative intensity of the resonance ascribed to bridging hydroxyls in hydrogen zeolites is strictly proportional to the amount of tetrahedral framework Al[62,63]. Structural defects caused by dealumination do not affect the accuracy of the measurement. ^{1}H MAS NMR is therefore an appropriate method for the determination

of framework Si/Al ratios in zeolites. However, the spectral resolution sometimes suffers from strong dipolar interactions which cannot be eliminated by magig angle spinning alone. Moreover, the samples under investigation must be absolutely dry and sealed in ampoules in order to prevent contact with moist air. As a further requirement for quantitative measurements it should be mentioned that the zeolites must be in the hydrogen form. This may restrict the application of ^{1}H MAS NMR to high–silica zeolites in which the charge compensating metal ions can easily and readily be exchanged against protons.

Conclusions

The quantitative determination of the amount of framework aluminum in dealuminated zeolites is still very difficult. The widely used techniques XRD, IR and ^{29}Si MAS NMR are useful or even indispensible structural tools, but provide no reliable quantitative information since structural defects, which are typically present in dealuminated zeolites, can impair the accurracy of the measurements. Quantitative NMR of quadrupole nuclei such as ^{27}Al is still not possible if the quadrupolar interaction of the species under investigation are known to be very large. The most promising technique at this time is ^{1}H MAS NMR of zeolites in the hydrogen form. However, this method also requires modern instrumentation and special experience with sample preparation (ampoule technique).

The knowledge of the amount of acid sites in modified zeolites is indispensible for the understanding of catalytic reactions. The problems arising with the quantitative determination of framework Si/Al ratios should be taken more seriously. Much more efforts should be made in order to develop or refine appropriate techniques for this purpose.

IV.5. REFERENCES

1   D.W. Breck, U.S. Patent 3.130.007 (1964).

2   D.W. Breck, "Zeolite Molecular Sieves", John Wiley & Sons, New York 1974, p. 95.

3   C.J. Plank, E.J. Rosinski and W.P. Hawthorne, Ind. Eng. Chem., Prod. Res. Dev. 3, 165 (1964).

4   C.J. Plank and E.J. Rosinski, U.S. Patent 3.140.249 (1964).

5   C.J. Plank and E.J. Rosinski, U.S. Patent 3.140.253 (1964).

6   A.G. Oblad, Oil Gas J. 70 (13), 84 (1972).

7   C.J. Plank and E.J. Rosinski, U.S. Patent 3.210.267 (1965).

8   K.M. Elliot and S.C. Eastwood, Oil Gas J. 60 (23), 142 (1962).

9   C.J. Plank and E.J. Rosinski, Chem. Eng. Prog. Symp. Ser. 73 (63), 26 (1967).

10   C.J. Plank and E.J. Rosinski, U.S. Patent 3.271.418 (1965).

11   C.V. McDaniel and P.K. Maher, in "Zeolite Chemistry and Catalysis" (R. Rabo, Ed.), ACS Monograph 171, 285 (1976).

12   N.Y. Chen, T.O. Mitchell, D.H. Olson and B.P. Pelrine, Ind. Eng. Chem., Prod. Res. Dev. 16, 244 (1977).

13   N.Y. Chen, T.O. Mitchell, D.H. Olson and B.P. Pelrine, Ind. Eng. Chem., Prod. Res. Dev. 16, 247 (1977).

14   A.W. Chester and W.A. Stover, Ind. Eng. Chem., Prod. Res. Dev. 16, 285 (1977).

15   C.V. McDaniel and P.K. Maher, in "Molecular Sieves", Society of Chemical Industries, London 1968, p. 186.

16   M.L. Poutsma, in "Zeolite Chemistry and Catalysis" (R. Rabo, Ed.), ACS Monograph 171, 437 (1976).

17   P.B. Venuto and E.T. Habib, Catal. Rev. Sci. Eng. 18 (1), 1 (1978).

18   S.C. Eastwood, R.D. Drew and F.D. Hartzell, Oil Gas J. 60 (44), 152 (1962).

19   L.A. Pine, P.J. Maher and W.A. Wachter, J. Catal. 85, 466 (1984).

20   J.J. De Jong, Ketjen Catalysts Symposium 1986.

21   C.–Y. Li and L.V.C. Rees, Zeolites 6, 60 (1986).

22   H. Rastelli, B.M. Lok, J.A. Duisman, D.E. Earls and J.T. Mullhaupt, Can. J. Chem. Eng. 60, 44 (1982).

23 A.L. Klyachko, G.I. Kapustin, T.R. Brueva and A.M. Rubinstein, Zeolites 7, 119 (1987).

24 W.O. Haag, R.M. Lago and P.B. Weisz, Nature 309, 589 (1984).

25 R. Beaumont and D. Barthomeuf, J. Catal. 26, 218 (1972).

26 R. Beaumont and D. Barthomeuf, J. Catal. 27, 45 (1972).

27 D. Barthomeuf and R. Beaumont, J. Catal. 30, 288 (1973).

28 R.A. Beyerlein, G.B. Vicker, L.N. Yacullo and J.J. Ziemiak, J. Phys. Chem. 92, 1967 (1988).

29 S.J. De Canio, J.R. Sohn, P.O. Fritz and J.H. Lunsford, J. Catal. 101, 132 (1986).

30 J.R. Sohn, S.J. De Canio, P.O. Fritz and J.H. Lunsford, J. Phys. Chem. 90, 4847 (1986).

31 A. Nock and R. Rudham, Zeolites 7, 481 (1987).

32 J. Arribas, A. Corma, V. Fornes and F. Melo, J. Catal. 108, 135 (1987).

33 R.M. Barrer and M.B. Makki, Can. J. Chem. 42, 1481 (1964).

34 R.M. Barrer and B. Coughlan, in "Molecular Sieves", Society of Chemical Industry, London 1968, p. 141.

35 G.K. Beier, I.M. Belen'kaya, M.M. Dubinin and F. Khange, Izv. Akad. Nauk. SSSR, Ser. Khim. 7, 1457 (1982), english translation.

36 E.F.T. Lee and L.V.C. Rees, J. Chem. Soc., Faraday Trans. I, 83, 1531 (1987).

37 G.T. Kerr, J. Phys. Chem. 72, 2594 (1968).

38 G.T. Kerr, J. Phys. Chem. 73, 2780 (1969).

39 G.T. Kerr, J. Catal. 15, 200 (1969).

40 T.H. Fleisch, B.L. Meyers, G.J. Ray, J.B. Hall and C.L. Marshall, J. Catal. 99, 117 (1986).

41 G.T. Kerr, J.N. Miale and R.J. Mikovsky, U.S. Patent 3.493.519 (1968).

42 N.Y. Chen and F.A. Smith, Inorg. Chem. 15 (2), 295 (1976).

43 J. Scherzer, J. Catal. 54, 285 (1978).

44 H.K. Beyer and I. Belenykaja, Stud. Surf. Sci. Catal., vol. 5, Elsevier Amsterdam 1980, p. 203.

45 H.K. Beyer, I. Belenykaja and F. Hange, J. Chem. Soc., Faraday Trans. I, 81, 2889 (1985).

46 P. Fejes, I. Kiricsi and I. Hannus, Acta phys. et chem. 28 (3–4), 173 (1982).

47 G.W. Skeels and D.W. Breck, in "Proc. 6th Int. Zeolite Conf. in Reno" (D. Olson et al., Eds.), Butterworths 1984, p. 87.

48   E.M. Flanigen, H. Khatami and H.A. Szymanski, in "Molecular Sieve Zeolites", Adv. Chem. Ser. 101, 201 (1971).

49   J.H. Scofield, J. Electron. Spectrosc. Relat. Phenom., 8, 129 (1976).

50   G. Engelhardt, U. Lohse, V. Patzelová, M. Mägi and E. Lippmaa, Zeolites 3, 233 (1983).

51   K. Suzuki, T. Sano, H. Shoji, T. Murakami, S. Ikai, S. Shin, H. Hagiwara and H. Takaya, Chem. Letters 1507 (1987).

52   R.D. Shannon, K.H. Gardner, R.H. Staley, G. Bergeret, P. Gallezot and A. Auroux, J. Phys. Chem. 89, 4778 (1985).

53   J. Dwyer, F.R. Fitch, F. Machado, G. Qin, S.M. Smyth and J.C. Vickerman, J. Chem. Soc., Chem. Comm. 422 (1981).

54   J. Dwyer, F.R. Fitch, G. Qin and J.C. Vickerman, J. Phys. Chem. 86, 4574 (1982).

55   J. Klinowski, J.M. Thomas, C.A. Fyfe, G.C. Gobbi and J.S. Hartman, Inorg. Chem. 22, 63 (1983).

56   L. Kubelková, L. Dudíková, Z. Bastl, G. Borbély and H.K. Beyer, J. Chem. Soc., Faraday Trans. I, 83, 511 (1987).

57   B.H. Ha, J. Cuidot and D. Barthomeuf, J. Chem. Soc., Faraday Trans. I, 75, 1245 (1979).

58   P.J. Grobet, P.A. Jacobs and H.K. Beyer, Zeolites 6, 47 (1986).

59   P. Bodart, J.B. Nagy, G. Debras, Z. Gabelica and P.A. Jacobs, J. Phys. Chem. 90, 5183 (1986).

60   D. Akporiaye, A.P. Chapple, D.M. Clark, J. Dwyer, I.S. Elliott and D.J. Rawlence, in "Proc. 6th Int. Zeolite Conf. in Tokyo", Elsevier Tokyo 1986, p. 351.

61   G. Engelhardt, U. Lohse, A. Samoson, M. Mägi, M. Tarmak and E. Lippmaa, Zeolites 2, 59 (1982).

62   D. Freude, M. Hunger, H. Pfeifer, G. Scheler, J. Hoffmann and W. Schmitz, Chem. Phys. Letters 105, 427 (1984).

63   G. Engelhardt, H.–G. Jerschkewitz, U. Lohse, P. Sarv, A. Samoson and E. Lippmaa, Zeolites 7, 289 (1987).

64   P.K. Maher, F.D. Hunter and J. Scherzer, Adv. Chem. Ser. 101, 266 (1971).

65   P. Gallezot, R. Beaumont and D. Barthomeuf, J. Phys. Chem. 78, 1550 (1974).

66   U. Lohse and M. Mildebrath, Z. anorg. allg. Chem. 476, 126 (1981).

67   A. Zukal, V. Patzelová and U. Lohse, Zeolites 6, 133 (1986).

68 V. Patzelová and N.J. Jaeger, Zeolites 7, 240 (1987).

69 I.E. Maxwell, W.A. van Erp, G.R. Hays, T. Couperus, R. Huis and A.D.H. Clague, J. Chem. Soc., Chem. Commun. 523 (1982).

70 J. Klinowski, J.M. Thomas, C.A. Fyfe and G.C. Gobbi, Nature 296, 533 (1982).

71 B. Kraushaar, L.J.M. van de Ven, J.W. de Haan and J.H.C. van Hooff, Stud. Surf. Sci. Catal., vol. 37, Elsevier Amsterdam 1988, p. 167.

72 B. Kraushaar, J.W. de Haan and J.H.C. van Hooff, J. Catal. 109, 470 (1988).

73 B. Kraushaar, J.W. de Haan, L.J.M. van de Ven and J.H.C. van Hooff, Z. anorg. allg. Chem. 564, 72 (1988).

74 T. Bein, R.R. Carver, R.D. Farlee and G.D. Stucky, J. Am. Chem. Soc. 110, 4546 (1988).

75 U. Lohse, E. Alsdorf and H. Stach, Z. anorg. allg. Chem. 447, 64 (1978).

76 M.W. Anderson and J. Klinowski, J. Chem. Soc., Faraday Trans. I, 82, 1449 (1986).

77 P. Pichat, R. Beaumont and D. Barthomeuf, J. Chem. Soc., Faraday Trans. I, 70, 1402 (1974).

78 J.R. Sohn, S.J. DeCanio, J.H. Lunsford and D.J. O'Donnell, Zeolites 6, 225 (1986).

79 E. Lippmaa, M. Mägi, A. Samoson, G. Engelhardt and A.–R. Grimmer, J. Am. Chem. Soc. 102, 4889 (1980).

80 E. Lippmaa, M. Mägi, A. Samoson, M. Tarmak and G. Engelhardt, J. Am. Chem. Soc. 103, 4992 (1981).

81 G. Engelhardt, U. Lohse, E. Lippmaa, M. Tarmak and M. Mägi, Z. anorg. allg. Chem. 482, 49 (1981).

82 C.A. Fyfe, G.C. Gobbi, J.S. Hartmann, J. Klinowski and J.M. Thomas, J. Phys. Chem. 86, 1247 (1982).

83 J.B. Nagy, Z. Gabelica, G. Debras, E.G. Derouane, J.–P. Gilson and P.A. Jacobs, Zeolites 4, 133 (1984).

84 D. Müller, W. Gessner, H.–J. Behrens and G. Scheler, Chem. Phys. Letters 79, 59 (1981).

85 E. Lippmaa, A. Samoson and M. Mägi, J. Am. Chem. Soc. 108, 1730 (1986).

86 D. Freude, T. Fröhlich, H. Pfeifer and G. Scheler, Zeolites 3, 171 (1983).

87 J.–P. Gilson, G.C. Edwards, A.W. Peters, K. Rajagopalan, R.F. Wormsbecher, T.G. Roberie and M.P. Shatlock, J. Chem. Soc., Chem.

Commun. 91 (1987).

88   D.R. Corbin, R.D. Farlee and G.D. Stucky, Inorg. Chem. 23, 2920 (1984).

89   A. Samoson, E. Lippmaa, G. Engelhardt, U. Lohse and H.–G. Jerschkewitz, Chem. Phys. Letters 134, 589 (1987).

90   G.J. Ray, B.L. Meyers and C.L. Marshall, Zeolites 7, 307 (1987).

91   A.P.M. Kentgens, K.F.M.G.J. Scholle and W.S. Veeman, J. Phys. Chem. 87, 4357 (1983).

92   K.F.M.G.J. Scholle and W.S. Veeman, J. Phys. Chem. 89, 1850 (1985).

93   A.P.M. Kentgens, J.J.M. Lemmens, F.M.M. Geurts and W.S. Veeman, J. Magn. Reson. 71, 62 (1987).

94   A. Samoson and E. Lippmaa, J. Magn. Reson. 79, 255 (1988).

95   P.P. Man and J. Klinowski, Chem. Phys. Letters 147, 581 (1988).

96   P.P. Man, J. Klinowski, A. Trokiner, H. Zanni and P. Papon, Chem. Phys. Letters 151, 143 (1988).

97   D. Freude, H. Pfeifer, W. Ploss and B. Staudte, J. Mol. Catal. 12, 1 (1981).

98   D. Freude, M. Hunger and H. Pfeifer, Chem. Phys. Letters 91, 307 (1982).

99   H. Pfeifer, D. Freude and M. Hunger, Zeolites 5, 274 (1985).

100   K.F.M.G.J. Scholle, A.P.M. Kentgens, W.S. Veeman, P. Frenken and G.P.M. van der Velden, J. Phys. Chem. 88, 5 (1984).

101   D. Freude, M. Hunger and H. Pfeifer, Z. Phys. Chem. NF 152, 171 (1987).

102   U. Lohse, E. Löffler, M. Hunger, J. Stöckner and V. Patzelová, Zeolites 7, 11 (1987).

V.1.   GENERAL INTRODUCTION

The Family of Microporous Aluminophosphates

The aluminophosphate family belongs to a new generation of crystalline microporous molecular sieves. The first members of this family with the framework composition $AlPO_4$ have been reported in 1982 by Wilson et al.[1,2]. Meanwhile, scientists of the Union Carbide Corporation reported more than two dozen different aluminophosphate structures, among them structural analogues of the zeolites sodalite, erionite–offretite, chabazite, gismondine, levynite, Linde Type A and faujasite[3].

Fig. V.1: The Family of Microporous Aluminophosphates.
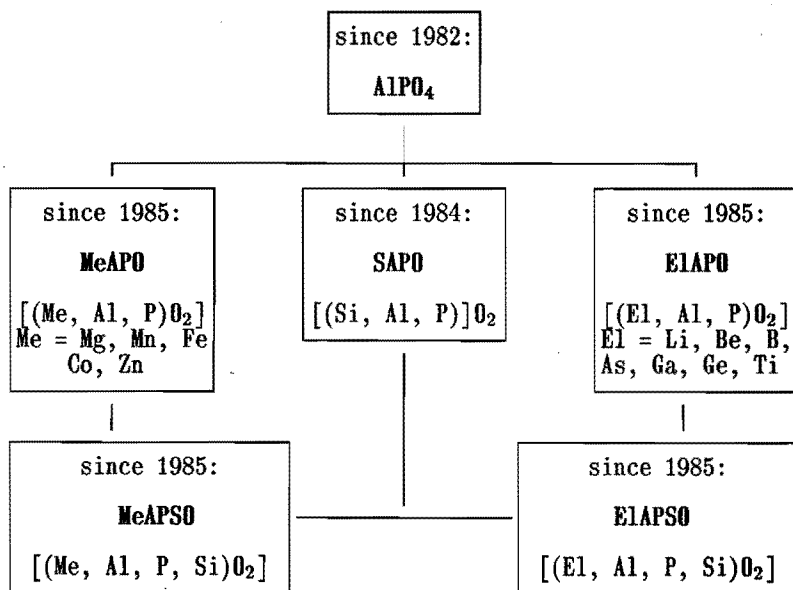
In 1984, the silicoaluminophosphate molecular sieves (SAPOs) were introduced[4,5], marking the beginning of a successful "Periodic Table strategy". The aluminophosphate family is illustrated in Fig. V.1. Until now, incorporation of thirteen elements into aluminophosphate frameworks has been reported resulting in the so–called MeAPO[6,7], ElAPO[8], MeAPSO[9-11] and ElAPSO[12] molecular sieves.

In Table V.1., the major structures of the aluminophosphate family are shown. The pore sizes, varying between 0.3 and 0.8 nm, are comparable with those in zeolites. An important difference with the aluminosilicates is the great variation in chemical compositions. Widely accepted is the Löwenstein rule as a structural guideline for the ordering of Si and Al atoms in zeolites. In the case of the aluminophosphate family, the situation is much more complicated. For these molecular sieves, Flanigen et al.[13] suggested a bonding concept which is summed up in Table V.2. From these rules, which are consistent with present structural and compositional evidence, mechanisms for the incorporation of Me and Si into hypothetical $AlPO_4$ frameworks can be derived:

TABLE V.1: *Selected Structures in the Aluminophosphate Family*[1].

Structure Type		Pore Size [nm]	$AlPO_4$	SAPO	MeAPO	MeAPSO	ElAPO	ElAPSO
5	novel	0.8	x	x	x	x	x	x
36	novel	0.8	—	—	x	x	x	—
37	faujasite	0.8	—	x	—	—	—	—
40	novel	0.7	—	x	—	—	—	—
46	novel	0.7	—	—	—	x	—	—
11	novel	0.6	x	x	x	x	x	x
31	novel	0.65	x	x	—	x	—	—
41	novel	0.6	—	x	—	—	—	x
14	novel	0.4	x	—	x	—	—	—
17	erionite	0.43	x	x	x	x	x	—
34	chabazite	0.43	—	x	x	x	x	x
44	novel	0.43	—	x	x	x	—	—
47	novel	0.43	—	—	x	x	—	—
20	sodalite	0.3	x	x	x	x	x	x

[1] *from ref. 3; x indicates compositions and structures observed in high purity.*

117

In MeAPOs, Me substitutes a hypothetical Al site, and in SAPOs, one Si substitutes a hypothetical P site (mechanism I) and/or two Si substitute Al+P (mechanism II). Some recent NMR studies on different SAPOs confirm the validity of the mechanisms I and II[14-16]. Figure V.2 shows the ternary composition diagrams of MeAPO and SAPO systems illustrating the bonding concept proposed by Flanigen et al.[13].

TABLE V.2: Bonding Concepts in AlPO₄–based Molecular Sieves.

Observed	Not Likely
Al – O – P	P – O – P
Si – O – Si	P – O – Si
Si – O – Al	Al – O – Al
Me – O – P	Me – O – Al
Me – O – P – O – Me	Me – O – Me
electroneutral and negatively charged frameworks	positively charged frameworks

Fig. V.2: Ternary Composition Diagrams of SAPO and MeAPO.
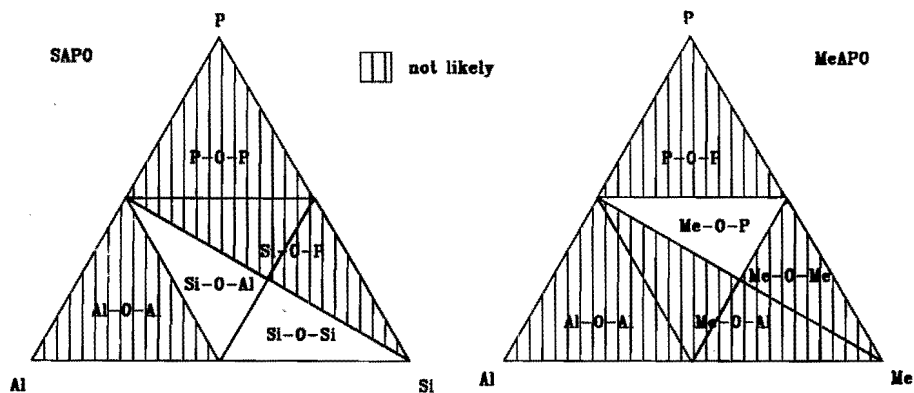
In multinary frameworks, the elements with oxidation states of $+1$, $+2$ and $+3$ tend to incorporate via the proposed Me—mechanism substituting hypothetical Al sites. Hypothetical P sites are occupied by elements with oxidation states of $+4$ or $+5$. Taking the substitution mechanisms into account, the net framework charges can be calculated from the chemical compositions. Obviously, $AlPO_4$ frameworks are electroneutral whereas MeAPO and SAPO frameworks exhibit a net negative charge. In MeAPOs, this negative charge is proportional to the mole fraction of Me incorporated. In SAPOs, only the fraction of Si substituting according to mechanism I causes negative charge whereas substitution mechanism II is electroneutral. Any negatively charged framework possesses cation exchange capacity and the potential for Brønsted acid sites. The $AlPO_4$—based molecular sieves with incorporated heterovalent elements exhibit weak to strong acidity depending on the charge and electronegativity of the framework[13,17].

Aluminophosphate Number 5 ($AlPO_4$—5)

$AlPO_4$—5 is the most prominent member of the aluminophosphate family since it is the first of which the crystal structure was determined[18]. The unit cell has hexagonal symmetry, and contains 24 tetrahedral oxide units, 12 Al and 12 P, with alternation of Al and P throughout the framework. The unconnected cylindrical channels are limited by 12—rings with a diameter of $0.7 - 0.8$ nm[18]. The as—synthesized material contains organic template encapsulated in the channels. It reveals its molecular sieve properties after removal of the template by calcination. As can be seen from Fig. V.3, the framework of $AlPO_4$—5, labeled Smith #81 (see part I), can most conveniently be built up from parallel sheets consisting of 4—, 6— and 12—rings. The alternation of Al and P in $AlPO_4$ frameworks restricts the order of the rings to an even number. The proposal of strict alternation of Al and P in $AlPO_4$—5 has also been confirmed by means of ^{27}Al and ^{31}P NMR investigations of the material before and after removal of the template[19].

Although $AlPO_4$—5 exhibits an electroneutral framework the surface character is moderately polar due to the difference in electronegativity between Al and P which also

119

Fig. V.3: Framework Model of AlPO$_4$-5.
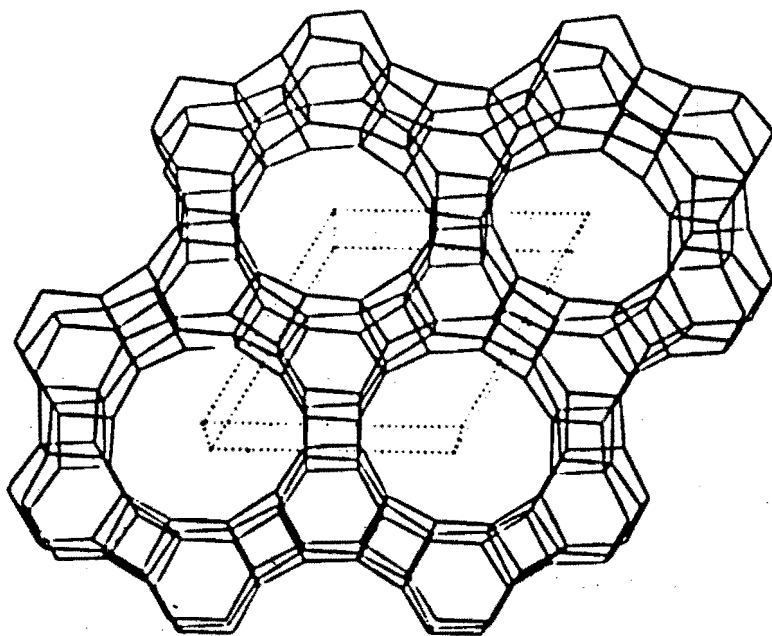
causes large displacements of oxygen from the centre of electron density[18]. The affinity of AlPO$_4$-5 for H$_2$O is less than in zeolites such as type A and type X, but more than in high silica molecular sieves[20].

Acidic and catalytic properties of AlPO$_4$-5 have been the subject of contradictory discussions. Based on catalytic data and studies on the temperature programmed desorption of pyridine, for instance, Choudhary et al. proposed the presence of strong Brønsted and Lewis acid sites in AlPO$_4$-5, but failed to comment on the nature or origin of these sites[21]. On the other hand, Flanigen et al.[13,20] and Hedge et al.[22] studied the hydroxyl infrared region of AlPO$_4$-5 which contains weak νOH absorptions at 3680 cm^{-1} and 3800 cm^{-1}. These absorptions have been assigned to terminal P–OH and Al–OH hydroxyls on the external surface of the crystals. The shift of these OH

120

stretchings after adsorption of weak bases like benzene and ethylene has been measured by Hedge et al. who conclude that the hydroxyl groups in $AlPO_4$–5 have only very weak acidic properties[22]. In agreement with these results, several authors reported very low or even nil activity of $AlPO_4$–5 in catalytic cracking and isomerization reactions[13,22,23].

However, it is obvious that $AlPO_4$ molecular sieves cannot compete with zeolites as far as catalytic properties are concerned. Regardless of the question whether there are a few strong acid sites present or not, the catalytic applications of $AlPO_4$–5 are practically nil. But, of course, there is a need for inert molecular sieve materials which can act as supports for active metal species in e.g. HDS, HDN or (de–)hydrogenation reactions. Aluminophosphate or silica molecular sieves may be promising candidates for these applications, provided that a loading with the catalytically active metal species is possible.

In the following, some aspects of the hydrothermal synthesis of $AlPO_4$–5 and the characterization of the products will be described. It will be shown that entrapment of metal species in the pores of $AlPO_4$–5 by means of conventional wet–chemical methods is complicated because of the lack of ion exchange capacity and the weak polarity of the framework. In contrast, chemical vapour deposition of an electroneutral organometallic compound can yield internal loadings of metal species and will be introduced as an appropriate method for the modification of inert molecular sieve materials.

V.2.   HYDROTHERMAL SYNTHESIS OF $AlPO_4$–5

Introduction

Aluminophosphate molecular sieves are prepared hydrothermally from gels containing an alumina source, a phosphate source, an organic template and water[1]. $AlPO_4$–5 is the structure with the lowest template specificity: It has been synthesized with 25 different organic templates, including primary, secondary and tertiary amines, quarternary

ammonium ions, cyclic amines, diamines and alkanolamines[13]. It is interesting to note that another $AlPO_4$ structure with unidimensional cylindrical channels, the medium–pore $AlPO_4$–11, also exhibits a low template specificity. In this specific channel type, space filling can be achieved by packing templates of quite different sizes and shapes. The typical template for the synthesis of $AlPO_4$–5 is tripropylamine (Pr_3N). It occupies one unit cell length (0.85 nm) of the 12–ring channel, resulting in a $(Al+P)O_2/Pr_3N$ ratio of 24 in the as–synthesized product[13].

Experimental

The gels were prepared by diluting orthophosphoric acid (85%, p.a., Merck) with water and subsequent addition of boehmite (Pural SB, Condea Chemie) and tripropylamine (p.s., Merck) under vigorous stirring. A very viscous gel was obtained. The crystallization was performed in stainless steel pressure bombs equipped with teflon inserts of 200 cm^3 capacity. The pressure bombs were heated in a drying oven without shaking. After crystallization, the pressure bombs were cooled down and the productes were filtered, washed and dried. The obtained powders were checked by means of XRD, using a Philips PW 7200 X–ray generator with Ni–filtered $CuK\alpha$ radiation. The composition of $AlPO_4$–5 phases was determined by means of chemical analyses. Prior to chemical analyses, the samples were calcined at 773 K in a stream of dry air.

Results and Discussion

The outcome of the gel crystallization depends on several parameters such as the gel composition, the crystallization temperature and time and the heating rate of the pressure bombs. As can be seen from Table V.3, the time and the temperature dependences of the $AlPO_4$–5 syntheses show similar effects: after short crystallization times or at low temperatures, some known $AlPO_4$ hydrates are formed, e.g. metavariscite ($AlPO_4 \cdot 2H_2O$), variscite ($AlPO_4 \cdot 2H_2O$), $AlPO_4 \cdot 1.67H_2O$, etc., whereas longer crystallization times or temperatures above 423 K result in the formation of dense

122

phase AlPO$_4$ with the berlinite, tridymite or cristobalite structures. The crystallographic and topologic properties of these AlPO$_4$ structures have been reviewed by Bennett et al.[24]. AlPO$_4$-5 without detectable impurities of hydrated or dense phase AlPO$_4$ could be obtained after 24 h crystallization at 423 K. However, a layer of Pr$_3$N on the final crystallization medium indicated an excess of template.

TABLE V.3: Effect of Crystallization Time and Temperature.

Gel composition: 1.5 Pr$_3$N · 1.0 Al$_2$O$_3$ · 1.0 P$_2$O$_5$ · 40 H$_2$O;
heating: 293 K → T(final) with about 3 K/min.

Time [h]	Temperature [K]	Products[1]
4	423	M + V + H4 + U
8	423	M + V + H4 + H3
22	423	5 >> H2 + H1
24	423	5 with Al/P=1.03
48	423	T + C + 5
24	373	H4 + M + V
24	393	5 + H4 + M
24	473	T + C + 5 + B

[1]*M = metavariscite (AlPO$_4$· 2H$_2$O),*   *V = Variscite (AlPO$_4$· 2H$_2$O),*
H1 = AlPO$_4$· 1.1–1.3H$_2$O,   *H2 = AlPO$_4$· 1.3−1.45H$_2$O,*
H3 = AlPO$_4$· 1.5H$_2$O,   *H4 = AlPO$_4$· 1.67H$_2$O,*
B = berlinite,   *T = tridymite,*
C = cristobalite,   *U = unidentified product,*
5 = AlPO$_4$−5.

TABLE V.4: Effect of Template Concentration.

Gel Composition: x Pr$_3$N · 1.0 Al$_2$O$_3$ · 1.0 P$_2$O$_5$ · 40 H$_2$O; crystallization time: 24 h;
crystallization temperature: 423 K; heating: 293 K → 423 K with ca. 3 K/min.

x	pH (initial)	pH (final)	Products
0.5	2.2	8.6	H3 + H4 + MV
1.0	3.0	8.3	5 with Al/P=1.07
1.2	3.5	8.4	5 with Al/P=1.05
1.5	4.2	8.5	5 with Al/P=1.04

The symbols for the products are explained in Tab. V.3.

The results in Table V.4 show that the synthesis of $AlPO_4$–5 can also succeed with lower concentrations of Pr_3N. But at a Pr_3N/Al_2O_3 ratio of 0.5 or lower, a mixture of hydrated $AlPO_4$ phases is formed, although only 0.17 moles of Pr_3N per mole of Al_2O_3 are required to fill the void space in $AlPO_4$–5. A certain excess of template in the reaction mixture seems to be necessary for the formation of $AlPO_4$–5.

The water content in the gel is also an important variable in the $AlPO_4$–5 synthesis. The higher the water content, the lower is the yield of $AlPO_4$–5 (Table V.5). The effect of gel dilution cannot only be a decrease in the rate of crystallization since prolonged crystallization times did not result in an increased $AlPO_4$–5 yield but rather favoured the formation of dense $AlPO_4$ phases.

TABLE V.5: Effect of Water Content and Crystallization Time.

Gel Composition: 1.0 Pr_3N · 1.0 Al_2O_3 · 1.0 P_2O_5 · x H_2O; crystallization temperature: 423 K; heating: 293 K → 423 K with ca. 3 K/min.

x	Time [h]	Products
40	24	5 with Al/P=1.07
60	24	5 >> V + H4
60	30	T + C + U
90	24	T + H2 + H4 + 5
90	48	T + C + H1 + H4

The symbols for the products are explained in Tab. V.3.

The rate of $AlPO_4$–5 crystallization can drastically be increased by increasing the heating rate. Usually, the pressure bombs were warmed up from room temperature to the desired crystallization temperature which is typically 423 K. The heating rate of the oven is about 3 K/min. Under these conditions, the crystallization of $AlPO_4$–5 is finished after 24 h. Table V.6 shows that the crystallization time can be reduced to 4 h if the pressure bombs are immediately exposed to the final crystallization temperature by transferring them to the preheated oven.

124

TABLE V.6: Effect of Heating Rate.

Gel Composition: 1.2 Pr$_3$N · 1.0 Al$_2$O$_3$ · 1.0 P$_2$O$_5$ · 40 H$_2$O;
crystallization temperature: 423 K.

Heating[1]	t [h]	Products[2]
slowly	24	5 with Al/P=1.05
fast	18	5 + H1 + T
fast	14	5 with Al/P=1.06
very fast	4	5 with Al/P=1.07

[1]*Slowly: from room temperature to 423 K with ca. 3 K/min;
fast: immediate exposure to 373 K, then slowly up to 423 K;
very fast: immediate exposure to 423 K;*
[2]*the symbols for the products are explained in Tab. V.3.*

TABLE V.7: Effect of Al$_2$O$_3$/P$_2$O$_5$ Ratio.

Gel Composition: 1.5 Pr$_3$N · 1.0 Al$_2$O$_3$ · x P$_2$O$_5$ · 40 H$_2$O; crystallization time: 4 h;
crystallization temperature: 423 K; heating: very fast.[1]

x	pH (initial)	pH (final)	Products	Al/P ratio
1.0	4.2	8.5	5	1.06
1.02	3.6	8.3	5	1.01
1.05	3.2	7.0	H2 + T + 5	—

[1]*see Table V.6; the symbols for the products are explained in Tab. V.3.*

Finally, it is important to note that the chemical analyses of the XRD–pure AlPO$_4$–5

samples always gave Al/P ratios larger than one. Assuming that a part of the alumina

component did not take part in the reaction, some crystallizations were performed with

gels containing excess orthophosphoric acid. The resulting decrease in pH values was

compensated by higher template concentrations. The results are listed in Table V.7, and

show that a slight excess of orthophosphoric acid results in final Al/P ratios closer to

one. However, the ideal stoichiometric ratio could not be obtained. Strikingly, this seems

to be a typical feature of AlPO$_4$–5 samples as can be shown by a careful study of the

present literature: The $AlPO_4$–5 samples under investigation exhibited non–stoichiometric Al/P ratios between 1.02 and 1.08[15,19,20-22,25,26].

Conclusions

It is difficult to prepare $AlPO_4$–5 with the stoichiometric Al/P ratio of one. All samples prepared by us as well as the samples reported in the literature contain too much aluminum. A small excess orthophosphoric acid in the gel provides a nearly stoichiometric composition of the final products, but requires at the same time a higher concentration of tripropylamine. The best results were achieved with the gel composition is: 1.5 Pr_3N · 1.0 Al_2O_3 · 1.02 P_2O_5 · 40 H_2O. The appropriate crystallization temperature is 423 K. The crystallization time can be reduced drastically if the gel is heated rapidly at the final crystallization temperature. This can be provided by transferring the autoclave into a preheated oven.

V.2.   PROPERTIES OF $AlPO_4$–5

Introduction

In the previous part, the hydrothermal synthesis of $AlPO_4$–5 was described, and the typical non–stoichiometric Al/P ratio of the obtained samples was stressed. Some further characteristics of the $AlPO_4$–5 molecular sieve will be given here. The applied techniques are standard methods for the characterization of zeolites and related molecular sieve materials and reveal useful information about the properties of $AlPO_4$–5 and the nature of the excess aluminum present in the samples.

Experimental

Four samples of $AlPO_4$–5 exhibiting different Al/P ratios have been investigated by means of scanning electron microscopy (SEM), X–ray diffraction (XRD), infrared

126

spectroscopy (IR), sorption of n—butane and temperature programmed desorption of ammonia (NH_3—TPD). These techniques have already been described in part II part III of this thesis. The thermal stabilities were typically tested with 2 g of template—free $AlPO_4$—5 placed in a vertical quartz tube reactor of 3 cm diameter. In a 100 ml/min stream of dry or moist air, respectively, the samples were heated with a rate of 10 K/min until the final temperature was reached which was retained for about 3 h. Finally, the crystallinities of the samples were checked by means of XRD. The chemical resistance of $AlPO_4$—5 was studied by treatments with aqueous NaOH or HCl solutions, respectively, of different concentrations. Typically, a suspension of 1 g in 300 ml solution was shaken for about 20 h at room temperature. After filtration, nitric ammonium molybdate solution was added to the liquid in order to check dissolution of the samples. The presence of phosphate ions is indicated by the formation of yellow ammonium molybdophosphate.

Results and Discussion

Framework ratios Al/P larger than 1 would require Al—O—Al bondings which are not likely according to the bonding concept proposed by Flanigen et al.[13]. The mean P—O and Al—O distances in $AlPO_4$—5 are 0.153 and 0.174 nm, respectively[18]. As a consequence of this considerable difference in bonding lengths, the unit cell constants must be expected to increase with increasing framework Al/P ratio. However, the data listed in Tab. V.8 show that the unit cell parameters are almost the same in all samples.

TABLE V.8: Unit Cell Parameters of Selected $AlPO_4$—5 Samples.

Sample	Al/P	a [nm]	c [nm]
1	1.07	1.3692	0.8440
2	1.05	1.3700	0.8443
3	1.03	1.3692	0.8442
4	1.01	1.3697	0.8451

In analogy to zeolites (see part IV), differences in framework Al/P ratios should moreover result in frequency shifts of the mid–infrared absorptions since the P–O bondings are stronger than Al–O bondings. But the IR spectra in Fig. V.4 give no evidence of any frequency shift. Both, XRD and IR results, indicate that the samples under investigation have the same framework compositions while containing different amounts of non–framework alumina.

Fig. V.4: IR Spectra of $AlPO_4-5$ with Different Al/P Ratios.
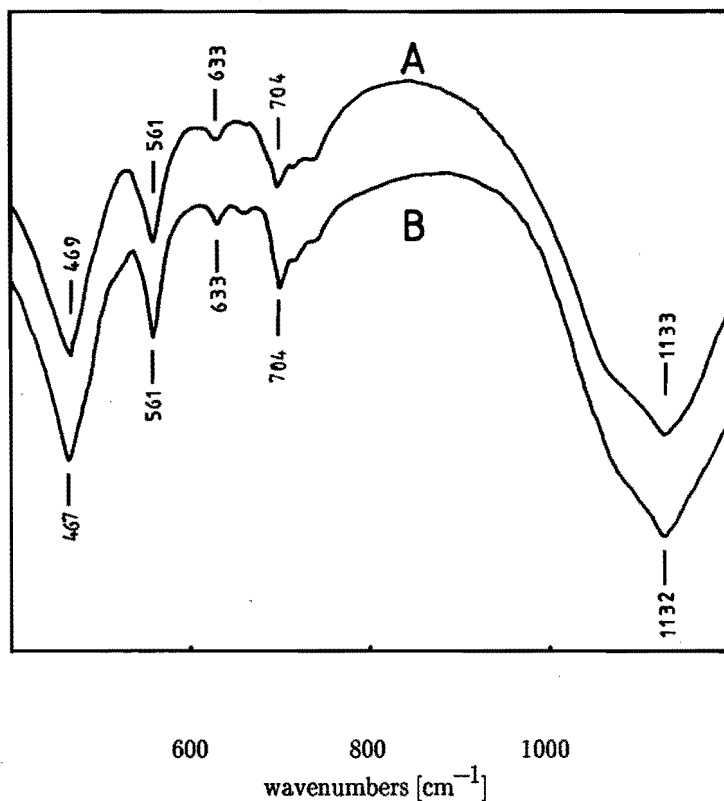*A = sample 1 with Al/P = 1.07; B = sample 4 with Al/P = 1.01*

TABLE V.9: *N−Butane Sorption Capacities of Selected AlPO$_4$−5 Samples.*

Sample	Al/P	Pore Volume [ml/g]
1	1.07	0.100
2	1.05	0.130
3	1.03	0.133
4	1.01	0.133

Adsorption of permanent gases and hydrocarbons into AlPO$_4$−5 gives isotherm shapes typical of micropore filling[20]. Therefore, n−butane adsorption capacities can be taken as a measure for the pore volumes of the calcined samples. The data in Table V.9 show that the pore volumes of the samples 2, 3 and 4 are almost the same. The small differences can be due to different amounts of dense phase alumina impurity. A typical scanning electron micrograph of AlPO$_4$−5 (sample 2) is shown in Fig. V.5. The sample consists of single crystal hexagonal prisms which are 5−10 μm long and 1−5 μm across.

Fig. V.5: *Scanning Electron Micrograph of AlPO$_4$−5 (sample 2, bar indicates 10 μm).*
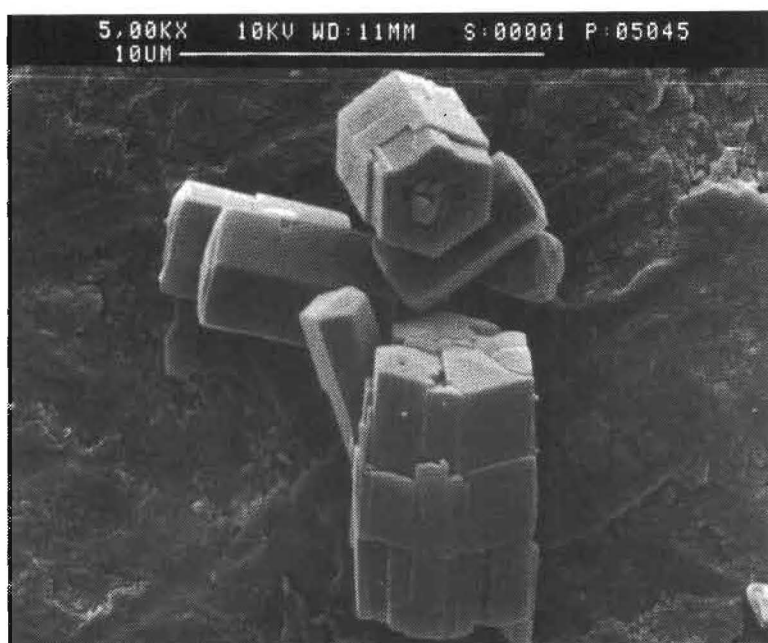
Additionally, some extraneous aggregates are visible, suggesting that the non–framework alumina forms particles which are physically mixed with the $AlPO_4$–5 crystals. The exceptional low pore volume of sample 1 can only be explained by additional internal alumina deposits blocking a part of the unidimensional channels.

From the similar crystal size distributions of the four samples it can be concluded that the amount of weakly acidic external terminal Al–OH and P–OH groups stemming from the $AlPO_4$–5 crystals is almost the same. Therefore, NH_3–TPD can be used in order to check whether the non–framework alumina provides additional acidic sites. The results are shown in Fig. V.6. Obviously, the TPD data show a similar trend as the Al/P ratios of the four samples: The higher the content of non–framework alumina, the higher is the amount of weak acidic sites. It should be emphasized here that there is no exact quantitative correlationship between the amount of extraneous alumina and the TPD data, since the amount of acidic sorption sites also depends on the nature and the

Fig. V.6: NH_3–TPD of $AlPO_4$–5 with Different Al/P Ratios.
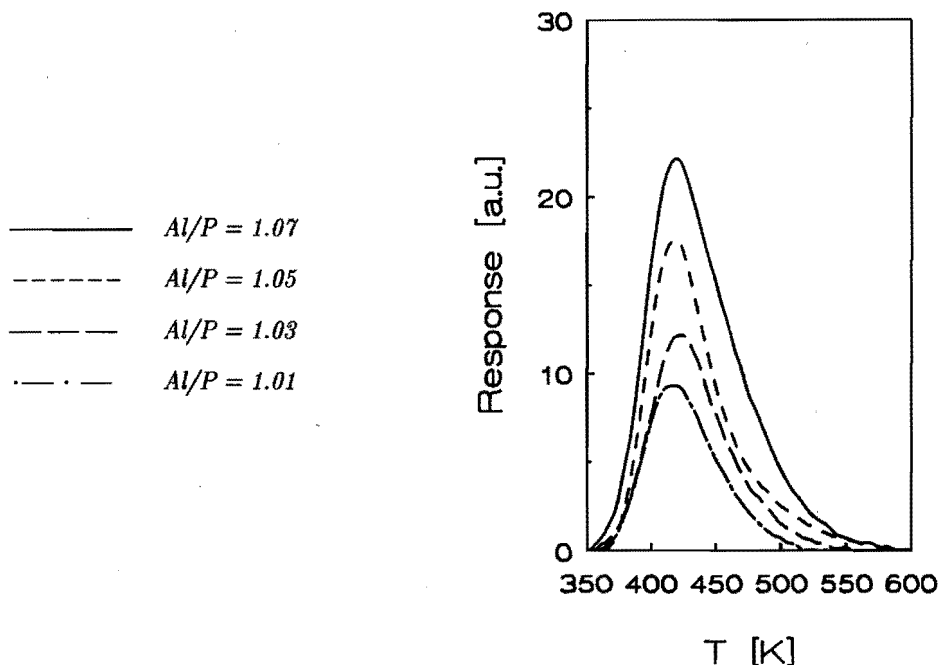
———————— Al/P = 1.07

– – – – – – Al/P = 1.05

—— —— Al/P = 1.03

·—— · —— Al/P = 1.01

capacity and the relatively apolar surface character make it difficult to load the channels with, for instance, nickel particles by means of conventional wet–chemical methods. In contrast, the chemical vapour deposition of an electroneutral metalorganic compound such as nickelocene has been shown to be a promising method for this purpose. Non–acidic molecular sieves can become particularly interesting supports for catalytically active metals or metal compounds because of their well–defined, high surface and their shape selective properties.

SAMENVATTING

Gemodificeerde zeolieten kennen vele commerciële toepassingen in het bijzonder als heterogene katalysatoren. Hoewel een grote varieteit aan zeolieten door directe synthese kan worden verkregen is modificatie in bepaalde gevallen de goedkoopste of soms zelfs de enige manier om een katalysator met de gewenste eigenschappen te verkrijgen. Bekende modificatie methoden die zijn ontwikkeld voor het verbeteren van de activiteit en/of de selectiviteit van zeoliet katalysatoren zijn ondermeer ionenwisseling, dealuminatie en belading met katalytisch actieve metaal deeltjes.

Het onderzoek dat in dit proefschrift wordt beschreven betreft de synthese, modificatie en karakterisiering van drie veel gebruikte kristallijne moleculaire zeven. De familie van kristallijne moleculaire zeven bestrijkt een groot gebied van verschillende structuren en chemische samenstellingen. In deel I wordt daarom begonnen met een korte beschrijving van een drietal nieuwe algemene concepten die kunnen worden gebruikt bij de beschrijving van de structurele, fysisch–chemische en katalytische eigenschappen van deze verschillende materialen.

In deel II wordt de karakterisering van zeoliet ZSM–5 besproken. Kenmerkend voor deze zeoliet zijn de interne silanol groepen, welke duiden op de aanwezigheid van structuurfouten. Een nieuwe methode, bestaande uit silylering van de silanol groepen

143

Conclusions

The framework of $AlPO_4-5$ exhibits excellent thermal and hydrothermal stability whereas the resistance towards acids and bases is poor. The sensitivity towards acids is comparable with that of the zeolites type A and type X. Samples of $AlPO_4-5$ typically contain impurities of alumina which are indicated by an over-all $Al/P > 1$. The alumina species can block the channels resulting in a decrease in accessible void space. Therefore, pore volume measurements are required even in the case of highly crystalline samples. Moreover, extraneous alumina can provide additional acidic sites, and care must be taken when acidic and catalytic properties of $AlPO_4-5$ with $Al/P > 1$ are considered.

V.4.   LOADING OF ALPO$_4$–5 WITH NICKEL PARTICLES

Introduction

Supported metal catalysts are typically prepared by means of wet chemical methods such as pore volume impregnation. The support materials are usually non-crystalline porous materials, e.g. silica, alumina, or titania, exhibiting polar terminal groups which provide adhesion of the ionic metal species on the support surface. A disadvantage of these supports is the wide range of pore sizes which enables broad distributions of the metal particle sizes. In contrast, crystalline silica or aluminophosphate molecular sieves provide well defined pore or channel systems. Application of these materials as supports would offer the possibility of shape selective metal catalysis. The problem arising here is the entrapment of the metal particles inside the pores. Silica and aluminophosphate molecular sieves don't possess ion exchange capacity, and polar hydroxyl groups are preferently located on the external surface of the crystallites. It will be shown here that ionic metal species can hardly be stabilized inside the channels of an electroneutral framework, and migration towards the polar external surface is the consequence. Several

132

procedures for the nickel loading of $AlPO_4$–5 will be evaluated, and chemical vapour deposition (CVD) of an electroneutral nickelcompound will be introduced as a promising method. Of course, nickeltetracarbonyl may be the most likely candidate for this purpose, but nickelocene has been preferred for reasons of safety.

Experimental

As starting material, a template–free $AlPO_4$–5 with $Al/P = 1.05$ was used. Ion exchange was performed by shaking 1 g $AlPO_4$–5 three times in 50 ml 0.5 M aqueous $Ni(NO_3)_2$ solution at room temperature. After washing with water, the product was dried overnight at 393 K in a stream of helium. Pore volume impregnations were performed with aqueous 1.0 m solutions of $Ni(NO_3)_2$ or $K_2[Ni(CN)_4]$, respectively, or with a 10 wt.% solution of nickelocene in benzene in order to provide cationic, anionic or electroneutral nickel species. After each impregnation step, the products were dried overnight in a stream of helium at 393 K. Reduction of the nickel species was achieved by heating up with 2 K/min in a flow of dry hydrogen and remaining for about 6 h at 673 K.

For the chemical vapour deposition (CVD) experiments, typically 500 mg nickelocene were sublimated at 383 K in a helium atmosphere. In a vertical quartz tube reactor, a thin layer of carefully dried $AlPO_4$–5 (1 g) was kept in a hydrogen atmosphere at 473 K. At reduced pressures between 0.6 and 13 kPa, a stream of nickelocene in helium was allowed to pass through the reactor and to mix there with hydrogen. After complete sublimation of the nickelocene, the sample was kept in a flow of hydrogen at ambient pressure and temperature for about 3 h.

The X–ray diffraction (XRD) and n–butane sorption experiments have been described in part II of this thesis. The transmission electron micrograph has been taken on a Jeol 200 CX electron microscope, equipped with a top entry $\pm 10^{o}$ double tilt.

Results and Discussion

In a molecular sieve with unidimensional channels such as $AlPO_4$–5, the accessible void space considerably decreases if a part of the channels is blocked by internal deposits. The effect of pore blocking on the sorption capacity is less pronounced in the case of short average channel lengths. But the parent sample of $AlPO_4$–5 consists of single crystals which are 5 – 10 μm along the c–axis (Fig. V.5), which is also the direction of the unidimensional channels. Therefore, pore volume measurements have been used here to give evidence of deposits inside the channel system.

TABLE V.12: Nickel Loading by Means of Wet–Chemical Methods.

Sample	Preparation[1]	Pore Volume [ml/g]		Ni content [wt.%]
		after drying	after reduction	
0	starting material	0.130	0.132	0
1	3 x exch. with $Ni(NO_3)_2$	0.131	0.132	0.05
2	1 x imp. with $Ni(NO_3)_2$	0.130	0.128	0.9
3	3 x imp. with $Ni(NO_3)_2$	0.127	0.125	2.9
4	3 x imp. with $K_2[Ni(CN)_4]$	0.125	0.128	3.0
5	3 x imp. with $Ni(C_5H_5)_2$	0.122	0.129	1.8

[1] *Exch. = ion exchange, imp. = pore volume impregnation.*

Table V.12 shows the results of chemical analyses and pore volume measurements of nickel loaded $AlPO_4$–5 prepared by means of wet–chemical methods. Only traces of nickel have been found in sample 1 which did undergo ion exchange including filtration and washing procedures. Due to the lack of electrostatic fields in $AlPO_4$–5, the nickel ions remained preferently in the aqueous solution. By means of pore volume impregnation, higher nickel loadings of about 1 – 3 wt.% could be obtained. But the changes in n–butane sorption capacities with respect to the nickel–free starting material

are within the experimental error, indicating that the channels are still completely accessible. The data in Tab. V.12 suggest that the nickel species are located on the external surface of $AlPO_4$–5 even before reduction. Possibly, drying of the impregnated samples causes a migration of Ni^{2+} or $Ni(CN)_4^{2-}$, respectively, towards the external surface since these ionic species can be stabilized there by polar terminal Al–OH and P–OH groups. In the case of the electroneutral nickelocene species it can be assumed that the interaction with the solvent benzene competes with the interaction with the channel walls. Supposing that the solvated nickelocene molecules are too large and the loss of coordinated solvent molecules is energetically unfavourable, the nickelocene will not even enter the channels.

A part of the XRD pattern of sample 3 after reduction with hydrogen is shown in Fig. V.7 (A), exhibiting a signal at $2\Theta = 44.5$ degrees that must be assigned to the Ni(111) reflection. Similar XRD spectra could be obtained from the samples 4 and 5. The Scherrer equation allows to estimate the apparent crystal size of the nickel particles from measurement of the half–peak width of the Ni(111) reflection:

$$L = \frac{0.94 \cdot \lambda}{B(2\Theta) \cdot \cos\Theta}$$

with   L = apparent cube edge dimension [nm],
        $B(2\Theta)$ = half maximum intensity width [rad],
        λ = X–ray wavelength [nm].

Without correction for the instrumental broadening an apparent crystal size of about 20 nm can be obtained for the samples 3, 4 and 5. For steric reasons, these particles cannot be located inside the channels without partial damage of the framework. However, this can be excluded from the XRD patterns. Therefore, XRD and pore volume measurements give evidence of the formation of large nickel particles on the external surface of the $AlPO_4$–5 crystals.

Fig. V.7: XRD Patterns of Nickel Loaded AlPO4−5.
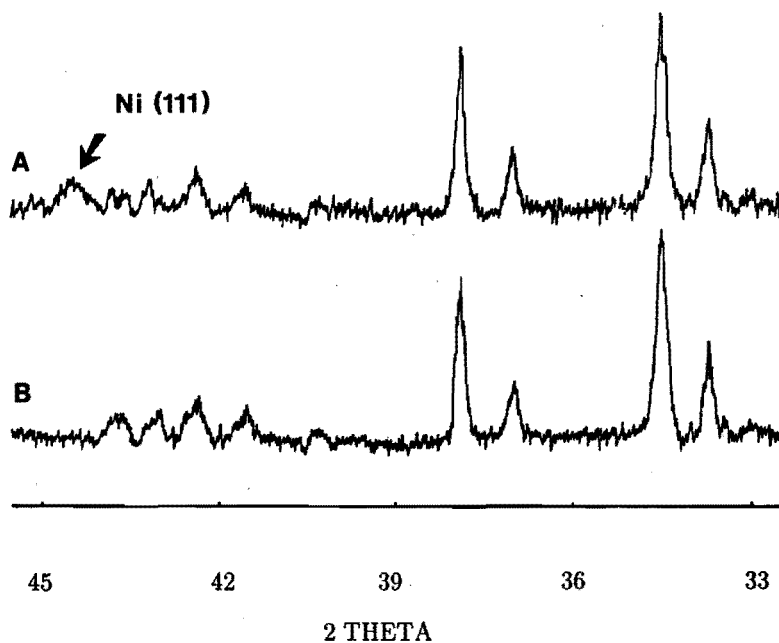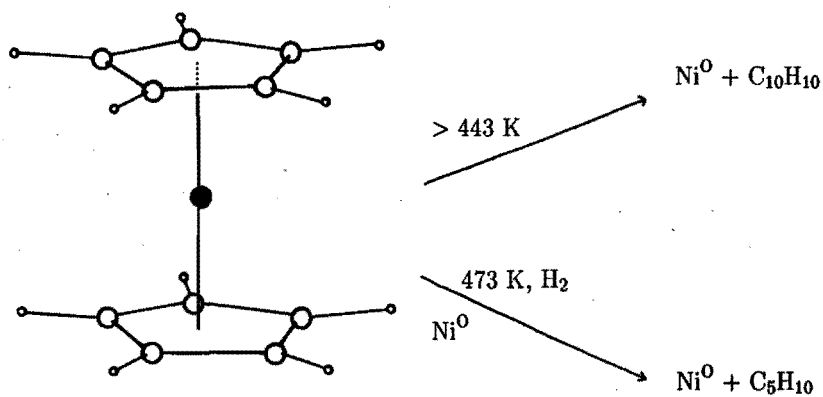*(A) = sample 3 with 2.9 wt.% Ni; (B) = sample 7 with 5.5 wt.% Ni.*

*Fig. V.8: Formation of Ni⁰ from Nickelocene*

Nickel species introduced via wet–chemical methods must be reduced with hydrogen in order to yield Ni^o. At least under optimal conditions this is not required after CVD of nickelocene. This compound should decompose upon passing through a layer of $AlPO_4$–5 at 473 K. However, in order to achieve a complete decomposition hydrogen can be passed through the reactor, providing hydrogenolysis of the nickelocene. This reaction is catalyzed by Ni^o which has already been formed upon thermal decomposition (Fig. V.8).

The samples obtained from CVD of nickelocene exhibit nickel loadings of about 3 – 10 wt.% (Tab. V.13). From the drastical decrease in n–butane sorption capacities it can be concluded that a considerable part of the nickel particles must be located inside the channel system. The XRD pattern of sample 7 (Fig. V.7, B) exhibits no Ni(111) reflection although the nickel content is about twice as high as in sample 3 (Fig. V.7, A). The broadening of the nickel reflection must be very pronounced due to the small size of the nickel crystals. A transmission electron micrograph of sample 7 is shown in Figure V.9. Nickel particles with diameters of about 2.5 nm are spread all over the $AlPO_4$–5 crystal. Looking at the edge of this crystal, it is obvious that nickel particles are formed on the external surface. It is impossible to conclude from this micrograph whether and to what extend nickel particles were also formed inside the channels. But it should be noticed that no nickel particles larger than about 2.5 nm are observed. Supposing this value to be the apparent crystalllite size, the Scherrer equation gives a half–peak width of the Ni(111) reflection of about 4 degrees. Indeed, this is a broadening that makes the nickel "XRD–invisible". For completion it should be added that none of the samples prepared by means of CVD of nickelocene exhibited the Ni(111) peak.

TABLE V.13: Nickel Loading by Means of CVD of Nickelocene.

Sample	CVD Pressure [kPa]	Pore Volume [ml/g]	Ni content [wt.%]
6	0.667	0.090	3.1
7	2.666	0.055	5.5
8	13.332	0.039	9.8

Fig. V.9: Transmission Electron Micrograph of Sample 7 (1 cm = 7.4 nm).
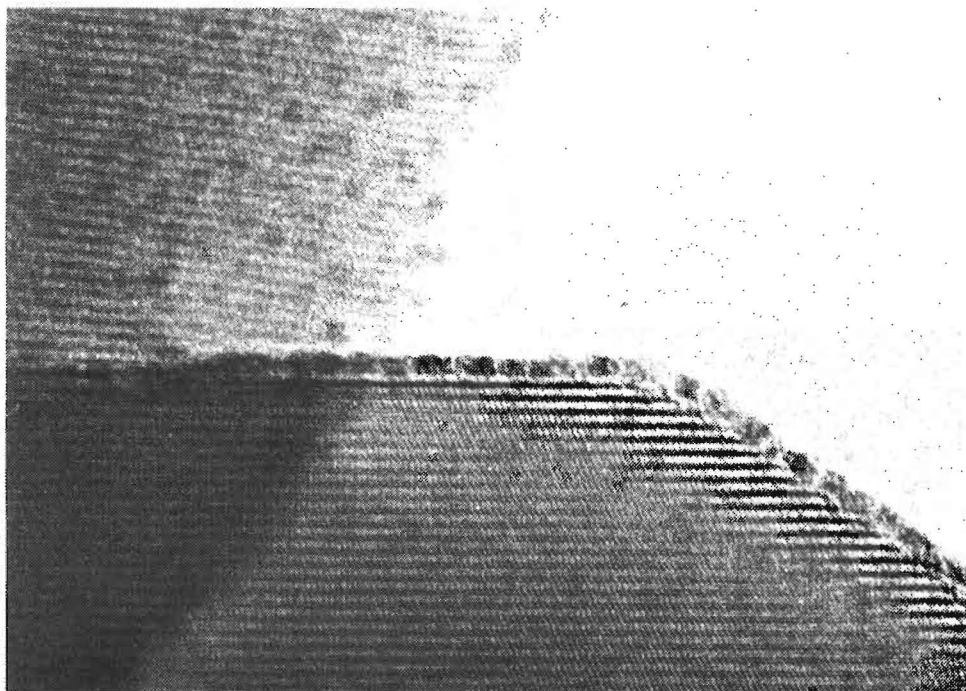
Conclusions

The preparation of nickel loaded $AlPO_4-5$ molecular sieve has been investigated by comparing some wet–chemical procedures with the chemical vapour deposition of nickelocene. Solvent effects and/or interaction with external terminal groups may be the reasons why the nickel species introduced by wet–chemical methods tend to concentrate on the external surface of the $AlPO_4-5$ crystals. Upon subsequent reduction, large XRD–visible nickel particles are formed. In contrast, the nickel particles deposited by means of CVD are highly dispersed. The combination of TEM and sorption measurements gives evidence of external as well as internal nickel loadings. Therefore, the CVD of metalorganic compounds such as nickelocene is a promising method for the metal loading of molecular sieves that don't possess ion exchange capacity. More extensive investigations including stability tests and catalytic reactions are required in order to evaluate and refine this interesting technique.

138

V.5. REFERENCES

1   S.T. Wilson, B.M. Lok and E.M. Flanigen, U.S. Patent 4.310.440 (1982).

2   S.T. Wilson, B.M. Lok, C.A. Messina, T.R. Cannan and E.M. Flanigen, J. Am. Chem. Soc. 104, 1146 (1982).

3   E.M. Flanigen, B.M. Lok, R.L. Patton and S.T. Wilson, in "Proc. 7th Int. Zeolite Conf. in Tokyo", Elsevier Tokyo 1986, p. 103.

4   B.M. Lok, C.A. Messina, R.L. Patton, R.T. Gajek, T.R. Cannan and E.M. Flanigen, U.S. Patent 4.440.871 (1984).

5   B.M. Lok, C.A. Messina, R.L. Patton, R.T. Gajek, T.R. Cannan and E.M. Flanigen, J. Am. Chem. Soc. 106, 6092 (1984).

6   C.A. Messina, B.M. Lok and E.M. Flanigen, U.S. Patent 4.544.143 (1985).

7   S.T. Wilson and E.M. Flanigen, U.S. Patent 4.567.029 (1986).

8   B.M. Lok, B.K. Marcus and E.M. Flanigen, U.S. Patent 4.500.651 (1985).

9   B.M. Lok, B.K. Marcus and E.M. Flanigen, Eur. Pat. Appl. EP 161.488 (1985).

10   B.M. Lok, B.K. Marcus and E.M. Flanigen, Eur. Pat. Appl. EP 161.489 (1985).

11   B.M. Lok, B.K. Marcus and E.M. Flanigen, Eur. Pat. Appl. EP 161.490 (1985).

12   B.M. Lok, B.K. Marcus, L.D. Vail, E.M. Flanigen, R.L. Patton and S.T. Wilson, Eur. Pat. Appl. EP 159.624 (1985).

13   E.M. Flanigen, R.L. Patton and S.T. Wilson, Stud. Surf. Sci. Catal., vol. 37, Elsevier Amsterdam 1988, p. 13.

14   C.S. Blackwell and R.L. Patton, J. Phys. Chem. 92, 3965 (1988).

15   D. Hasha, L.S. de Saldarriaga, C. Saldarriaga, P. Hathaway, D.F. Cox and M.E. Davis, J. Am. Chem. Soc. 110, 2127 (1988).

16   I.P. Appleyard, R.K. Harris and F.R. Fitch, Chem. Lett. 1747 (1985).

17   E.M. Flanigen, B.M. Lok, R.L. Patton and S.T. Wilson, in "New Developments in Zeolite Science and Technology", (Y. Murakami, A. Iijima and J.W. Ward, Eds.), Elsevier New York 1986, p. 103.

18   J.M. Bennet, J.P. Cohen, E.M. Flanigen, J.J. Pluth and J.V. Smith, Am. Chem. Soc. Symp. Ser. 218, 109 (1983).

19 D. Müller, E. Jahn, B. Fahlke, G. Ladwig and U. Haubenreisser, Zeolites 5, 53 (1985).

20 S.T. Wilson, B.M. Lok, C.A. Messina, T.R. Cannan and E.M. Flanigen, Am. Chem. Soc. Symp. Ser. 218, 79 (1983).

21 V.R. Choudhary and D.B. Akolekar, J. Catal. 103, 115 (1987).

22 S.G. Hedge, P. Ratnasamy, L.M. Kustov and V.B. Kazansky, Zeolites 8, 139 (1988).

23 D.R. Pyke, P. Whitney and H. Houghton, Appl. Catal. 18, 173 (1985).

24 J.M. Bennet, W.J. Dytrych, J.J. Pluth, J.W. Richardson and J.V. Smith, Zeolites 6, 349 (1986).

25 V.R. Choudhary, D.B. Akolekar, A.P. Singh and S.D. Sansare, J. Catal. 111, 23 (1988).

26 H. Stach, H. Thamm, K. Fiedler, B. Grauert, W. Wieker, E. Jahn and G.Ohlmann, in "Proc. 7th Int. Zeolite Conf. in Tokyo", Elsevier Tokyo 1986, p. 539.

SUMMARY

Modified zeolites play an important role in many commercial applications and particularly in the field of heterogeneous catalysis. In spite of the great variety of zeolites and related crystalline, microporous materials which can be synthesized directly, modification is sometimes the cheapest or even the only way to prepare a catalyst with the desired properties. Ion exchange, dealumination or loading with catalytically active metal particles, for instance, are familair modification procedures which have been developed in order to improve activity and/or selectivity of zeolite catalysts.

The investigations described in this thesis are concerned with the synthesis, modification and characterization of some selected crystalline molecular sieves. The family of crystalline molecular sieves covers a wide range of different structures and chemical compositions. Part I therefore gives a short introduction to some novel, unifying concepts that account for this variety and may be helpful in the rationalizing of structural, physico–chemical and catalytic properties.

In part II, the characterization of zeolite ZSM–5 has been described. This zeolite typically exhibits internal silanol groups which indicate the presence of structural defects. A novel method has been developed, consisting of silylation of the silanol groups and subsequent ^{29}Si CP MAS NMR analyses of the products, which enables a deeper insight into the kind and position of these structural defects in ZSM–5. It could be shown that the internal silanol groups in ZSM–5 surround T–atom vacancies, lattice positions where a tetrahedrally coordinated silicon or aluminum atom is missing. Manipulation of the amount of internal silanol groups is possible by means of hydrothermal treatments or exposure to mineralic acids. The catalytic results presented in chapter II.4 show that structural defects can considerably affect the intrinsic activity and the deactivation characteristics of H–ZSM–5 in catalytic cracking, suggesting that changes in the amount of internal silanol groups alter the surface character in the zeolite channels and hence the interaction between framework and reagent molecules.

141

The investigations presented in part III demonstrate that the same structural defects unfavourable in catalytic cracking can be considered as useful functional groups in modification reactions. Reaction of titanium tetrachloride vapour with a defective ZSM–5 results in a refilling of the T–atom vacancies with titanium atoms. The material obtained is called titanium silicalite and exhibits remarkable catalytic properties in the oxidation of organic compounds involving hydrogen peroxide. The direct hydrothermal synthesis reported in the patent literature is difficult to reproduce and yields only titanium silicalites with the structure of ZSM–5. In contrast, the modification route can also be applied to other zeolites, provided the aluminum content is low and the amount of T–atom vacancies is high.

Dealumination of zeolite Y and characterization of the resulting structural defects are the subjects of part IV of this thesis. Acid leaching, hydrothermal treatment and the reaction with silicon tetrachloride have been investigated as the three most important dealumination procedures. The characterizations of the products clearly show that any of the methods applied causes the formation of T–atom vacancies. It depends on the dealumination conditions whether these T–atom vacancies are isolated from each other or accumulated, forming small cavities or even secondary pores in the lattice. Dealumination is usually applied in order to improve the thermal stability of zeolite Y which is the most important industrial cracking catalyst. Moreover, the selectivity towards gasoline fractions with high octane numbers can be enhanced. However, the structural defects typically present in dealuminated zeolite Y are surrounded by silanol groups which may enable incorporation of titanium atoms or other interesting reactions. Dealuminated zeolite Y should therefore also be considered as a useful starting material for further modifications.

The investigations described in the last part of this thesis do not concern the incorporation of metal ions into the framework of a molecular sieve but rather the deposition of metal particles in the channels. The material under investigation is $AlPO_4$–5, a molecular sieve with an electroneutral framework. The lack of ion exchange

142

capacity and the relatively apolar surface character make it difficult to load the channels with, for instance, nickel particles by means of conventional wet–chemical methods. In contrast, the chemical vapour deposition of an electroneutral metalorganic compound such as nickelocene has been shown to be a promising method for this purpose. Non–acidic molecular sieves can become particularly interesting supports for catalytically active metals or metal compounds because of their well–defined, high surface and their shape selective properties.

SAMENVATTING

Gemodificeerde zeoliten kennen vele commerciële toepassingen in het bijzonder als heterogene katalysatoren. Hoewel een grote varieteit aan zeoliten door directe synthese kan worden verkregen is modificatie in bepaalde gevallen de goedkoopste of soms zelfs de enige manier om een katalysator met de gewenste eigenschappen te verkrijgen. Bekende modificatie methoden die zijn ontwikkeld voor het verbeteren van de activiteit en/of de selectiviteit van zeoliet katalysatoren zijn ondermeer ionenwisseling, dealuminatie en belading met katalytisch actieve metaal deeltjes.

Het onderzoek dat in dit proefschrift wordt beschreven betreft de synthese, modificatie en karakterisering van drie veel gebruikte kristallijne moleculaire zeven. De familie van kristallijne moleculaire zeven bestrijkt een groot gebied van verschillende structuren en chemische samenstellingen. In deel I wordt daarom begonnen met een korte beschrijving van een drietal nieuwe algemene concepten die kunnen worden gebruikt bij de beschrijving van de structurele, fysisch–chemische en katalytische eigenschappen van deze verschillende materialen.

In deel II wordt de karakterisering van zeoliet ZSM–5 besproken. Kenmerkend voor deze zeoliet zijn de interne silanol groepen, welke duiden op de aanwezigheid van structuurfouten. Een nieuwe methode, bestaande uit silylering van de silanol groepen

143

gevolgd door ^{29}Si CP MAS NMR analyse van de gevormde producten, is ontwikkeld, om de aard en de plaats van deze structuurfouten te kunnen bepalen. Hiermee kon worden aangetoond dat de silanol groepen in ZSM–5 zijn gegroepeerd rond een vacante roosterplaats voor een silicium– of een aluminiumatoom. Beïnvloeding van het aantal interne silanolgroepen is mogelijk door hydrothermale behandeling of door behandeling met minerale zuren. De katalytische resultaten voor het kraken van hexaan en butaan in hoofdstuk II.4 geven aan dat de structuurfouten in H–ZSM–5 in belangrijke mate de activiteit en deactivering beïnvloeden. Dit duidt op een beïnvloeding van de interne oppervlakte eigenschappen door de aanwezige silanol groepen waardoor ook de interactie tussen het zeoliet rooster en de reagerende moleculen verandert.

Deel III laat zien dat dezelfde structuurfouten die bij het katalytisch kraken zo'n ongunstige werking hebben nuttig kunnen zijn als functionele groepen bij bepaalde modificatie reacties. Reactie van titaan–tetrachloride damp met een defecte ZSM–5 zeoliet resulteert bijvoorbeeld in de inbouw van titaanatomen in het zeolietrooster. Het op deze wijze verkregen materiaal wordt titaan silikaliet genoemd en bezit bijzondere katalytische eigenschappen voor de oxidatie van bepaalde organische verbindingen met waterstofperoxide. De directe hydrothermale synthese zoals beschreven in de patent literatuur blijkt moeilijk te reproduceren en is bovendien alleen toepasbaar voor de bereiding van titaan silikalieten met de structuur van ZSM–5. De modificatie methode met titaan–tetrachloride kan daarentegen ook voor andere typen zeolieten worden gebruikt, mits het aluminiumgehalte laag en het aantal vacante roosterplaatsen hoog is.

Dealuminering van zeoliet Y en karakterisering van de hierbij ontstane structuurfouten is het onderwerp van deel IV van dit proefschrift. Extractie met zuur, hydrothermale behandling en reactie met silicium–tetrachloride zijn als de drie belangrijkste dealumineringsmethoden onderzocht. De karakterisering van de verkregen producten toont duidelijk aan dat in elk van deze gevallen vacante roosterplaatsen worden gevormd. Afhankelijk van de dealumineringscondities zijn deze geïsoleerd danwel geaccumuleerd waardoor kleine holten of zelfs secundaire poriën kunnen worden

144

gevormd. De voornaamste reden voor dealuminering van zeoliet Y is verbetering van de voor het gebruik als kraak–katalysator zo belangrijke thermische stabiliteit. Daarnaast kan dealuminering ook leiden tot een verhoging van het octaangetal van de bij het kraken gevormde benzine. De structuurfouten in zeoliet Y kunnen echter ook worden gebruikt voor de inbouw van titaanatomen of voor andere interessante reacties. Gedealumineerde zeoliet Y moet daarom gezien worden als een belangrijk uitgangsmateriaal voor modificatie.

Het onderzoek dat in het laatste deel van dit proefschrift wordt beschreven betreft niet de introductie van afzonderlijke metaalionen in het rooster van een moleculaire zeef maar het aanbrengen van kleine metaaldeeltjes in de poriën. Het onderzochte materiaal is in dit geval $AlPO_4$–5, een moleculaire zeef met een electroneutraal rooster. Het ontbreken van ionenwisselingseigenschappen en het relatieve apolaire oppervlak maken het inbrengen van nikkelatomen met behulp van de conventionele natchemische methoden onmogelijk. Het aanbrengen van kleine nikkeldeeltjes in de poriën blijkt echter wel mogelijk door thermische ontleding van gasvormig electroneutraal nikkeloceen ($Ni(C_5H_5)_2$). Met metaal beladen niet–zure moleculaire zeven kunnen door hun goed gedefiniëerde oppervlak en hun vormselectieve eigenschappen interessante nieuwe mogelijkheden bieden.

List of Publications

Part II:

B. Kraushaar, J.W. de Haan, L.J.M. van de Ven and J.H.C. van Hooff, "Cation Assisted Lattice Improvement of Highly Siliceous ZSM–5 upon Prolonged Heat Treatment", Chem. Lett. 1523, 1986.

Part II:

B. Kraushaar, L.J.M. van de Ven, J.W. de Haan and J.H.C. van Hooff, "Clusters of Terminal Groups in ZSM–5: A Study Performed by Silylation and ^{29}Si CP MAS NMR", Stud. Surf. Sci. Catal., vol. 37, Elsevier Amsterdam 1988, p. 167.

Part II:

B. Kraushaar, J.W. de Haan and J.H.C. van Hooff, "On the Presence of Internal Silanol Groups in ZSM–5 and the Annealing of these Sites by Steaming", J. Catal. 109, 470 (1988).

Part II and IV:

B. Kraushaar, J.W. de Haan, L.J.M. van de Ven and J.H.C. van Hooff, "A Method for the Identification of T–Atom Vacancies in the Lattices of Zeolites", Z. anorg. allg. Chem. 564, 72 (1988).

Part III:

B. Kraushaar and J.H.C. van Hooff, "A New Method for the Preparation of Titanium Silicalite (TS–1)", Catal. Lett. 1, 81 (1988).

Part III:

B. Kraushaar–Czarnetzki and J.H.C. van Hooff, "A Test Reaction for Titanium Silicalite Catalysts", Catal. Lett., in press.

Part V:

B. Kraushaar–Czarnetzki and J.H.C. van Hooff, "On the Preparation of Nickel Loaded $AlPO_4$–5", Stud. Surf. Sci. Catal., in press.

Part II:

B. Kraushaar–Czarnetzki and J.H.C. van Hooff, "Effect of Internal Silanol Groups on the Catalytic Properties of H–ZSM–5", in preparation.

146

Curriculum Vitae

Bettina Kraushaar werd geboren op 20 januari 1958 te Zwesten (deelstaat Hessen, Bondsrepubliek Duitsland). Op 18 juni 1977 behaalde zij het "Zeugnis der allgemeinen Hochschulreife" aan het Immanuel–Kant–Gymnasium te Heiligenhaus (deelstaat Nordrhein Westfalen, BRD). Aansluitend begon zij haar studie scheikunde aan de Rheinisch–Westfälisch Technische Hochschule te Aken. Na het behalen van het "Vordiplom" op 9 maart 1991 zette zij de studie scheikunde voort aan de Universiteit Bremen. Op 6 maart 1985 legde zij de "Diplomprüfung" af. Het afstudeeronderwerp werd uitgevoerd in de Vakgroep voor Fysische en Toegepaste Chemie onder de leiding van prof. dr. G. Schulz–Ekloff and prof. dr. N. Jaeger. Aansluitend begon zij met haar promotieonderzoek in de Vakgroep voor Anorganische Chemie en Katalyse aan de Technische Universiteit Eindhoven. Op 19 augustus 1988 trad zij in het huwelijk met Lothar Rüdiger Czarnetzki.

STELLINGEN

behorende bij het proefschrift

Characterization and Modification

of Zeolites and Related Materials

van

Bettina Kraushaar–Czarnetzki

1   Mixing or segregation of polymers and bilayer constituents is often exclusively studied by means of Differential Scanning Calorimetry. It is advisable to involve also solid–state ^{13}C nuclear magnetic resonance spectroscopy (^{13}C CP MAS NMR).

P.M. Henrichs, J. Tribone, D.J. Massa and J.M. Hewitt, Macromolecules 21, 1282 (1988).
G.H.W.M. Meulendijks, J.W. de Haan, A.H.J.A. Vos, L.J.M. van de Ven and H.M. Buck, J. Phys. Chem., in press.

2   Boiling and subsequent quenching of tetramethylammonium silicate solutions results in the formation of silica gel. The silicate species observed by Knight et al. after thawing are therefore stemming from re–dissolution of gel particles rather than from slow rearrangements between silicate anions in solution.

P.W.J.G. Wijnen, T.P.M. Beelen, J.W. de Haan, C.P.J. Rummens, L.J.M. van de Ven and R.A. van Santen, in preparation.
C.T.G. Knight, R.J. Kirkpatrick and E. Oldfield, J. Chem. Soc., Chem. Commun. 66, 1986.

3   Analyses of thermal desorption spectra within the Polanyi–Wigner model are often performed according to simplified methods involving easily accessible spectral features such as peak maximum temperatures and widths. These simplified methods do not take the coverage–dependence of the preexponential factor ν into consideration and give unreliable values for the activation energy of desorption $E(\Theta)$. In contrast, the "complete analysis" as described by King results in correct $E(\Theta)$ and $\nu(\Theta)$ values and reveals lateral interactions of adsorbed species.

D.A. King, Surf. Sci. 47, 384 (1975).
J.W. Niemantsverdriet and K. Wandelt, J. Vac. Sci. Technol. A 6 (3), 757 (1988), and references therein.

4   The ^{29}Si–{^{1}H} cross–polarization characteristics (^{29}Si CP MAS NMR amplitudes versus contact time) of many silica gels and their derivatives exhibit more than one maximum. In these cases, ^{29}Si CP MAS NMR will hardly yield quantitative results, but it does reveal new structural information.

B. Pfleiderer, K. Albert, E. Bayer, L.J.M. van de Ven, J.W. de Haan and C. Cramers, submitted for publication.

5   The extraordinary bad performance of the sulfided NiMo catalysts in the pyridine HDN reaction as reported by Ledoux et al. is a result of the extraordinary preparation and pretreatment conditions applied by the authors and does not justify the general conclusion that nickel and sulfur have a poisoning effect.

M.J. Ledoux, G. Agostini, R. Benazouz and O. Michaux, Bull. Soc. Chim. Belg. 93, 635 (1984).

6   Der kollektiven Machtzunahme durch den naturwissenschaftlichen und technischen Fortschritt steht eine Abnahme der Einflussmöglichkeiten des einzelnen Wissenschaftlers gegenüber. Eine "Ethik für die technologische Zivilisation", wie sie von Jonas angeregt wird, sollte daher nicht die Verantwortung des Einzelnen in den Vordergrund stellen sondern Richtlinien für gesellschaftliches Handeln, zum Beispiel in der Gesetzgebung, Erziehung, Wissenschafts– und Wirtschaftsförderung herauskristallisieren.

H. Jonas, "Das Prinzip Verantwortung. Versuch einer Ethik für die technologische Zivilisation", Suhrkamp Taschenbuch Verlag, Frankfurt a.M. 1984.

7   The lack of cracking activity of calcined TPA/Na–ZSM–5 indicates that the product of the calcination is not H/Na–ZSM–5.